

Habilitation à Diriger des Recherches

présentée par

Xavier Bombois

TITRE

**Travaux sur l'identification pour la
commande et la synthèse optimale de
l'expérience d'identification**

December 13, 2013

Contents

I	Curriculum et bilan des activités	7
1	Curriculum Vitae	9
1.1	Renseignements généraux	9
1.2	Formation	9
1.3	Expérience professionnelle	10
1.4	Connaissance des langues	10
1.5	Formations complémentaires	10
2	Activités d’enseignement	11
2.1	Aperçu général	11
2.2	Détail des activités	11
2.2.1	Activités à la TU Delft	11
2.2.2	Activités dans le cadre de l’Ecole doctorale hollandaise en Automatique (DISC)	13
2.2.3	Activités à l’Université Catholique de Louvain	13
3	Activités de recherche	15
3.1	Aperçu général	15
3.2	Encadrement de thèses de doctorat	16
3.3	Encadrement d’un postdoctorat	17
3.4	Gestion de projets de recherche	17
3.4.1	Projet européen EU-FP7 STREP “Autoprofit” (2010-2013)	17
3.4.2	Projet “Octopus” - Smart System Adaptability (2007-2012)	18
3.4.3	Projet “Automatic autorotation of a rotorcraft Unmanned Aerial Vehicle (UAV)” (2006-2014)	19
3.4.4	Batch Crystallization Control for Pharmaceutical Manu- facturing (2007-2013).	19
3.5	Collaborations nationales et internationales	20
3.6	Séjours en laboratoire	20
3.7	Activités éditoriales	21
3.8	Participation à des jurys de thèse de doctorat	21
3.9	Autres activités académiques	22
4	Travaux et publications	23

II Synthèse des travaux de recherche	33
5 Introduction	35
6 Robustness analysis	41
6.1 Prediction-error Identification	41
6.2 Controller design and controller validation	44
6.2.1 Controller design	44
6.2.2 Controller validation	45
6.3 Robustness tools	46
6.3.1 Robust performance analysis - controller validation for performance	46
6.3.2 Robust stability analysis - controller validation for stability	48
6.4 Conclusions	49
7 Least costly identification for control	51
7.1 Problem statement	51
7.2 Convex formulation	53
7.3 Shaping the spectrum	54
7.4 Extensions	56
7.5 Conclusions	58
8 Closed-loop performance diagnosis	59
8.1 Problem statement	59
8.2 Performance diagnosis	61
8.2.1 Hypothesis testing framework	61
8.2.2 Decision rule	62
8.2.3 After performance diagnosis	64
8.3 Experiment Design Framework	65
8.4 Conclusions	67
9 Iterative model improvement for control	69
9.1 Problem statement	69
9.2 Iterative identification and control design	72
9.3 Cost \mathcal{T}_i of interval i	73
9.4 Optimal experiment design problem	74
9.5 Conclusions	75
10 Identification and control of inkjet printheads	77
10.1 Problem statement	77
10.2 Modeling the inkjet printhead	79
10.3 Model-based design of the actuation procedure	81
10.4 Experimental results	84
10.5 Conclusions	85
11 Informative data and network identification	89
11.1 Introduction	89
11.2 How to get a sufficiently rich excitation signal?	89
11.3 Identification of a particular system in a complex network	90

<i>CONTENTS</i>	5
12 Other research projects	93
13 Conclusions	95

Part I

Curriculum et bilan des activités

Chapter 1

Curriculum Vitae

1.1 Renseignements généraux

Date et lieu de naissance : 16 octobre 1974 à Bruxelles, Belgique

Fonction actuelle: Professeur Assistant (maître de conférences) à la TU Delft
(Delft University of Technology)

Adresse professionnelle : Delft Center for Systems and Control, Delft University of Technology
Mekelweg 2
NL-2628 CD Delft
Pays-Bas
Internet: <http://www.dsc.tudelft.nl>

Téléphone : 00.31.15.278.51.50

E-mail : x.j.a.bombois@tudelft.nl

Page WEB : www.dsc.tudelft.nl/~xbombois

1.2 Formation

- **1997-2000:** Doctorat de troisième cycle, Grade de Docteur en Sciences Appliquées de l'Université Catholique de Louvain (Belgique) obtenu le 14 novembre 2000, après soutenance de la Thèse intitulée :

*Connecting Prediction Error Identification and Robust Control Analysis:
a new framework*

Directeur de thèse : Michel Gevers

Membres du jury: Michel Gevers, Lennart Ljung, Paul Van den Hof,
Gérard Scorletti, Georges Bastin et Vincent Blondel.

- **1992-1997:** Diplôme d'Ingénieur Civil Electricien de l'Université Catholique de Louvain (Belgique).

1.3 Expérience professionnelle

- **Mai 2001 – ... :** Professeur Assistant (maître de conférences) au *Delft Center for Systems and Control*, Delft University of Technology, Delft, Pays-Bas
- **Novembre 2000 – Avril 2001:** Assistant de recherche (post-doctorat), *Signals, Systems and Control Group*, Delft University of Technology, Delft, Pays-Bas
- **Septembre 1997 – Octobre 2000:** Assistant (doctorant), CESAME, Université Catholique de Louvain, Louvain-la-Neuve, Belgique

1.4 Connaissance des langues

- Français: langue maternelle
- Anglais: langue de travail et d'enseignement; niveau C2 (le plus haut niveau) dans le cadre européen commun de référence pour les langues
- Néerlandais: langue de travail et d'enseignement

1.5 Formations complémentaires

- *Active and Collaborative learning (2004)*. Faculty of Technology, Policy and Management, TU Delft. Charge horaire: 70 heures
- *Coaching leadership (2011)*. DORFL leadership training. Charge horaire: 40 heures
- *English Pronunciation Workshop (2011)*. Faculty of Technology, Policy and Management, TU Delft. Charge horaire: 14 heures

Chapter 2

Activités d'enseignement

2.1 Aperçu général

Depuis le début de mon activité d'enseignement en octobre 1997, j'ai eu la chance d'enseigner sur des sujets assez différents (électronique, mécanique, mécatronique, analyse du signal, identification des systèmes, automatique) et pour une large diversité de publics:

- étudiants en science de l'Ingénieur au niveau licence (Bachelor of Science)
- étudiants en science de l'Ingénieur au niveau maîtrise (Master of Science)
- doctorants et chercheurs.

Mes tâches d'enseignements m'ont permis de donner des cours magistraux, des séances de travaux dirigés et pratiques, d'encadrer des élèves en projets de laboratoire et d'encadrer des travaux de fin d'étude. Elle m'a aussi permis de bâtir des cours, des sujets d'examen, de mettre au point des travaux dirigés et pratiques. De façon plus générale, j'ai pris part à l'organisation de l'enseignement sous ses différentes formes : organisation matérielle, discussions sur le contenu des cours, suivi et évaluation des élèves.

J'enseigne pour le moment en anglais et en néerlandais, mais j'ai aussi enseigné en français de 1997 à 2000.

Le volume annuel de mes activités d'enseignement s'élève actuellement à environ 50 heures de cours magistraux, quatre heures de travaux dirigés et 150 heures environ pour l'encadrement d'étudiants (travaux de fin d'études,...). Si l'on fait le bilan depuis 1997, j'estime avoir donné environ 350 heures de cours magistraux et 600 heures de travaux dirigés et pratiques. Le temps passé à l'encadrement de travaux de fin d'études peut être évalué à environ 1500 heures.

2.2 Détail des activités

2.2.1 Activités à la TU Delft

La TU Delft est la plus importante "Ecole d'Ingénieurs" néerlandaise avec ses 17000 étudiants. Je donne mes enseignements dans la faculté de mécanique qui

est une des plus grandes de la TU Delft.

- *Sc4110 Identification des systèmes (2002-...)*. Je suis le titulaire de ce cours de maîtrise (bac+4) ayant une charge de cinq ECTS et qui est suivi par une trentaine d'étudiants chaque année. Ce cours comporte 13 cours magistraux, cinq séances de travaux dirigés (en salle et sur ordinateur) et est achevé à la fois par un projet que les étudiants doivent réaliser en laboratoire et par un examen oral. J'ai complètement renouvelé ce cours à partir de celui que donnait Paul van den Hof auparavant. Ma philosophie a été de présenter une méthode systématique pour aborder le problème d'identification (càd déduire un modèle mathématique d'un système physique à partir de mesures entrée-sortie). Cette méthode systématique considère les différents choix que l'on doit effectuer dans la procédure d'identification (choix du signal d'excitation, choix de l'ordre du modèle) et leur influence sur la qualité du modèle identifié. Les transparents du cours sont disponibles à l'adresse internet suivante:
<http://www.dcsc.tudelft.nl/~xbombois/sc4110slides.pdf>
- *WBTP211 Mécatronique (2009-...)*: Je suis le responsable de ce cours/projet de licence (bac+2) ayant une charge de 10 ECTS et qui est suivi par 300 étudiants chaque année. Ce cours comporte 11 cours magistraux, 40 heures de travaux pratiques en laboratoire et un projet final consistant à construire un système mécatronique (système de distribution automatisé). En tant que responsable de ce cours, je m'occupe de l'organisation générale et dirige l'équipe pédagogique qui compte quatre enseignants et neuf assistants. Je suis aussi responsable de la moitié des cours magistraux¹. Ces cours magistraux portent sur l'électronique (analyse des circuits, amplificateur opérationnel, synthèse de filtres passifs et actifs) et sur le moteur électrique à courant continu. J'ai fortement renouvelé la manière d'enseigner cette partie du cours (qui lui existe depuis une dizaine d'années).
- *Encadrement de mémoires de fin d'études (2004-...)*. Depuis 2004, j'ai encadré une trentaine de travaux de fin d'études (TFE). Ce travail de fin d'études couvre la totalité de la deuxième année de maîtrise (bac+5) et consiste en une étude bibliographique (15 ECTS) et en un travail de recherche sur un sujet donné (45 ECTS). Parmi ces TFEs, la moitié a été effectuée en collaboration avec différentes entreprises (Shell, British Petroleum, NEM, OCE, Laborelec, Philips,...) et l'autre moitié sur des sujets plus théoriques. Une liste est disponible à l'adresse internet suivante:
<http://www.dcsc.tudelft.nl/~xbombois/research.html>
- *WB3250 Analyse du signal (2005-2009)*. Paul Van den Hof et moi avons monté ce cours de licence (bac+3) ayant une charge de 3 ECTS et qui est suivi par 300 étudiants chaque année. Je me suis plus particulièrement occupé du développement d'une série d'exercices (travaux dirigés) qui sont rassemblés dans un document de 130 pages. Ce document est disponible à

¹Le cours doit être donné deux fois par an vu le nombre d'étudiants.

l'adresse internet suivante: <http://www.dsc.tudelft.nl/~xbombois/SR3exercises.pdf>.

Jusqu'en 2009, je donnais les sept séances de travaux dirigés de ce cours et j'étais responsable de l'examen écrit. Depuis lors, le cours est donné par d'autres enseignants, mais le matériel de cours est resté inchangé.

- *Sc4140ap Automatique (2002-2005)*: J'ai développé et encadré le projet en laboratoire qui terminait ce cours de quatrième année (bac+4). Ce projet consistait en la synthèse et l'application de deux régulateurs pour une manipulation à disques tournants.

2.2.2 Activités dans le cadre de l'Ecole doctorale hollandaise en Automatique (DISC)

Depuis 2002, j'assure avec Paul Van den Hof le cours *System Identification for Control* de l'école doctorale hollandaise en Automatique (DISC). Ce cours, qui consiste en 8 séances de 2 heures partagées entre Paul Van den Hof et moi-même (quatre séances chacun), est destiné aux doctorants en automatique des différentes universités hollandaises. Il a pour objectif de fournir à ces doctorants les bases en identification pour la commande nécessaires à leur travail de recherche. La réussite de ce cours requiert l'accomplissement de trois séries d'exercices. L'adresse du site internet de ce cours est <http://www.dsc.tudelft.nl/~discsysid>. En 2003 et 2011, à la demande des responsables de l'équivalent belge du DISC, nous avons également assuré ce cours pour les doctorants belges.

2.2.3 Activités à l'Université Catholique de Louvain

En ma qualité d'assistant à la Faculté des Sciences Appliqués (Sciences de l'Ingénieur), j'ai assuré, de 1997 à 2000, des séances de travaux dirigés et/ou pratiques pour les cours de Mécanique et d'Analyse des Circuits Electriques. Le cours de Mécanique s'adressait à des étudiants en deuxième année (bac+2) et le cours d'Analyse des Circuits Electriques à des étudiants en troisième année, spécialisation Electricité (bac+3). Le volume horaire annuel pour le cours de Mécanique était de 90 heures et pour celui d'Analyse des Circuits de 35 heures.

Chapter 3

Activités de recherche

3.1 Aperçu général

J'effectue, depuis 2001, ma recherche au sein du *Delft Center for Systems and Control* (DCSC) en tant que professeur assistant (contrat à durée indéterminée). Le Delft Center for Systems and Control est un groupe fort de treize académiques et d'une cinquantaine de doctorants et de postdocs. Ce laboratoire a pour vocation de concentrer, dans la faculté de mécanique, la recherche en automatique de toute la TU Delft aussi bien au niveau théorique qu'au niveau des applications (industrie des procédés, systèmes mécatroniques, robotique, ...).

Depuis le début de ma carrière académique, je suis parvenu à devenir un expert reconnu dans le domaine de l'identification pour la commande robuste et la synthèse de l'expérience d'identification. J'ai initié et développé une ligne de recherche originale et cohérente à la frontière de différents domaines, ce qui a permis la publication de 22 articles de journal dans les meilleures revues en automatique. J'ai établi, dans ce cadre, des collaborations de longue durée avec certains des principaux chercheurs en automatique (Prof. Gevers, Scroletti, Hjalmarsson, Van den Hof et Anderson). J'ai également travaillé en tant que chercheur invité dans de nombreuses universités à travers le monde (KTH Stockholm, Australian National University, Université Catholique de Louvain et Ecole Centrale de Lyon,...).

Mes idées de recherche sont à l'origine du projet *Autoprofit*, un projet européen EU-FP7 STREP (2010-2013). Celui-ci a un budget de 2,5 millions d'euros et regroupe différents partenaires académiques (TU Delft, TU Eindhoven, KTH Stockholm, RWTH Aachen) et industriels (ABB, SASOL, Boliden). En plus d'avoir initié ce projet par mes idées de recherche, j'ai également participé à son élaboration avec P. Van den Hof et J. Ludlage et je suis le responsable d'un de ses modules de travail (work package leader). La coordination scientifique de l'ensemble du projet est réalisée par Prof. Van den Hof.

J'encadre pour le moment trois doctorants. J'ai également encadré dans le passé deux autres doctorants ainsi qu'un Postdoc. Ces thèses et ce postdoctorat portent sur des sujets à la fois théoriques et pratiques.

Finalement, je suis éditeur associé pour le journal *Control Engineering Practice* et pour le *Conference Editorial Board of the IEEE Control Society*.

Mes différentes contributions en recherche seront détaillées dans le chapitre 5. Dans ce chapitre, nous nous limiterons aux activités proprement dites.

3.2 Encadrement de thèses de doctorat

Cette section est composée de deux parties: une partie concernant les thèses que j'ai encadré dans le passé et une autre pour les thèses qui sont encore en cours. Il est important de noter que, comme c'est aussi le cas en France, un professeur assistant aux Pays-Bas n'a pas le droit d'être promoteur d'une thèse de doctorat. Il a cependant la possibilité d'être encadrant (daily supervisor) et, depuis quelques années, co-promoteur. La décision de nommer l'encadrant journalier comme co-promoteur se fait généralement à la fin de la thèse.

Thèses achevées

- Robert Bos, *Monitoring of industrial processes using large-scale first-principles models*. Thèse soutenue le 21 décembre 2006. J'étais l'encadrant de cette thèse dont Paul van den Hof était le promoteur. Cette thèse a été réalisée avec le soutien de l'institut de recherche TNO-TPD. Voir aussi les publications J.11, C.17, C.18 et C.23.¹ Robert Bos travaille chez Shell en tant que *reservoir engineer* depuis la fin de son doctorat.
- Amol Khalate, *Model-based feedforward control for inkjet printheads*. Thèse soutenue le 17 décembre 2013. Je suis le co-promoteur de cette thèse dont Robert Babuska est le promoteur. Cette thèse a été réalisée dans le cadre du projet *Octopus* avec le soutien de Senter Novem, de l'entreprise Océ et de l'*Embedded Systems Institute (ESI)*. Voir aussi les publications J.16, J.19, J.20, L.05, C.37, C.40, C.41, C.43 et C.45. Amol Khalate travaille chez Océ en tant que *hardware designer* depuis la fin de son contrat à la TU Delft.

J'ai aussi encadré Märta Barentin Syberg, une doctorante de H. Hjalmarsson à la KTH, lors de sa visite de trois mois à Delft en 2006. Des résultats de cette visite, Märta a tiré un chapitre de sa thèse intitulée *Complexity issues, validation and input design for control in system identification* (KTH, Stockholm, 2008). Ce chapitre a été également publié sous la forme d'un article de journal (article J.09).

Thèses que j'encadre pour le moment.

- Marco Forgone, *Batch-to-batch model learning for control in process systems with application to cooling crystallization*. Je suis le co-promoteur de cette thèse de doctorat qui est dans sa phase de rédaction et devrait être

¹La liste de mes publications est donnée au Chapitre 4.

soutenue mi-2014. Cette thèse est réalisée avec le soutien de l'*Institute for Sustainable Process Technology (ISPT)*. Voir les articles S.01, C.48, C.54, C.57 et CS.03.

- Skander Tamaallah, *Automatic autorotation of a rotorcraft Unmanned Aerial Vehicle (UAV)*. Je suis l'encadrant de cette thèse de doctorat qui devrait se terminer fin 2014. La thèse de Skander, ingénieur au NLR (Dutch Aerospace Laboratory) est réalisée avec le soutien de son employeur. Voir les articles C.47 et C.60.
- Max Potters, *Optimal identification experiment design for closed-loop systems operated with Model Predictive Control*. Je suis l'encadrant de cette thèse de doctorat qui devrait se terminer début 2016. Cette thèse est réalisée dans le cadre du projet *Autoprofit* avec le soutien de la Commission Européenne (EU-FP7). Voir l'article CS.02 et le livrable D.03.

Paul Van den Hof est le promoteur des trois thèses ci-dessus. Je participe aussi à l'encadrement d'Arne Dankers, un doctorant dont Paul est l'encadrant principal. La thèse d'Arne (*Identification of dynamic models in complex networks with prediction error identification*) est dans sa phase de rédaction et devrait être soutenue mi-2014. Voir les publications J.21, C.46, C.51, C.55, C.56 et S.03.

J'encadre également Vedran Peric, un doctorant de L. Vanfretti à la KTH, durant la visite de neuf mois (octobre 2013-juin 2014) qu'il effectue à Delft. Son sujet de thèse est l'identification des oscillations dans les réseaux électriques.

3.3 Encadrement d'un postdoctorat

Pendant un période de deux ans (2010-2012), j'ai encadré Ali Mesbah durant son postdoctorat à la TU Delft. Ce postdoctorat a été réalisé dans le cadre du projet *Autoprofit* avec le soutien de la Commission Européenne (EU-FP7). Le sujet de recherche était *Least costly performance diagnosis and plant re-identification* et a conduit aux articles S.02, C.44, C.49, C.53, CS.01 et aux livrables D.01, D.02 et D.04. Ali Mesbah travaille au MIT en tant que *senior postdoctoral associate* depuis la fin de son postdoctorat à la TU Delft.

3.4 Gestion de projets de recherche

3.4.1 Projet européen EU-FP7 STREP "Autoprofit" (2010-2013)

Mes contributions sur la synthèse d'expériences d'identification faiblement perturbatrices (voir Chapitre 5) et mon intention de les utiliser en vue d'améliorer la maintenance des systèmes de commande des procédés industriels sont à l'origine du projet européen *Autoprofit*. Le nom complet de ce projet est *Advanced Autonomous Model-Based Operation of Industrial Process Systems* (grant agreement number: 257059). Celui-ci a un budget de 2,5 millions d'euros et regroupe différents partenaires académiques (TU Delft, TU Eindhoven, KTH Stockholm, RWTH Aachen) et industriels (ABB, SASOL, Boliden). En plus d'avoir initié

ce projet par mes idées de recherche, j'ai également participé à son élaboration avec P. Van den Hof et J. Ludlage et je suis le responsable d'un de ses modules de travail (work package leader). La coordination scientifique de l'ensemble du projet est réalisée par Prof. Van den Hof.

En tant que responsable du quatrième module de travail (WP4) de ce projet,

- je suis responsable de l'animation de l'équipe de chercheurs impliqués dans ce module de travail. Cette équipe comprend les membres de trois partenaires du projet (ABB, KTH et TU Delft)
- je suis également responsable de la qualité scientifique des livrables liés à ce module de travail. Voir D.01, D.02, D.03 et D.04.
- je suis le représentant du module de travail aux réunions semestrielles du projet.
- je suis responsable de la rédaction du rapport annuel sur l'avancement des travaux de ce module de travail et chargé de la présentation sur cet avancement lors des réunions annuelles d'évaluation du projet à la Commission Européenne à Bruxelles. Les évaluateurs nommés par la Commission Européenne ont particulièrement apprécié nos résultats dans leur dernier rapport (novembre 2012):

“WP4 has progressed exceptionally well. Methods have been proposed which have been validated on the two benchmark problems, and corresponding software has been developed. This WP has exhibited very good collaboration between the academic and industrial partners (in particular TUD, KTH and ABB), also good liaison with WP3, and several papers have been written.”

A côté de mon rôle de *work package leader*,

- je suis membre du comité de pilotage (steering committee) du projet
- j'anime les activités de recherche de la TU Delft dans ce projet. Ces activités sont concentrées principalement sur deux modules de travail (WP3 et WP4)
- je gère avec P. Van den Hof le budget alloué à la TU Delft pour ce projet (540 kilo-euros)
- j'ai organisé la procédure de recrutement des deux jeunes chercheurs (Ali Mesbah et Max Potters) que l'on a pu engager (temporairement) pour ce projet

3.4.2 Projet “Octopus” - Smart System Adaptability (2007-2012)

Le projet Octopus a regroupé un consortium composé d'un partenaire industriel *Océ Technologies* et différents partenaires académiques (TU Delft, TU

Eindhoven, l'Université de Nijmegen et l'Université de Twente); l'institut de recherche *Embedded Systems Institute (ESI)* ayant la responsabilité de la gestion du projet. Ce projet a été partiellement financé par Senter Novem (Ministère néerlandais des Affaires Economiques) dans le cadre du programme Bsik (projet P90600).

Le budget alloué à l'équipe du *Delft Center for Systems and Control* dans ce projet était de 220 kilo-euros. Cette équipe était composée de Prof. Babuska et de moi-même ainsi que d'un doctorant (Amol Khalate) engagé dans le cadre de ce projet. Mon rôle dans ce projet a été

- d'organiser la procédure de recrutement de ce doctorant
- d'animer les activités de recherche de notre équipe au sein de ce projet multi-disciplinaire.
- de représenter notre équipe lors des réunions des partenaires de ce projet. Robert Babuska et moi-même nous rendions alternativement à ces réunions.

Les résultats du module de travail dans lequel nous avons travaillé avec l'équipe de la TU Eindhoven ont été particulièrement appréciés par notre partenaire industriel. En effet, on peut lire dans les minutes de la réunion finale du projet:

“Océ is very happy with the results achieved in inkjet print head control. This research line is very successful; the results can be picked up on short term, very nice!”.

Notre doctorant a d'ailleurs été le seul doctorant à avoir été engagé par Océ au terme du projet.

3.4.3 Projet “Automatic autorotation of a rotorcraft Unmanned Aerial Vehicle (UAV)” (2006-2014)

Ce projet est un projet de collaboration entre le *NLR (Dutch Aerospace Laboratory)* et le *Delft Center for Systems and Control*. Dans ce projet, le *NLR* finance la thèse de doctorat d'un de ses ingénieurs (Skander Taamallah); thèse de doctorat qu'il effectue à mi-temps tout en continuant une partie de ses activités au *NLR*. Je suis responsable de l'animation scientifique de ce projet ainsi que du budget alloué par le *NLR* pour l'encadrement de Skander (50 kilo-euros).

3.4.4 Batch Crystallization Control for Pharmaceutical Manufacturing (2007-2013).

Bien qu'étant principalement responsable depuis 2011 de l'encadrement du doctorant (Marco Forgione) de notre groupe travaillant dans ce projet, j'ai également participé aux réunions des partenaires de ce projet depuis ce moment. Ce projet regroupe un consortium de partenaires industriels (Albemarle, Bruker Optics, DSM, Friesland Campina, IPCOS, MSD, Perdix Analytical Systems et Zeton) et de deux partenaires académiques (TU Delft et TU Eindhoven). Ce

projet a un budget total de 2,4 millions d'euros (dont 240 kilo-euros pour le doctorat de Marco Forgione) et est réalisé avec le soutien de l'*Institute for Sustainable Process Technology (ISPT)*.

3.5 Collaborations nationales et internationales

J'ai eu la chance de pouvoir travailler et publier des articles avec un cinquantaine de chercheurs différents. Dans la liste suivante, je me limite cependant aux collaborations principales.

1. G. Scorletti, professeur à l'Ecole Centrale de Lyon, sur les aspects de l'analyse de la robustesse. Voir les articles J.01 à J.04, J.07, J.09, J.13, J.18 et J.19.
2. M. Gevers, professeur à l'Université Catholique de Louvain, sur différents aspects de l'identification des systèmes (identifiabilité, identification pour la commande, ...). Voir les articles J.01 à J.04, J.07, J.12, J.15 et J.17.
3. H. Hjalmarsson, professeur à la KTH Stockholm, sur la synthèse optimale de l'expérience d'identification. Voir les articles J.09, J.13, J.22 et S.02.
4. P.M.J. Van den Hof, professeur à la TU Delft et à la TU Eindhoven, sur différents aspects de l'identification des systèmes (identification des réseaux, synthèse optimale de l'expérience d'identification). Voir les articles J.07, J.08, J.11, J.21, S.01, S.02 et S.03.
5. B.D.O. Anderson, professeur à l'Australian National University, sur l'identification pour la commande et la commande H_∞ . Voir les articles J.02 à J.06 et J.10.
6. P. Heuberger, professeur assistant à la TU Eindhoven, sur l'identification de modèles dynamiques dans les réseaux complexes. Voir les articles J.21 et S.03.
7. A. Bazanella, professeur associé à l'Université de Porto-Alegre, sur les problèmes d'identifiabilité. Voir les articles J.12 et J.17.
8. R. Babuska, professeur à la TU Delft, sur la commande et l'identification des systèmes d'impression. Voir les articles J.16, J.19 et J.20.
9. P-J. van Overloop, professeur assistant à la TU Delft, sur l'identification des canaux d'irrigation. Voir les articles J.14 et C.52.
10. A. Lanzon, professeur à l'Université de Manchester, sur la commande H_∞ . Voir les articles J.05 et J.10.

3.6 Séjours en laboratoire

- à la KTH (Stockholm, Suède), invité par H. Hjalmarsson: nombreux séjours d'une semaine ou deux ainsi qu'un séjour d'un mois en 2007

- à l’Australian National University (Canberra, Australie), invité par B.D.O. Anderson: deux séjours d’un mois en 2001 et 2002 et dix jours en 2006
- à l’Université de Caen et à l’Ecole Centrale de Lyon, invité par G. Scorletti: nombreux séjours d’une ou deux semaines. En mai 2014, je ferai un séjour d’un mois en tant que *professeur invité* à l’Ecole Centrale de Lyon.
- à l’Université Catholique de Louvain (Belgique), invité par M. Gevers: nombreux séjours d’une ou deux semaines
- à l’Université de Linköping (Suède), invité par L. Ljung: deux mois en 2001
- à l’Université de Cambridge (Royaume-Uni), invité par G. Vinnicombe: une semaine en 2000
- à l’Université de Lorraine, invité par M. Gilson: une semaine en 2005

3.7 Activités éditoriales

- Editeur associé pour le journal IFAC *Control Engineering Practice* depuis 2012
- Editeur associé depuis 2012 pour le *Conference Editorial Board of the IEEE Control Society* qui organise la *Conference on Decision and Control (CDC)* et l’*American Control Conference (ACC)*
- Membre du comité international de programmation pour les conférences suivantes:
 - Mathematical Theory of Networks and Systems (MTNS) en 2004
 - IFAC Symposium on System Identification (SYSID) en 2012
 - European Control Conference (ECC) en 2013
- Co-président du programme (*program co-chair*) du prochain workshop annuel de l’ERNSI (European Network on System Identification) à Ostende (Belgique), septembre 2014

3.8 Participation à des jurys de thèse de doctorat

- pour la thèse de Robert Bos à la TU Delft en 2006
- pour la thèse de Jonas Mårtensson à la KTH Stockholm en 2007
- pour la thèse de Jakob Kjøbsted Huusom à la Technical University of Denmark en 2008
- pour la thèse d’Amol Khalate à la TU Delft en décembre 2013

3.9 Autres activités académiques

- Présentation plénière intitulée *Design of optimal identification experiments for control*, donnée aux 3èmes Journées Identification et Modélisation Expérimentale (JIME) à Douai en 2011. L'article J.18 est l'article de journal qui a été tiré de cette présentation plénière.
- Membre de deux comités de sélection pour un maître de conférence à l'Ecole Centrale de Lyon en 2010 et 2012
- Lecteur pour les journaux Automatica, IEEE Transactions on Automatic Control, Control Engineering Practice, Journal of Process Control, International Journal of Adaptive Control and Signal Processing
- *Outstanding reviewer* pour Automatica en 2001
- Organisateur des colloques hebdomadaires de mon laboratoire en 2012
- Mon directeur de thèse (M. Gevers) a utilisé les résultats de ma recherche pour sa présentation plénière à la 44th IEEE Conference on Decision and Control (2005).
- Arne Dankers (voir section 3.2) a obtenu le "Best Junior Paper Award" à la 12th European Control Conference (2013) pour le papier C.59
- (Co-)organisateur de deux sessions invitées au 16th IFAC Symposium on System Identification (2012) et d'un mini-symposium au 16th International Symposium on Mathematical Theory of Networks and Systems (2004)
- Membre du comité d'organisation locale du workshop annuel de l'ERNSI (European Network on System Identification) à Maastricht (Pays-Bas) en 2011 (60 participants)
- Membre du comité d'organisation du symposium *Systems and Control: Challenges for the 21st Century* à Delft en juin 2004 (151 participants).

Chapter 4

Travaux et publications

Un grand nombre de mes publications sont disponibles à l'adresse internet suivante: www.dsc.tudelft.nl/~xbombois/pub.html

Mémoire de thèse

- T.01** X. Bombois. *Connecting Prediction Error Identification and Robust Control Analysis: a new framework*. Université Catholique de Louvain (Belgique), 163 pages, novembre 2000.

Articles de journal, publiés ou acceptés

- J.01** X. Bombois, M. Gevers et G. Scorletti, "A measure of robust stability for a set of parametrized transfer functions", *IEEE Transactions on Automatic Control*, Vol. 45(11), pages 2141-2145, 2000.
- J.02** X. Bombois, M. Gevers, G. Scorletti et B.D.O. Anderson, "Robustness analysis tools for an uncertainty set obtained by prediction error identification", *Automatica*, Vol. 37(10), pages 1629-1636, 2001.
- J.03** M. Gevers, X. Bombois, B. Codrons, G. Scorletti et B.D.O. Anderson, "Model validation for control and controller validation in a prediction error identification approach - Part I : theory", *Automatica* Vol. 39(3), pages 403-415, 2003.
- J.04** M. Gevers, X. Bombois, B. Codrons, G. Scorletti et B.D.O. Anderson, "Model validation for control and controller validation in a prediction error identification approach - Part II : illustrations", *Automatica* Vol. 39(3), pages 417-427, 2003.
- J.05** A. Lanzon, B.D.O. Anderson et X. Bombois, "Selection of a single uniquely specifiable Hinf controller in the chain-scattering framework", *Automatica*, Vol. 40(6), pages 985-994, 2004.

- J.06** X. Bombois, B.D.O. Anderson and M. Gevers, "Quantification of frequency domain error bounds with guaranteed confidence level in Prediction Error Identification", *Systems and Control Letters*, Vol. 54(5), pp. 471-482, 2005.
- J.07** X. Bombois, G. Scorletti, M. Gevers, P. Van den Hof and R. Hildebrand, "Least costly identification experiment for control", *Automatica*, Vol. 42(10), pp. 1651-1662, 2006.
- J.08** S. Douma, X. Bombois and P. Van den Hof, "Validity of the standard cross-correlation test for model structure validation", *Automatica*, Vol. 44(5), pp. 1285-1294, 2008.
- J.09** M. Barenthin, X. Bombois, H. Hjalmarsson and G. Scorletti, "Identification for control of multivariable systems: controller validation and experiment design via LMIs", *Automatica*, Vol. 44(12), pp. 3070-3078, 2008.
- J.10** B.D.O. Anderson, A. Lanzon, A. Dehghani and X. Bombois, , "Quantitative effects of weight adjustments in H-infinity control", *Optimal Control, Applications and Methods*, Vol. 30, pp. 267-286, 2009.
- J.11** R. Bos, X. Bombois and P. Van den Hof, "Accelerating simulations of computationally intensive first principle models using accurate quasi linear parameter varying models", *Journal of Process Control*, Vol. 19, pp. 1601-1609, 2009.
- J.12** M. Gevers, A.S. Bazanella, X. Bombois and L. Miskovic, "Identification and the information matrix: how to get just sufficiently rich", *IEEE Transactions on Automatic Control*, Vol. 54(12), pp. 2828-2840, 2009.
- J.13** X. Bombois, H. Hjalmarsson and G. Scorletti, "Identification for robust H2 deconvolution filtering", *Automatica*, Vol 46(3), pp. 577-584, 2010.
- J.14** P.J. van Overloop, I.J. Miltenburg, X. Bombois, A.J. Clemmens, R.J. Strand, N.C. van de Giesen and R. Hut, "Identification of resonance waves in open water channels", *Control Engineering Practice*, Vol. 18, pp. 863-872, 2010.
- J.15** M. Gevers, X. Bombois, R. Hildebrand and G. Solari, "Optimal experiment design for open and closed-loop system identification", *Communications in Information and Systems*, Vol 11(3), pp. 197-224, 2011.
- J.16** A. Khalate, X. Bombois, R. Babuska, H. Wijshoff and R. Waarsing, "Performance improvement of a drop-on-demand inkjet printhead using an optimization-based feedforward control method", *Control Engineering Practice*, Vol. 19, pp. 771-781, 2011.
- J.17** A.S. Bazanella, X. Bombois and M. Gevers, "Necessary and sufficient conditions for uniqueness of the minimum in prediction error identification", *Automatica*, Vol. 48(8), pp. 1621-1630, 2012.

- J.18** X. Bombois and G. Scorletti, “Design of least costly identification experiments - the main philosophy accompanied by illustrative examples”, *Journal Européen des Systèmes Automatisés*, Vol 46(6-7), pp. 587-610, 2012.
- J.19** A.A. Khalate, X. Bombois, G. Scorletti, R. Babuska, S. Koekebakker, W. de Zeeuw, “A waveform design method for a piezo inkjet printhead based on robust feedforward control”, *IEEE/ASME Journal of Microelectromechanical Systems*, Vol 21(6), pp. 1365-1374, 2012.
- J.20** A.A. Khalate, X. Bombois, S. Ye, R. Babuska and S. Koekebakker, “Minimization of cross-talk in a piezo inkjet printhead based on system identification and feedforward control”, *Journal of Micromechanics and Microengineering*, Vol 22(11), paper 115035 (21 pages), 2012
- J.21** P. Van den Hof, A. Dankers, P. Heuberger, X. Bombois, “Identification of Dynamic Models in Complex Networks with Prediction Error Methods - Basic Methods for Consistent Module Estimates”, *Automatica*, Vol. 49(10), pp. 2994-3006, 2013.
- J.22** D. Katselis, C. Rojas, M. Bengtsson, E. Bjornson, X. Bombois, N. Shariati, M. Jansson and H. Hjalmarsson, “Training Sequence Design for MIMO Channels: An Application-Oriented Approach”, accepté en octobre 2013 en vue d’une publication dans *EURASIP Journal on Wireless Communications and Networking*

Articles de journal, soumis

- S.01** M. Forgone, X. Bombois and P. Van den Hof, “Optimal data-driven model improvement for model-based control”, soumis à *Automatica*, mai 2013
- S.02** A. Mesbah, X. Bombois, J. Ludlage, H. Hjalmarsson, M. Forgone, P. Van den Hof, “Least Costly Closed-loop Performance Diagnosis and Plant Re-identification” soumis à *Journal of Process Control*, juin 2013
- S.03** A. Dankers, P. Van den Hof, X. Bombois, P. Heuberger, “Identification of Dynamic Models in Complex Networks with Prediction Error Methods - Predictor Input Selection”, soumis à *IEEE Transactions on Automatic Control*, octobre 2013

Chapitres de livre

- L.01** M. Gevers, X. Bombois, B. Codrons, F. De Bruyne et G. Scorletti, *The Role of Experimental Conditions in Model Validation for Control*, dans “Robustness in Identification and Control”, A. Garulli, A. Tesi and A. Vicino eds., *Lecture Notes in Control and Information Sciences*, Vol.245, Springer Verlag, 1999, pages 72-86 (15 pages).

- L.02** X. Bombois, B.D.O. Anderson et M. Gevers , *Mapping parametric confidence ellipsoids to Nyquist plane for linearly parametrized transfer functions*, dans "Model Identification and Adaptive Control", G.C. Goodwin ed., Springer Verlag, 2000, pages 53-71 (18 pages).
- L.03** B.D.O. Anderson and X. Bombois, *Analysis of weight change in H_∞ control design*, dans "Control and Modeling of Complex Systems: Cybernetics in the 21st Century", K. Hashimoto, Y. Oishi and Y. Yamamoto eds., Birkhauser Boston Inc., 2002, pages 113-130 (18 pages).
- L.04** M. Gevers, X. Bombois, G. Scorletti, P. Van den Hof and R. Hildebrand, *Experiment design for robust control: why do more work than is needed?*, dans "Control of Uncertain Systems: Modelling, Approximation and Design", B. Francis and J.C. Willems Eds., Springer Verlag, Lecture Notes in Control and Information Sciences, Volume 329, 2006, pp. 139 - 162 (24 pages).
- L.05** S. Koekebakker, M. Ezzeldin, A. Khalate, R. Babuska, X. Bombois, P. van den Bosch, G. Scorletti, S. Weiland, H. Wijshoff, R. Waarsing, W. de Zeeuw, *Piezo printhead control: jetting any drop at any time*, dans "Model-based design of adaptive embedded systems", T. Basten, R. Hamberg, F. Reckers et J. Verriet Eds, Springer, 2013, pp. 41 - 85 (45 pages).

Articles de conférence, avec comité de lecture

Les articles C.03, C.04, C.06, C.19, C.20, C.22, C.25, C.39, C.42, C.49, C.50 et C.52 ont été présentés dans des sessions invitées.

- C.01** B.D.O. Anderson, X. Bombois, M. Gevers and K. Kulcsar, "Caution in iterative modelling and control design", IFAC Workshop on Adaptive Control and Signal Processing, Glasgow, pp. 13-19, 1998.
- C.02** X. Bombois, M. Gevers and G. Scorletti, "Controller Validation for a Validated Model Set", 5th European Control Conference, paper 869 (CD-ROM), Karlsruhe, 1999.
- C.03** X. Bombois, M. Gevers and G. Scorletti, "Controller Validation based on an identified model", 38th IEEE Conference on Decision and Control, pp. 2816-2821, Phoenix, Arizona, 1999.
- C.04** M. Gevers, X. Bombois, B. Codrons, G. Scorletti and F. De Bruyne , "Model validation for robust control and controller validation in a prediction error framework", 12th IFAC Symposium on System Identification, paper WeAM1-1 (CD-ROM), Santa Barbara, California, 2000.
- C.05** X. Bombois, M. Gevers, G. Scorletti and B.D.O. Anderson , "Controller Validation for Stability and for Performance based on an uncertainty region designed from an identified model", 12th IFAC Symposium on System Identification, paper WePM1-6 (CD-ROM), Santa Barbara, California, 2000.

- C.06** X. Bombois, M. Gevers and G. Scorletti , "Controller Validation for Stability and for Performance based on a frequency domain uncertainty region designed with stochastic embedding", 39th IEEE Conference on Decision and Control, paper TuM06-5 (CD-ROM), Sydney, Australia, 2000.
- C.07** B. Codrons, X. Bombois, M. Gevers and G. Scorletti, "A practical application of recent results in model and controller validation to a ferrosilicon production process", 39th IEEE Conference on Decision and Control, paper WeP07-6 (CD-ROM), Sydney, Australia, 2000.
- C.08** X. Bombois, B.D.O. Anderson and M. Gevers , "Frequency domain image of a set of linearly parametrized transfer functions", 6th European Control Conference, paper WeA07-1, pp. 1416-1421, Porto, 2001.
- C.09** X. Bombois, G. Scorletti, B.D.O. Anderson, M. Gevers and P. Van den Hof, "A new robust control design procedure based on a PE identification uncertainty set", 15th IFAC World Congress, Barcelona, 2002.
- C.10** X. Bombois and B.D.O. Anderson, "On the influence of weight modification in Hinf control design", 41th IEEE Conference on Decision and Control, Las Vegas, 2002.
- C.11** A. Lanzon, B.D.O. Anderson and X. Bombois, "On uniqueness of central H-infinity controllers in the chain-scattering framework", 4th IFAC Symposium on Robust Control Design, Milano, 2003.
- C.12** X. Bombois and Paresh Date , "Connecting PE Identification and robust control theory: the multiple-input single-output case. Part I: Uncertainty region validation", 13th IFAC Symposium on System Identification, paper WeA01-02, Rotterdam, 2003.
- C.13** X. Bombois and Paresh Date , "Connecting PE Identification and robust control theory: the multiple-input single-output case. Part II: Controller validation", 13th IFAC Symposium on System Identification, paper WeA01-03, Rotterdam, 2003.
- C.14** S. Douma, X. Bombois and P. Van den Hof , "Validation test based parameter uncertainty versus assumption-based confidence bounds", 13th IFAC Symposium on System Identification, paper FrP03-03, Rotterdam, 2003.
- C.15** A. Lanzon, X. Bombois and B.D.O. Anderson , "On weight adjustments in Hinf control design", 7th European Control Conference, Cambridge, 2003.
- C.16** X. Bombois, G. Scorletti, P. Van den Hof and M. Gevers, "Least costly identification experiment for control. A solution based on a high-order model approximation", 2004 American Control Conference, pp. 2818-2823, Boston, 2004.

- C.17** R. Bos, X. Bombois and P. Van den Hof, "Accelerating large-scale non-linear models for monitoring and control using spatial and temporal correlations", 2004 American Control Conference, pp. 3705-3710, Boston, 2004.
- C.18** R. Bos, X. Bombois and P. Van den Hof, "On model selection for state estimation for nonlinear systems", 7th International Symposium on Dynamic and Control of Process systems, Cambridge, Massachusetts, 2004.
- C.19** X. Bombois, G. Scorletti, P. Van den Hof, M. Gevers and R. Hildebrand, "Least costly identification experiment for control", 16th International Symposium on Mathematical Theory of Networks and Systems, Louvain, 2004.
- C.20** X. Bombois, B.D.O Anderson and M. Gevers, "Frequency domain uncertainty sets with guaranteed probability level in Prediction Error Identification", 16th International Symposium on Mathematical Theory of Networks and Systems, Louvain, 2004.
- C.21** X. Bombois, G. Scorletti, M. Gevers, R. Hildebrand and P. Van den Hof, "Cheapest open-loop identification for control", 43th IEEE Conference on Decision and Control, Atlantis, Bahamas, 2004.
- C.22** X. Bombois, G. Scorletti and P. Van den Hof, "Least disturbing closed-loop identification experiment for control", IFAC World Congress, Praha, 2005.
- C.23** R. Bos, X. Bombois and P. Van den Hof, "Designing a Kalman filter when no noise covariance information is available", IFAC World Congress, Praha, 2005.
- C.24** S. Douma, X. Bombois and P. Van den Hof, "Validity of the standard cross-correlation test for model structure validation", IFAC World Congress, Praha, 2005.
- C.25** X. Bombois, M. Gevers, G. Scorletti, "Open-loop vs. closed-loop identification of Box-Jenkins models: a new variance analysis", CDC-ECC'05, Sevilla, 2005
- C.26** A. Lanzon, B.D.O. Anderson and X. Bombois, "A Newton-Raphson algorithm for calculating the effects of changes in weights on an Hinf design", CDC-ECC'05, Sevilla, 2005.
- C.27** R. Bos, X. Bombois and P. Van den Hof, "Accelerating simulations of first principle models of complex industrial systems using quasi linear parameter varying models", CDC-ECC'05, Sevilla, 2005.
- C.28** X. Bombois and M. Gilson, "Cheapest identification experiment with guaranteed accuracy in the presence of undermodeling", 14th IFAC Symposium on System Identification, pp. 505-510, Newcastle, 2006

- C.29** M. Gevers and X. Bombois, "Input design: from open-loop to control-oriented design", 14th IFAC Symposium on System Identification, pp. 1329-1334, Newcastle, 2006
- C.30** M. Barenthin, X. Bombois and H. Hjalmarsson, "Mixed H₂ and H_{inf} input design for multivariable systems", 14th IFAC Symposium on System Identification, pp. 1335-1340, Newcastle, 2006.
- C.31** X. Bombois, B.D.O. Anderson and G. Scorletti, "Open loop vs. Closed-loop identification of Box-Jenkins systems in a Least Costly Identification context", European Control Conference 2007, pp. 4510-4517, Kos, 2007
- C.32** A.J. den Dekker, X. Bombois and P. Van den Hof, "Likelihood Based Uncertainty Bounding in Prediction Error Identification using ARX models: a simulation study", European Control Conference 2007, pp. 2879-2886, Kos, 2007
- C.33** G. Scorletti, X. Bombois, M. Barenthin and V. Fromion, "Improved efficient analysis for systems with uncertain parameters", 46th IEEE Conference on Decision and Control, pp 5038-5043, New Orleans, 2007
- C.34** A.J. den Dekker, X. Bombois and P. Van den Hof, "Finite Sample Confidence Regions for Parameters in Prediction Error Identification using Output Error Models", 17th IFAC World Congress, pp. 5024-5029, Seoul, 2008
- C.35** X. Bombois, M Barenthin and P. Van den Hof, "Finite-time experiment design with multisines", 17th IFAC World Congress, pp. 11445-11450, Seoul, 2008,
- C.36** M. Gevers, A.S. Bazanella and X. Bombois, "Connecting informative experiments, the information matrix and the minima of a prediction error identification criterion", 15th Symposium on System Identification, pp. 675-680, Saint Malo, 2009
- C.37** A. Khalate, X. Bombois, R. Toth and R. Babuska, "Optimal experimental design for LPV identification using a local approach", 15th Symposium on System Identification, pp. 162-167, Saint Malo, 2009
- C.38** X. Bombois and H. Hjalmarsson, "Optimal input design for robust H₂ deconvolution filtering", 15th Symposium on System Identification, pp. 934-939, Saint Malo, 2009
- C.39** X. Bombois, A.J. den Dekker, M. Barenthin and P. Van den Hof, "Effect of model structure and signal-to-noise ratio on finite-time uncertainty bounding in prediction error identification", 48th IEEE Conference on Decision and Control, pp. 494-499, Shanghai, 2009
- C.40** A. Khalate, X. Bombois, R. Babuska, H. Wijshoff and R. Waarsing, "Optimization-based feedforward control for a drop-on-demand inkjet printer", American Control Conference, pp. 2182-2187, Baltimore, July 2010

- C.41** A. Khalate, X. Bombois, G. Scorletti, R. Babuska, R. Waarsing, W. de Zeeuw, “Robust feedforward control for a drop-on-demand inkjet printhead”, 18th IFAC World Congress, pp. 5795-5800, Milano, 2011
- C.42** X. Bombois, A.J. den Dekker, C. Rojas, H. Hjalmarsson and P. Van den Hof, “Optimal experiment design for hypothesis testing applied to functional magnetic resonance imaging”, 18th IFAC World Congress, pp. 9953-9958, Milano, 2011
- C.43** A. Khalate, X. Bombois, R. Babuska, G. Scorletti, S. Koekebakker, H. Wijshoff, W. de Zeeuw and R. Waarsing, “Performance improvement of a drop-on-demand inkjet printhead: a feedforward control based approach”, International Conference on Digital Printing Technologies (NIP), pp. 74-78, Minneapolis, 2011
- C.44** Ali Mesbah, X. Bombois, J. Ludlage and P. Van den Hof, “Closed-loop performance diagnosis using prediction error identification”, IEEE Conference on Decision and Control, pp. 2969-2974, Orlando, 2011
- C.45** A. Khalate, B. Bayon, X. Bombois, G. Scorletti and R. Babuska, “Drop-on-demand inkjet printhead performance improvement using robust feedforward control”, IEEE Conference on Decision and Control, pp. 4183-4188, Orlando, 2011
- C.46** A. Dankers, R. Toth, P. Heuberger, X. Bombois and P. Van den Hof, “Informative data and identifiability for LPV-ARX prediction error identification”, IEEE Conference on Decision and Control, pp. 799-804, Orlando, 2011
- C.47** S. Taamallah, X. Bombois and P. Van den Hof, “Optimal Control For Power-Off Landing Of A Small-Scale Helicopter - A Pseudospectral Approach”, American Control Conference, pp. 914-919, Montreal, 2012 .
- C.48** M. Forgione, A. Mesbah, X. Bombois and P. Van den Hof, “Iterative Learning Control of Supersaturation in Batch Cooling Crystallization”, American Control Conference, pp. 6455-6460, Montreal, 2012
- C.49** A. Mesbah, X. Bombois, J. Ludlage, P. Van den Hof, “Experiment Design for Closed-loop Performance Diagnosis”, IFAC Symposium on System Identification, pp. 1341-1346, Brussels, 2012
- C.50** S. Narasimhan, X. Bombois, “Plant friendly input design for system identification in closed loop”, IFAC Symposium on System Identification, pp. 1335-1340, Brussels, 2012
- C.51** A. Dankers, P. Van den Hof, P. Heuberger, X. Bombois, “Dynamic network structure identification with prediction error methods - basic examples” , IFAC Symposium on System Identification, pp. 876-881, Brussels, 2012
- C.52** P.-J. van Overloop, X. Bombois, “Identification of Properties of Open Water Channels for Controller Design” , IFAC Symposium on System Identification, pp. 1019-1024, Brussels, 2012

- C.53** A. Mesbah, X. Bombois, M. Forgone, J. Ludlage, P. Moden, H. Hjalmarsson, P. Van den Hof, “A Unified Experiment Design Framework for Detection and Identification in Closed-loop Performance Diagnosis”, IEEE Conference on Decision and Control, pp. 2152-2157, Maui, 2012.
- C.54** M. Forgone, A. Mesbah, X. Bombois, P. Van den Hof, “Batch-to-batch Strategies for Cooling Crystallization”, IEEE Conference on Decision and Control, pp. 6364-6369, Maui, 2012.
- C.55** A. Dankers, P. Van den Hof, P. Heuberger, X. Bombois, “Dynamic Network Identification Using the Direct Prediction-Error Method”, IEEE Conference on Decision and Control, pp. 901-906, Maui, 2012.
- C.56** P. Van den Hof, A. Dankers, P. Heuberger, X. Bombois, “Identification in dynamic networks with known interconnection topology”, IEEE Conference on Decision and Control, pp. 895-900, Maui, 2012.
- C.57** M. Forgone, X. Bombois, P. Van den Hof, “Experiment design for batch-to-batch learning control”, American Control Conference, Washington, 2013.
- C.58** C. Larsson, M. Annergren, H. Hjalmarsson, C. Rojas, X. Bombois, A. Mesbah, P. Moden, “Model predictive control with integrated experiment design for output error systems”, European Control Conference, Zurich, 2013.
- C.59** A. Dankers, P. Van den Hof, X. Bombois, P. Heuberger, “Predictor Input Selection for two stage identification in dynamic networks”, European Control Conference, Zurich, 2013.
- C.60** S. Taamallah, X. Bombois and P. Van den Hof, “Affine LPV Modeling: An Hinfinity Based Approach”, IEEE Conference on Decision and Control, Florence, 2013

Articles de conférence, soumis

- CS.01** X. Bombois and A. Mesbah, “Closed-loop Performance Diagnosis for Model Predictive Control Systems” soumis à l’European Control Conference, Strasbourg, 2014
- CS.02** M. Potters, X. Bombois, M. Forgone, P. Modén, M. Lundh, H. Hjalmarsson and P. Van den Hof, “Optimal Experiment Design in Closed Loop with Unknown, Nonlinear or Implicit Controllers using Stealth Identification” soumis à l’European Control Conference, Strasbourg, 2014
- CS.03** M. Forgone, X. Bombois, P. Van den Hof, H. Hjalmarsson, “Experiment design for parameter estimation in nonlinear systems based on multilevel excitation” soumis à l’European Control Conference, Strasbourg, 2014

Livrables (deliverables) liés au projet européen Autoprofit

- D.01** A. Mesbah, X. Bombois, “Performance monitoring and diagnosis”, livrable 4.1 du projet Autoprofit, 53 pages, 2011
- D.02** P-E. Moden, A. Mesbah, X. Bombois, “Fundamentals on least costly detection and performance monitoring”, livrable 4.2 du projet Autoprofit, 41 pages, 2012
- D.03** M. Potters, M. Lund, P-E. Moden, X. Bombois, “Matlab software for performance monitoring”, livrable 4.3 du projet Autoprofit, 23 pages, 2012
- D.04** X. Bombois, A. Mesbah, “Least costly detection in the industry”, livrable 4.4 du projet Autoprofit, 45 pages, 2013

Brevet, soumis

- B.01** “Providing improvements in relation to a model of a process”, soumis en juin 2013 à l’Office européen des brevets (référence de soumission EP13166342). Inventeurs: P-E. Moden (25 %), H. Hjalmarsson (5 %) et X. Bombois (70 %)¹

¹Les pourcentages correspondent à la contribution relative de chaque inventeur dans cette invention. Ces pourcentages ont été convenu entre les trois inventeurs.

Part II

Synthèse des travaux de recherche

Chapter 5

Introduction

Model-based engineering is the dominant engineering paradigm to systematic design and maintenance of engineering systems. In those technology fields where dynamics plays a role, *model-based control* acts as an enabling technology that is essential for the design and realization of high-performance and robustly operating systems.

The design of a control loop for a real-life system (the so-called true system) can generally be divided in two essential steps:

1. Modelling: the determination of a mathematical model of the true system coupled with information about the model uncertainty. This step can be performed using a first-principles approach (physical modelling), using experimental data collected on the system (system identification) or a combination of both approaches.
2. Robust Control Design: The design of a controller using the identified model of the true system; followed by the verification of the robustness of this controller against model uncertainty (see e.g. [54]¹).

The first step (i.e. modelling systems in order to control them) is a complicated task. The model must, on the one hand, be sufficiently accurate to guarantee high performance, but the model should also remain relatively simple since, otherwise, it would become impossible to design a controller based on that model. This is a challenge for both modelling approaches (first principles and system identification). In my research until now, I have mostly concentrated on (linear) system identification as modelling technique for control and I will thus from now on restrict attention to this modelling technique. Note nevertheless that we have also addressed the question of accelerating first-principles models (see J.11 et C.60). Indeed, if such models can be very accurate², they are generally much too complicated and computationally expensive to be used in a model-based control strategy.

¹The references [.] pertain to the reference list at the end of this document; the other references to the list in Chapter 4.

²especially if their unknown parameters have been calibrated using experimental data

System identification [33, 38] can be an elegant technique to obtain models that are both simple and accurate. A system identification procedure is made up of different steps. First, an *experiment* has to be performed on the true system to collect informative data. This is done by applying an excitation signal to the system either in open or in closed loop. Once data have been collected, an identification criterion (e.g. the prediction error criterion) determines, within an a-priori selected set of candidate-models, the particular model that is best able to explain the data. The choice of the model set is in this sense crucial and techniques are available to make this choice³.

Even if the model set has been intelligently chosen, obtaining accurate models for control using system identification remains a difficult task. Indeed, the quality of the identified model highly depends on the *identification experiment* that has been performed and a badly designed experiment generally leads to models for which the uncertainty is too high for the design of a satisfactory controller for the true system. Consequently, it is very important to optimize the path that starts by the design of the identification experiment and finally leads to a satisfactory control performance. This has been the main objective of my research since the beginning of my academic career.

Since the mid-eighties, intensive research has been conducted in this area by the groups of Prof. Gevers and Van den Hof (see e.g. [14, 10, 23, 9]). These efforts have shown the advantages of closed-loop identification techniques with respect to open-loop techniques. Techniques alternating (closed-loop) identification steps and control design steps have also been developed [44]. The reasoning is that, to obtain an accurate model for control, the data have to be collected in circumstances close to the ones the plant will face when operated with the to-be-designed controller.

In these early years, the apparent incompatibility between the uncertainty information delivered by classical system identification [33] and the uncertainty descriptions used in mainstream robust control theory [54] meant that limited attention was paid to the concept of uncertainty region, in general, and to its possible use to verify the robustness of the controller designed with the identified model, in particular. Consequently, there was still no technique that allows one to verify whether a controller designed with the identified model stabilizes and achieves sufficient performance with the true system.

The uncertainty region deduced after an identification experiment is indeed quite particular. If a full-order model set is used, the uncertainty region is a set of parametrized transfer functions whose parameter vector is constrained to lie in an ellipsoid (see [33] or the thesis T.01). The size of the ellipsoid is given by the covariance matrix of the identified parameter and is therefore dependent on the identification experiment. The structure is also particular when reduced-

³We will make often the assumption that the model set is rich enough to describe the system (full-order model structure). Such a model set can be determined iteratively using model structure validation based on residual tests. See [33], the publication J.08 or the identification slides <http://www.dsc.tudelft.nl/~xbombois/sc4110slides.pdf>.

order model sets are used (see [18, 20] or T.01). Indeed, the uncertainty region is, in this case, a set containing all transfer functions whose frequency response lies, at each frequency, in an ellipse in the Nyquist plane.

Due to these particular structures, the classical results of robustness analysis could not be applied to the uncertainty descriptions delivered by system identification. We have bridged this gap by developing new robustness analysis tools adapted to those particular types of uncertainty regions. These robustness tools allow one to verify whether a controller designed from the identified model will stabilize and achieve sufficient performance with the unknown true system. Note also that the development of these new robustness analysis tools required extensive use of the computational possibilities provided by the optimization problems using Linear Matrix Inequalities constraints; an approach that could be considered as entirely novel for the system identification community. The results have been first developed for SISO systems whose performance is measured in the H_∞ framework (see J.01, J.02, J.03 and C.06). They have been then extended towards MIMO systems in J.09 and towards H_2 performance measures in J.13.

These novel robustness tools have been my first step in optimizing the path between the identification experiment and a satisfactory control performance. However, because little attention had been devoted to analyzing the choice of data used to identify the model and its uncertainty region, we still had no insight into the best way to design the identification experiment to guarantee that, with the identified model and its uncertainty, a robust controller meeting the performance requirements can be designed. The size of the model uncertainty is indeed directly related to the performed identification experiment. Consequently, if we do not design correctly the identification experiment, the identified uncertainty could prove too large to meet all the performance requirements. This is especially true for systems (such as systems in the process industry) for which collecting identification data entails a very important economical cost. Indeed, because of that high economical cost, the experiments are, in those cases, generally short and the excitation signal of low power; which in turn leads to large model uncertainty if the excitation signal is not chosen with care.

This observation led me to the development of a new framework for optimal identification experiment design, in the context of “identification for robust control”. It is novel essentially in that it takes the dual viewpoint to the classical way of posing optimal experiment design problems. To state this in a nutshell, the classical way is to seek the optimal input signal (or the optimal input signal spectrum) that minimizes some control-oriented measure of the quality of the identified model, subject to constraints on the input signal power (and/or on the output signal power). Representative examples of such approach can be found in [16, 24, 33, 12, 32, 8, 21, 27]. From a robust control point of view, such an approach is not always the most sensible choice: one should not spend more effort on the identification than what is needed to achieve the required robust control performance. Or in other words, one should just spend the necessary efforts to obtain an uncertainty region which is *just* small enough for the design

of satisfactory controller.

In our new optimal experiment design framework, the objective is to design the least costly identification experiment which nevertheless guarantees that the collected data are sufficiently informative about the dynamics of the true system for the corresponding identification to deliver a model with a sufficiently small uncertainty for the design of a robust controller meeting the performance requirements. The least costly experiment is, among all experiments satisfying the control performance requirements, the one that causes the least perturbation to the normal operations of the plant. Technically speaking, the framework is based on the robustness tools for the uncertainty regions delivered by system identification and on the affine relation existing between the power spectrum of the excitation signal and the inverse of the covariance matrix (i.e. the size of the uncertainty region) [32]. This framework was first developed in a SISO H_∞ framework in J.07, but has been extended to a MIMO framework and H_2 performance measures in J.09 and J.13, respectively. In [22], H. Hjalmarsson has also proposed a methodology which, at the cost of a second-order approximation, allows one to consider a large variety of performance measures in the least costly framework.

One of the main conclusions of the work so far is that the cost of the identification can be dramatically decreased by optimizing the excitation signal. As an example, the paper [2] shows that we can identify an accurate model using an identification experiment that is ten times shorter when using an optimized excitation signal. Other illustrative examples are given in J.18.

It is worth noticing that we have been able to interest the industry for the least costly identification paradigm. As expected, because of the important economical costs linked to identification experiments in those areas, this interest mainly comes from the large process industries. As an example, one of my MSc students has applied the developed techniques to identify a small-scale direct sheet plant at Tata Steel (IJmuiden, The Netherlands) in 2012. On a larger scale, within the Autoprofit project (2010-2013), we have gathered a consortium of industrial partners (ABB, SASOL and Boliden) which will allow the applications of these optimal experiment ideas under realistic industrial circumstances.

The Autoprofit project is an EU-KP7 STREP project (budget 2.5 million) that is mainly based on my research ideas. This project not only aims at developing our least costly framework towards industrial applications, but also at improving the maintenance of model-based control systems using the least costly philosophy.

Once a model has been identified and a satisfactory controller has been designed, it is indeed important to maintain the performance of this controller over time. The performance of a controller can indeed be significantly reduced by the inherent (gradual) time-varying nature of the plant dynamics. For this purpose, the closed-loop performance has to be continuously monitored and the

cause of any performance drop should be determined before any re-identification of the plant dynamics is decided. Indeed, if a re-identification of the plant dynamics seems the only solution to restore the initial closed-loop performance when the cause of the performance drop is a control-relevant plant change. It is by far not the optimal solution when the cause of the performance drop is to be found elsewhere. As a matter of fact, in real practice, closed-loop performance degradation mostly results from (temporary) variations in disturbance characteristics or sensor/actuator failures. Knowing the relatively high economical costs of a re-identification (even in the least costly context), a sustainable controller maintenance procedure should therefore contain a so-called performance diagnosis step that would be performed when a closed-loop performance drop is observed. The performance diagnosis should verify whether it is likely that the performance degradation is due to a control-relevant plant change.

Within the Autoprofit project, we have developed a general closed-loop performance diagnosis method formulated as an hypothesis test and involving a diagnosis experiment on the plant. This diagnosis experiment boils down to a short identification experiment from which a model of the current plant dynamics can be deduced. We have also addressed the problem of optimal experiment design for the diagnosis problem at stake. The optimal experiment design is performed in the least-costly context in order to minimize the cost of the diagnosis experiment while guaranteeing a pre-specified accuracy for detecting the cause of the performance drop. An optimal trade-off is sought between the contradictory objectives of obtaining an accurate diagnosis and obtaining a cheap diagnosis experiment (particularly with respect to a re-identification experiment). To our knowledge, the design of optimal experiments for closed-loop performance diagnosis had not been investigated in the literature.

As the diagnosis step is closely intertwined with the re-identification step performed if a control-relevant plant change is diagnosed, a unified framework is furthermore proposed for the optimal design of both the diagnosis experiment and the possible re-identification experiment. In a nutshell, the diagnosis and re-identification experiments are designed in such a way that the sum of the excitation costs related to these two experiments is minimized while guaranteeing a pre-specified diagnosis accuracy and, in the cases where a re-identification is needed, guaranteeing that the re-identified model is accurate enough for re-designing the controller. These contributions can be found in the publications C.44,C.49,C.53 and S.02.

As part of the PhD project of Marco Forgione (see Section 3.2), we have also recently proposed another alternative framework for *optimal identification experiment design for control* (see C.57 et S.01). In this new framework, there is no longer a strict distinction between an identification phase and a phase where the designed controller operates the true system without any excitation. As opposed to this classical setup, an optimal excitation signal is (or, at least, can be) applied throughout the lifetime of the closed loop. This allows to gradually reduce the model uncertainty and improve the controller (that is updated at fixed interval). It is important to note that this excitation increases the perfor-

mance (in the future) by reducing the model uncertainty, but also reduces the present performance (due to the perturbation caused on the normal operation). We therefore seek the excitation signal that maximizes the overall performance over the entire lifetime of the closed loop. Since the overall performance is negatively influenced by both the model uncertainty and the excitation signal, the objectives of the least costly and of the more classical optimal experiment design frameworks are somehow combined in this novel framework.

The philosophy on *identification for robust control* developed since the beginning of my academic career has also allowed me to participate to more applied research projects such as the Octopus project in collaboration with the printer manufacturer OCE. In this project, we addressed the question of improving the printing quality of inkjet printheads. This printing quality is severely affected by oscillations in the ink channel. These oscillations are created by the drop jetting process and the cross-talk between neighbouring channels. Consequently, the printing quality could be improved if the actuation pulse that commands the drop jetting process could be re-designed to effectively damp these oscillations. To achieve this pulse redesign (feedforward control) in a robust way, we have identified a model of the printhead at different setpoints (i.e. for different jetting frequencies). This has allowed us to design a robust pulse whose efficacy has been demonstrated using both simulation and experimental results. See e.g. J.20.

In Chapters 6 to 10, the above research results will be presented in more details. In Chapters 11 and 12, some other research projects that are further away from my main research line will also be presented. Finally, in Chapter 13, I will present some ideas for future research.

Chapter 6

Robustness analysis for uncertainty regions delivered by identification

6.1 Prediction-error Identification

In this chapter, we will present the robustness analysis tools we have developed for the uncertainty regions delivered by system identification. We will restrict attention to the case where the chosen model structure (model set) for the identification is rich enough to describe the true system. The results corresponding to reduced-order model structures can be found in T.01 or C.06. To simplify the notations, we will present the mathematical framework assuming that the true system is SISO. Note however that the (main) differences between the SISO and MIMO cases will be reported after each stage. We will also assume that the true system is operated in closed loop with an existing controller C_{id} . We therefore consider the case where we want to perform an identification to design a new controller C that will improve the performance of the existing controller C_{id} . Note that the open-loop setting is a special case of the closed-loop setting where the controller C_{id} is zero. Let us first present some results of system identification and, in particular, prediction-error identification [33].

We consider the identification of a linear time-invariant single input single output system with a model structure $\mathcal{M} = \{G(z, \theta), H(z, \theta)\}$, $\theta \in \mathbf{R}^k$, that is able to represent the true system. Thus, the true system is given by:

$$\begin{aligned} \mathcal{S}: \quad y(t) &= G_0(z)u(t) + \overbrace{H_0(z)e(t)}^{=v(t)} \\ &= G(z, \theta_0)u(t) + H(z, \theta_0)e(t) \end{aligned} \quad (6.1)$$

for some unknown parameter vector $\theta_0 \in \mathbf{R}^k$, and with $e(t)$ a white noise of variance σ_e^2 . With some abuse, we use the symbol “ z ” both for the shift operator (see (6.1)) and for the Z -transform variable. We further assume that the true system \mathcal{S} is operated in closed loop with an existing LTI controller C_{id} (see Figure 6.1).

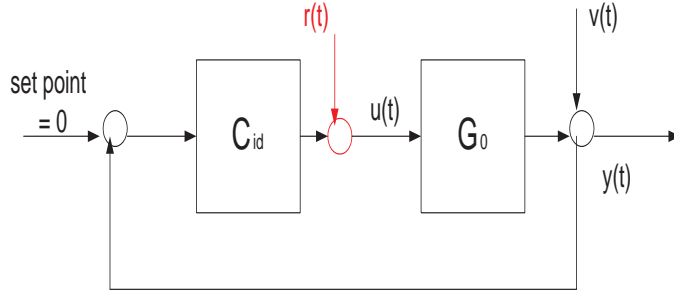


Figure 6.1: Closed-loop identification: the data set Z^N is collected by exciting the closed loop made up of the true system and a controller C_{id} using an external signal $r(t)$

In order to identify the true system, an identification experiment has to be performed. For this purpose, an excitation signal $r(t)$ ($t = 1 \dots N$) is applied to the closed loop as shown in Figure 6.1 and the corresponding input and output data are measured: $Z^N = \{y(t) \ u(t) \mid t = 1 \dots N\}$. During the identification experiment, we have the following relations:

$$y(t) = \overbrace{G_0 S_{id} r(t)}^{y_r(t)} + S_{id} v(t) \quad (6.2)$$

$$u(t) = \overbrace{S_{id} r(t)}^{u_r(t)} - C_{id} S_{id} v(t) \quad (6.3)$$

with $S_{id} = (1 + C_{id} G_0)^{-1}$ the sensitivity function of the closed loop $[C_{id} \ G_0]$. When designing the experiment, besides the choice of the duration N of the identification experiment, the user has also to determine the excitation signal $r(t)$ (in particular, the power spectrum $\Phi_r(\omega)$ of r). Consequently, when we will optimally design the identification experiment (see Chapter 7), these two variables will be the design variables. In this chapter, we will suppose that these variables have been a-priori chosen. The only condition imposed on the excitation signal is that the data set Z^N has to be informative enough for the identification of (6.1). This can be easily achieved e.g. by choosing the excitation signal as a (filtered) white noise.

Once the data set Z^N has been collected, prediction error identification can be used to determine a consistent estimate $\hat{\theta}_N$ of the true parameter vector θ_0 using the following criterion:

$$\hat{\theta}_N \triangleq \arg \min_{\theta} \frac{1}{N} \sum_{t=1}^N \epsilon^2(t, \theta) \quad (6.4)$$

with $\epsilon(t, \theta) \triangleq H(z, \theta)^{-1} (y(t) - G(z, \theta)u(t))$.

The identified parameter vector $\hat{\theta}_N$ is asymptotically normally distributed around θ_0 :

$$\hat{\theta}_N \sim \mathcal{N}(\theta_0, P_\theta) \quad (6.5)$$

and, given the full-order model structure assumption, the covariance matrix P_θ has the following expression [33]: $P_\theta = \frac{\sigma_e^2}{N} (\bar{E}(\psi(t, \theta_0)\psi(t, \theta_0)^T))^{-1}$ with $\psi(t, \theta) = -\frac{\partial \epsilon(t, \theta)}{\partial \theta}$. It is possible to rewrite the expression of P_θ in such a way that its dependence on the identification duration N and on the excitation spectrum $\Phi_r(\omega)$ becomes visible (see J.07):

$$\begin{aligned} P_\theta^{-1} &= \left(\frac{N}{\sigma_e^2} \frac{1}{2\pi} \int_{-\pi}^{\pi} F_r(e^{j\omega}, \theta_0) F_r(e^{j\omega}, \theta_0)^* \Phi_r(\omega) d\omega \right) \\ &+ \left(N \frac{1}{2\pi} \int_{-\pi}^{\pi} F_v(e^{j\omega}, \theta_0) F_v(e^{j\omega}, \theta_0)^* d\omega \right) \end{aligned} \quad (6.6)$$

with $F_r(z, \theta_0) = \frac{S_{id}}{H_0} \Lambda_G(z, \theta_0)$, $F_v(z, \theta_0) = \frac{\Lambda_H(z, \theta_0)}{H_0} - C_{id} S_{id} \Lambda_G(z, \theta_0)$, $\Lambda_G(z, \theta) = \frac{\partial G(z, \theta)}{\partial \theta}$ and $\Lambda_H(z, \theta) = \frac{\partial H(z, \theta)}{\partial \theta}$. We observe in (6.6) that the covariance matrix “decreases” both when N and $\Phi_r(\omega)$ “increase”. It is also important to note that the covariance matrix can easily be estimated using the identified parameter vector $\hat{\theta}_N$ and the data set Z^N :

$$P_\theta \approx \frac{\hat{\sigma}_e^2}{N} \left(\sum_{t=1}^N \psi(t, \hat{\theta}_N) \psi^T(t, \hat{\theta}_N) \right)^{-1} \quad (6.7)$$

with $\hat{\sigma}_e^2 = \frac{1}{N} \sum_{t=1}^N \epsilon^2(t, \hat{\theta}_N)$.

Let us now assess the uncertainty of the identified parameter vector $\hat{\theta}_N$. This can be done by using (6.5) to construct a confidence ellipsoid U centered at the identified parameter vector $\hat{\theta}_N$ and containing the unknown true parameter vector θ_0 at an user-chosen probability level α :

$$U = \{\theta \in \mathbf{R}^k \mid (\theta - \hat{\theta}_N)^T P_\theta^{-1} (\theta - \hat{\theta}_N) < \chi_\alpha\} \quad (6.8)$$

with χ_α such as $Pr(\chi^2(k) < \chi_\alpha) = \alpha$. This ellipsoid in the parameter space in turn defines an uncertainty region in the space of transfer functions $G(z, \theta)$ and that contains $G_0(z) = G(z, \theta_0)$ at the same probability α :

$$\mathcal{D} = \{G(z, \theta) \mid \theta \in U\} \quad (6.9)$$

After an identification experiment in a full-order model structure, we are thus able to determine an uncertainty region \mathcal{D} centered at the identified model $G(z, \hat{\theta}_N)$ and containing the true system G_0 at a self-chosen probability α (e.g. $\alpha = 0.95$). This uncertainty region \mathcal{D} is a set of parametrized transfer function whose parameter vector is constrained to lie in an ellipsoid U . \mathcal{D} is only a function of the identified model $G(z, \hat{\theta}_N)$ and of the (estimated) covariance matrix P_θ of $\hat{\theta}_N$. It is important to realize that the uncertainty region \mathcal{D} is therefore different for each set of data collected on the true system $G_0(z)$. Indeed, for each set of data, you obtain a different model $G(z, \hat{\theta}_N)$, a different covariance matrix

P_θ and thus a different uncertainty set \mathcal{D} . Moreover, the smaller the covariance matrix of $\hat{\theta}_N$ is, the smaller the uncertainty region is and thus the more we have confidence that the true system $G_0(z)$ is “close” to the identified model $G(z, \hat{\theta}_N)$.

Remark 1. Since we identify the true system in a full-order model structure, the only source of uncertainty is the stochastic noise $v(t)$ which makes of the identified parameter vector $\hat{\theta}_N$ a random variable. This can also be observed in the expression of the uncertainty region where we see that the size of the uncertainty is determined by the covariance matrix P_θ of $\hat{\theta}_N$. When identifying in a reduced-order model structure, the uncertainty is function of both the structural mismatch and of the noise [18, 20].

Remark 2. For the sequel, it is important to note that the classical parametrizations of $G(z, \theta)$ in system identification are all Linear Fractional Transformations (LFTs) of the parameter vector θ [54].

Remark 3 (MIMO systems). The uncertainty region \mathcal{D} in the case of a MIMO true system would be identical. The parametrization $G(z, \theta)$ is however in this case a matrix of transfer functions. Each element of this matrix is an LFT in θ .

Remark 4. The expression of the uncertainty ellipsoid U is based on the asymptotic distribution (6.5) which is thus in theory only valid for $N \rightarrow \infty$. We have analyzed the validity of this uncertainty ellipsoid for small values of N in the papers C.32, C.34 and C.39. One of the main observations of these papers is that, in order to guarantee $Pr(\theta_0 \in U) \approx \alpha$, a smaller data set can be somehow *compensated* by a larger excitation signal.

6.2 Controller design and controller validation

6.2.1 Controller design

The identified model $G(z, \hat{\theta}_N)$ can now be used to design a new controller $C(z)$ for the true system $G_0(z)$. This controller C stabilizes and achieves satisfactory performance with the model $G(z, \hat{\theta}_N)$. Despite all the care brought in the design of the identification experiment, the model $G(z, \hat{\theta}_N)$ is nevertheless only an approximation of the true system G_0 . Consequently, the controller that has been designed from $G(z, \hat{\theta}_N)$ is not guaranteed to either stabilize G_0 or achieve the desired performance with G_0 .

In order to derive this guarantee, the framework of Robustness Theory, introduced in the early 80’s in [53, 11], is an elegant solution. Based on the concept of uncertainty regions of which the set \mathcal{D} given in (6.9) is a particular example, this framework allows one to verify whether the model-based controller C stabilizes all systems in the considered uncertainty set and achieves sufficient performance with all these systems. In other words, the controller is a-posteriori validated for stability and for performance.

Remark. Another approach would consist in directly designing a robust controller which stabilizes and achieves sufficient performance with all plants in the uncertainty set. We will here disregard this approach since the optimization to deduce this robust controller leads to a very complicated iteration process (D-K iteration [54]) that is not guaranteed to converge and that leads to an explosion of the order of the controller. This direct design of the robust controller is nevertheless much more simpler for feedforward controller (see e.g. Chapter 10) and for (deconvolution) filters (see J.13).

6.2.2 Controller validation

Since \mathcal{D} is the uncertainty region delivered by the identification experiment, the validation of the controller C designed from the identified model $G(z, \hat{\theta}_N)$ has to be performed using this uncertainty region \mathcal{D} . Recall that this uncertainty contains the unknown true system at an user-chosen probability α . The main challenge in using \mathcal{D} in a robustness analysis procedure is that this uncertainty region is not standard in mainstream robust control (see Section 6.3).

The validation of the designed controller $C(z)$ is made up of two essential steps:

- controller validation for stability: verification whether C stabilizes all systems in \mathcal{D} (and therefore also the true system G_0)
- controller validation for performance: we compute the worst case performance achieved by C over the plants in \mathcal{D} and we verify if this worst case performance is sufficient with respect to the controller specifications. This worst case performance is of course a lower bound of the performance achieved by the controller C with G_0 .

The controller validation procedure for stability is unequivocal. The controller validation for performance involves the computation of the worst case performance. In order to define the worst case performance, we first need to define a performance measure of a closed-loop system $[C \ G]$. There are many ways to measure the performance of a closed-loop system. However, most commonly used criteria uses some norm of a weighted closed-loop transfer function $T(G, C)$, e.g.

$$T(G, C) = \frac{W(z)}{1 + G(z)C(z)} \quad (6.10)$$

with W an user-chosen weight. Instead of a scalar transfer function, $T(G, C)$ can also be a matrix containing all four (weighted) closed-loop transfer functions:

$$T(G, C) = W_l \begin{pmatrix} \frac{GC}{1+GC} & \frac{G}{1+GC} \\ \frac{C}{1+GC} & \frac{1}{1+GC} \end{pmatrix} W_r \quad (6.11)$$

with some prescribed weights $W_l = \text{diag}(W_{l1}(z), W_{l2}(z))$ and $W_r = \text{diag}(W_{r1}(z), W_{r2}(z))$.

A possible norm that can be considered to define the performance is the largest singular value of T at each frequency ω . The performance of the loop is thus defined at each frequency as:

$$J(G, C, \omega) = \sigma_{max}(T(G(e^{j\omega}), C(e^{j\omega}))) \quad (6.12)$$

For scalar T , (6.12) reduces to the modulus of T at each frequency. The H_∞ norm of T is the maximum over the frequency of $J(G, C, \omega)$.

With (6.12) as performance measure, we can state that the loop $[C \ G]$ achieves sufficient performance if $J(G, C, \omega)$ remains below some threshold γ at each frequency (i.e. $\|T(G, C)\|_\infty < \gamma$). At a given frequency ω , the worst case performance achieved by the controller C over all plants in the uncertainty region \mathcal{D} is then defined as:

$$J_{WC}(\mathcal{D}, C, \omega) = \sup_{G \in \mathcal{D}} J(G, C, \omega) \quad (6.13)$$

where $J(G, C, \omega)$ is defined in (6.12). Consequently, a controller will be deemed validated for performance if $J_{WC}(\mathcal{D}, C, \omega) < \gamma$ at each frequency.

Instead of the largest singular value, we can also consider the H_2 norm to define the performance. The worst-case performance achieved by C over the plants in \mathcal{D} is then:

$$J_{WC}(\mathcal{D}, C) = \sup_{G \in \mathcal{D}} J(G, C) \quad \text{with } J(G, C) = \|T(G, C)\|_2 \quad (6.14)$$

Here, the worst case performance is not dependent on the frequency and a controller is deemed validated if $J_{WC}(\mathcal{D}, C) < \gamma$.

Remark 1 (MIMO systems). The validation of a controller in the MIMO case is completely equivalent to the SISO case (except for some obvious notational changes when defining the closed-loop transfer functions).

Remark 2. In [22], H. Hjalmarsson shows that a very large variety of performance measures can in fact be used in our framework at the cost of a second-order Taylor approximation. The condition is e.g. that the performance of the loop $[C \ G]$ is defined as a deviation with respect to the performance of the designed loop $[C \ G(z, \hat{\theta}_N)]$. An example of such a measure will be used in Chapter 9. For the performance measures considered in [22], the designed controller C can also be nonlinear (such as a MPC controller).

6.3 Robustness tools

6.3.1 Robust performance analysis - controller validation for performance

Let us first focus on the controller validation for performance. The worst case performance defined in the previous section can be computed as $\sqrt{\zeta_{opt}}$ with ζ_{opt} the solution of the following optimization problem:

$$\text{minimize } \zeta \quad (6.15)$$

subject to

$$J^2(G(z, \theta), C) < \zeta \quad \forall \theta \in U \quad (6.16)$$

Here J represents both the frequency-dependent and frequency-independent performance measures. Owing to this formulation, we will be able to compute the worst case performance if we can rewrite (6.16) as a tractable constraint.

Consider the loop $[C \ G(z, \theta)]$ with $G(z, \theta)$ a plant in the uncertainty region \mathcal{D} . Due to the particular parametrization of $G(z, \theta)$ (see Remarks 2 and 3 in Section 6.1), the loop $[C \ G(z, \theta)]$ can be rewritten in the so-called LFT framework represented in Figure 6.2. In this representation, we represent the transfer function/matrix T :

$$z = T(G(z, \theta), C) w$$

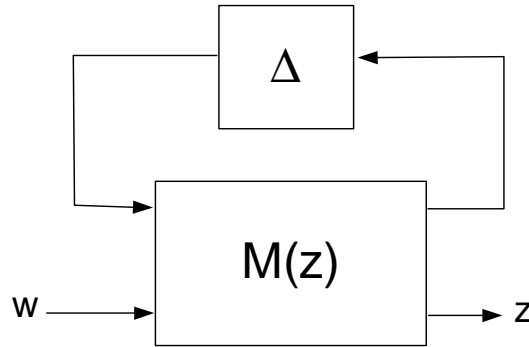


Figure 6.2: LFT representation of $T(G, C)$

by separating a fixed/known part $M(z)$ from an varying/uncertain part Δ . The uncertain part $\Delta(\theta)$ is here a known function of θ . Depending on the situation, Δ will be equal to θ or to $I \otimes \theta$ (I represents the identity matrix and \otimes represents the Kronecker product). More particularly, if the system is SISO, we will have that $\Delta = \theta$, while Δ is given by $I \otimes \theta$ when $G(z, \theta)$ represents a MIMO system (see J.09).

Once the loop has been rewritten in the LFT framework, we can rewrite the constraint (6.16) using the so-called separation of graph theorem¹ [17, 45, 46]. An important ingredient of this approach is to determine an explicit parametrization (called set of multipliers) of the quadratic constraints satisfied by the graphs $[I \ \Delta^T]^T$ of all uncertainties $\Delta(\theta)$, $\theta \in U$. In [46], such set of multipliers is derived for the classical uncertainty sets encountered in the robustness

¹The separation of graph theorem is equivalent to the μ -analysis approach [54]

analysis literature. However, the set corresponding to the uncertainty region \mathcal{D} is not classical. The uncertainty $\Delta(\theta)$ has indeed a very particular structure, especially in the MIMO case i.e. a block-diagonal matrix with a parameter vector constrained in an ellipsoid repeated on the diagonal. A very general set of multipliers has been deduced in J.09 for this type of uncertainty. With this set of multipliers, we can deduce a LMI constraint which implies (6.16). Using this LMI constraint in the optimization problem (6.15), we thus obtain an upper bound on the worst case performance².

The procedure above is a very general procedure which is absolutely necessary for many cases, e.g. MIMO systems (see J.09), performance measure expressed with the H_2 norm (see J.13). However, in the case of a SISO system and an H_∞ performance measure such as (6.12), we can **exactly** compute the worst case performance $J_{WC}(\mathcal{D}, C, \omega)$. Indeed, it is proven in J.02 that the constraint $J^2(G(\theta), C, \omega) < \zeta$ can be expressed as a quadratic expression in θ for each ω . Since U is an ellipsoid, $\theta \in U$ can also be expressed as a quadratic expression in θ . The \mathcal{S} -procedure [6] can then be used to derive an LMI constraint linear in ζ which is **equivalent** to the original constraint (6.16) (see J.02 for more details). This equivalent LMI constraint has the following form:

$$\exists \tau > 0 \text{ such that } \mathcal{A}(\zeta, C) - \tau \mathcal{B}(P_\theta^{-1}, \hat{\theta}_N) < 0 \quad (6.17)$$

with τ a scalar decision variable, $\mathcal{A}(\zeta, C)$ a known matrix that is linear in ζ and function of the controller C and $\mathcal{B}(P_\theta^{-1}, \hat{\theta}_N)$ also a known matrix that is linear in P_θ^{-1} and function of $\hat{\theta}_N$.

Remark. If we use the performance measures proposed in [22] and approximated by a Taylor expansion, the constraint (6.16) can be rewritten as:

$$\zeta P_\theta^{-1} > R_{\hat{\theta}_N, C} \quad (6.18)$$

where P_θ is the known covariance matrix of the identified parameter vector $\hat{\theta}_N$ and $R_{\hat{\theta}_N, C}$ is also a known matrix which is a function of $\hat{\theta}_N$, the controller C designed from $G(z, \hat{\theta}_N)$ and the particular choice of performance measure. Since (6.18) is an LMI constraint linear in ζ , the worst case performance can also be easily computed.

6.3.2 Robust stability analysis - controller validation for stability

Let us now consider the controller validation for stability. Using similar tools³, we can deduce, in the SISO case, a necessary and sufficient condition for the stabilization of all plants in \mathcal{D} by a given controller C (see J.02 for more details). In the MIMO case, only a sufficient condition for robust stability can be

²The conservatism is among other things due to the fact that the set of multipliers gives a linear parametrization of the quadratic constraints satisfied by the graphs of all uncertainties $\Delta(\theta)$, $\theta \in U$. If this linear parametrization makes the robustness analysis problem tractable, it does not include all possible quadratic constraints.

³The separation of graph theorem is basically a robust stability result that is extended for robust performance analysis.

deduced (see J.09 for more details).

Note that a controller validated for performance is also directly validated for stability. Indeed, if the controller C does destabilizes some plants in \mathcal{D} , there is always one plant $G(z, \theta)$ for which $1 + G(e^{j\omega}, \theta)C(e^{j\omega}) = 0$ at one frequency. Consequently, the worst case performance $J_{WC}(\mathcal{D}, C, \omega)$ (see (6.13)) defined in the H_∞ framework will be infinite at that frequency and the worst case performance $J_{WC}(\mathcal{D}, C)$ (see (6.14)) defined in the H_2 framework will also be infinite.

6.4 Conclusions

Using the robustness tools presented in this chapter, we can validate a controller C designed from an identified model both for stability and for performance. If the controller is deemed validated, it can be subsequently applied to the true system. However, if the uncertainty of the identified model is too large, the controller may be well invalidated. In the next chapter, we will present tools to design the identification experiment in such a way that the controller designed from the model identified with this experiment is guaranteed to be validated.

Chapter 7

Design of least costly identification experiments for control

7.1 Problem statement

If the uncertainty region \mathcal{D} of the identified model $G(z, \hat{\theta}_N)$ is too large (i.e. if the covariance matrix P_θ defining the size of \mathcal{D} is too large), a controller designed with $G(z, \hat{\theta}_N)$ may be invalidated and can therefore not be applied to the true system since it may achieve unsatisfactory performance with the true system G_0 . In this chapter, we will present a framework for the design of optimal identification experiments to avoid such issues. In a nutshell, the optimal experiment in our framework is the cheapest identification experiment that nevertheless guarantees that the uncertainty of the identified model is small enough for the design of a controller achieving satisfactory performance with G_0 .

As in the previous chapter, we will present the mathematical framework for a SISO true system in a closed-loop setting and we will assume that the identification is performed in a full-order model structure \mathcal{M} . We thus consider the framework of Section 6.1. For the ease of discussion, we will also consider an H_∞ performance measure (see (6.12)). Extensions to the other cases (MIMO, H_2, \dots) will nevertheless be discussed in Section 7.4.

As we already mentioned in Section 6.1, when designing an identification experiment in closed loop, the design variables are the duration N of the identification experiment and the excitation sequence $r(t)$ ($t = 1 \dots N$). In a first stage, we will suppose that N has been chosen a-priori and the design variables therefore reduce to the excitation signal $r(t)$. To make the problem tractable, we will in fact consider the power spectrum $\Phi_r(\omega)$ of $r(t)$ as design variable and, once this spectrum has been determined, we will realize an excitation sequence $r(t)$ having that particular spectrum.

The major constraint for the to-be-designed identification experiment is that the controller C that will be designed with the identified model achieves suffi-

cient performance with all plants in the uncertainty \mathcal{D} of this model (and thus also with G_0). As shown in Chapter 6, this robust performance constraint is equivalent to the following constraint that must hold at each ω :

$$J(G(z, \theta), C, \omega) < \gamma \quad \forall \theta \in U \quad (7.1)$$

with γ an user-chosen bound on the acceptable performance. It is important to note that U (see (6.8)) here represents the ellipsoidal uncertainty that will be derived after the to-be-designed experiment and C is the controller that will be designed from the model identified with this experiment. In the sequel, it will be supposed that we have a-priori fixed a control design method in such a way that C can be considered as a *known* function¹ $C = C(\hat{\theta}_N)$ of the to-be-identified model $G(z, \hat{\theta}_N)$. Note also that this robust performance constraint also ensures robust stability over the uncertainty set \mathcal{D} (see Section 6.3).

To formalize our optimal experiment design problem, we still need to define what we mean by the cost \mathcal{J}_r of an identification experiment. In a closed-loop setting, this cost can be e.g. measured by the power \mathcal{P}_r of the excitation signal $r(t)$. However, we can also consider an alternative definition which seems closer to the actual cost of a closed-loop experiment. Suppose that the closed-loop presented in Figure 6.1 represents a production unit with a product $y(t)$. In normal operation the signals $u(t)$ (control signal) and $y(t)$ (the product) are given by: $y(t) = S_{id}v(t)$ and $u(t) = -C_{id}S_{id}v(t)$ ($v(t) = H_0(z)e(t)$). By applying an external signal $r(t)$ to the loop during the identification, we introduce *disturbances* $y_r(t)$ and $u_r(t)$ on top of the normal operation signals such as shown in (6.2)-(6.3). Those disturbances induce a loss of production quality. Consequently, we can measure the cost caused by the application of a signal with power spectrum $\Phi_r(\omega)$ using the following cost function:

$$\begin{aligned} \mathcal{J}_r &= \beta_y \mathcal{P}_{y_r} + \beta_u \mathcal{P}_{u_r} \\ &= \beta_y \left(\frac{1}{2\pi} \int_{-\pi}^{\pi} \Phi_{y_r}(\omega) d\omega \right) + \beta_u \left(\frac{1}{2\pi} \int_{-\pi}^{\pi} \Phi_{u_r}(\omega) d\omega \right) \end{aligned} \quad (7.2)$$

$$= \frac{1}{2\pi} \int_{-\pi}^{\pi} (\beta_y |G_0(e^{j\omega})S_{id}(e^{j\omega})|^2 + \beta_u |S_{id}(e^{j\omega})|^2) \Phi_r(\omega) d\omega \quad (7.3)$$

where the scalars β_u and β_y can be freely chosen.

We are now able to formulate our optimal experiment design problem problem:

Least costly experiment design problem (fixed N). *Determine the power spectrum $\Phi_r(\omega)$ of the excitation signal $r(t)$ corresponding to the smallest cost \mathcal{J}_r while guaranteeing that the model $G(z, \hat{\theta}_N)$ and its uncertainty U identified with this excitation signal satisfies the accuracy constraint (7.1) at each ω .*

¹The control design procedure is chosen in such a way that the nominal performance $J(G(z, \hat{\theta}_N), C(\hat{\theta}_N), \omega)$ is (slightly) better than the acceptable performance level γ .

7.2 Convex formulation

The optimization problem presented above can be formulated as follows:

$$\min_{\Phi_r(\omega)} \mathcal{J}_r \quad (7.4)$$

subject to the constraints that, at each ω ,

$$J^2(G(z, \theta), C, \omega) < \gamma^2 \quad \forall \theta \in U \quad (7.5)$$

Let us first note that the objective function \mathcal{J}_r (see (7.3)) of this optimization problem is a linear function of the decision variable $\Phi_r(\omega)$. Moreover, we have also seen in Section 6.3 that the constraint (7.5) can be transformed into an equivalent constraint (6.17) that can be rewritten as:

$$\exists \xi > 0 \text{ such that } \xi \mathcal{A}(\gamma^2, C) - \mathcal{B}(P_\theta^{-1}, \hat{\theta}_N) < 0 \quad (7.6)$$

Since \mathcal{B} is linear in P_θ^{-1} , (7.6) is thus an LMI constraint linear in the inverse P_θ^{-1} of the covariance matrix (γ^2 being here a given constant). If we further observe that P_θ^{-1} is affine in the design variable $\Phi_r(\omega)$ (see (6.6)), we can thus conclude that the constraint (7.5) can be replaced by an equivalent LMI constraint affine in the decision variable $\Phi_r(\omega)$. Consequently, the optimization problem boils down to a convex LMI optimization problem.

Before being able to use this optimization problem to design the least costly identification experiment, we have nevertheless to resolve a couple of issues related to this optimization problem. The first issue is that this optimization problem has an infinite number of constraints since (7.5) must hold at each frequency. Even though more elaborated solutions exist (see e.g. J.07), the easiest and more efficient way to circumvent this issue is to grid the frequency range in order to obtain a finite number of constraints. A second issue is the fact that the constraint (7.6) depends on unknown variables: the to-be-identified parameter vector $\hat{\theta}_N$ (via $C = C(\hat{\theta}_N)$ and \mathcal{B}) and the true parameter vector θ_0 (via P_θ^{-1} ; see (6.6)). The cost \mathcal{J}_r (see (7.3)) is also function of θ_0 . This is the well-known chicken-and-egg problem related to each optimal experiment design problem: see e.g. [33]. To circumvent this issue, θ_0 and $\hat{\theta}_N$ are replaced by an initial estimate θ_{init} of the parameter vector of the underlying system². This initial estimate can be obtained by performing, prior to the design of the optimal experiment, a short identification experiment with e.g. white noise. For more elaborated techniques to circumvent the chicken-and-egg problem, we refer the reader to J.07 and [13, 41].

Remark 1. Until now, we have considered the duration N of the identification experiment as fixed a-priori. The reason for this is the fact that N and $\Phi_r(\omega)$ appears as a product in the expression (6.6) of P_θ^{-1} . However, if we want to also consider N as a design variable, a good approach is to determine, with the

²The constraint (7.5) is also function of the unknown noise variance σ_e^2 . This variance has also to be replaced by some estimate $\sigma_{e,init}^2$.

optimization problem (7.4)-(7.5), the optimal spectrum $\Phi_r(\omega)$ for different values of the length N . Since, for increasing values of N , the optimal cost function \mathcal{J}_r will decrease, such approach allows one to find the *optimal* combination for the duration of the identification and the induced cost \mathcal{J}_r . It is also to be noted that, if the controller C_{id} is sufficiently complex, (7.5) can be satisfied with no excitation at all (i.e. $\Phi_r(\omega) = 0 \forall \omega$) once N is chosen larger than a certain value. This concept of *costless identification* is further developed in J.07 and J.12 and has been tested by Shardt and Huang on an experimental setup in [48].

Remark 2. In order to solve the optimization problem (7.4)-(7.5), the spectrum $\Phi_r(\omega)$ must be parametrized. This parametrization must be linear for the optimization problem to remain convex and it must allow one to easily realize an excitation sequence $r(t)$ having that spectrum. Different parametrizations having these features are available and lead to excitation sequences under the form of filtered white noises or multisines i.e. the signals that are generally used in system identification (see [32, 27] or J.07 for more details).

7.3 Shaping the spectrum

As already mentioned previously, an important property of the optimal identification experiment framework presented above is the a-priori guarantee that the uncertainty of the identified model will be small enough for the design of a satisfactory robust controller. Another important property, though, is the objective of designing experiments that are perturbing as little as possible the normal operations of the system. Using the parametrizations discussed in Remark 2 above, this optimization of the identification cost is achieved by appropriately shaping the power spectrum of the excitation signal over the frequencies, rather than using a common white noise excitation. Shaping the spectrum can be quite beneficial as shown in the following two figures extracted from the paper J.18. In these figures, the perturbation y_r induced by the excitation signal r on the output of the system (see (6.2)) is represented for four different experiments on the same closed loop. All these four experiments are the solution of a least costly design (7.4)-(7.5) and thus leads to an uncertainty region which is just small enough for the design of a robust controller. The two experiments in Figure 7.1 have both a duration $N = 500$, but, in the bottom plot, the spectrum $\Phi_r(\omega)$ is constrained to be flat (white noise) while, in the top plot, the spectrum has been shaped in frequency by the optimization problem. In Figure 7.2, the top plot pertains to a flexible spectrum $\Phi_r(\omega)$ and $N = 500$ and the bottom plot pertains to $N = 1000$ and a flat spectrum. We observe that shaping the spectrum allows to reduce the perturbation y_r significantly (Figure 7.1) or to reduce the identification duration by a factor two (Figure 7.2). Other illustrative examples can be found in J.18 and in [2].

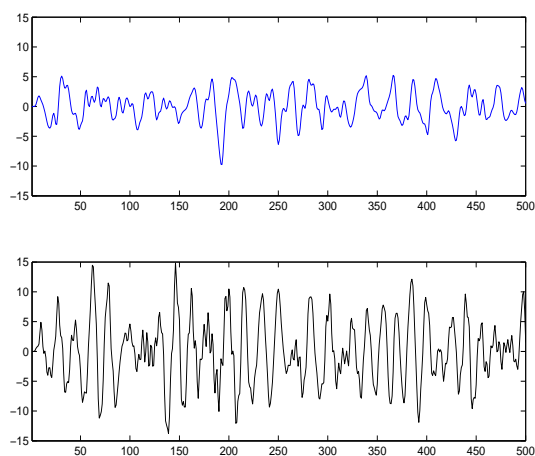


Figure 7.1: Induced output perturbation $y_r(t)$ corresponding to a flexible spectrum (top) and to a flat spectrum (bottom) for $N = 500$

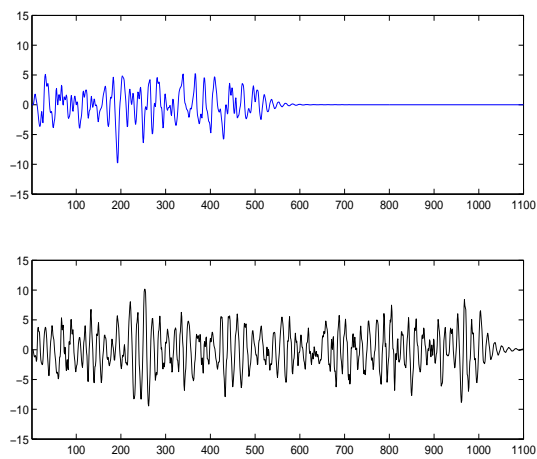


Figure 7.2: Induced output perturbation $y_r(t)$ corresponding to a flexible spectrum and $N = 500$ (top) and to a flat spectrum and $N = 1000$ (bottom)

7.4 Extensions

As in the previous chapter, we have supposed when presenting the least costly framework that the identification experiment is performed in a full-order model structure \mathcal{M} . The least costly framework has nevertheless been also extended to the case where the identification is performed in a reduced-order model structure (see C.28 for more details). Another assumption in the previous sections is that the true system is SISO and that the performance is measured in the H_∞ framework. The framework can nevertheless be extended to the MIMO case (see J.09) and to H_2 performance measures (see J.13). As shown in Section 6.3, the separation of graph theorem allows us in these cases to derive a constraint which implies (7.1) and that can be used in an optimization problem. As shown in J.09 and J.13, this constraint is unfortunately bilinear in P_θ^{-1} and the multipliers (these multipliers are also decision variables of the optimization problem). Consequently, the optimization problem (7.4)-(7.5) has to be solved in an iterative way (see J.09 and J.13 for more details).

The performance measures that are proposed in [22] and that are approximated by a Taylor expansion can also be used in the least costly framework. Indeed, the constraint (7.5) can in this case be replaced by the following LMI constraint linear in P_θ^{-1} (see Section 6.3):

$$\gamma^2 P_\theta^{-1} > R_{\hat{\theta}_N, C} \quad (7.7)$$

As mentioned in Section 6.2, these measures are also appropriate for controllers C that are nonlinear. However, if the controller C_{id} is also nonlinear, the optimal excitation spectrum can no longer be determined because P_θ^{-1} is no longer an affine relation of $\Phi_r(\omega)$. Indeed, if we inspect (6.6), we observe that this affine relation relies on the LTI sensitivity function S_{id} of the loop $[C_{id} G_0]$. Such an LTI sensitivity function does no longer exist if C_{id} is nonlinear (e.g. a MPC controller).

One simple solution to the issue of a nonlinear C_{id} is of course the approximation consisting of linearizing this nonlinear controller. Another solution to this problem is the so-called *stealth excitation*. The idea behind this concept is to ensure that the excitation $r(t)$ affects the true system in an open-loop fashion. Our objective is thus to have the following relations:

$$y(t) = G_0(z)r(t) + y_e(t)$$

$$u(t) = r(t) + u_e(t)$$

where $y_e(t)$ and $u_e(t)$ correspond to the output and input signals that would be generated by the closed loop if there was no excitation $r(t)$. Such relations can be obtained by modifying the feedback term: instead of feeding back $y(t)$ to the controller, we feed back $y(t) - G_0(z)r(t)$. We ensure in this way that the nonlinear controller C_{id} does not “see” $r(t)$ via the feedback term. Because of that, the inverse of the covariance matrix becomes affine in the spectrum $\Phi_r(\omega)$ and has the following expression:

$$P_\theta^{-1} = \left(\frac{N}{\sigma_e^2} \frac{1}{2\pi} \int_{-\pi}^{\pi} \bar{F}_r(e^{j\omega}) \bar{F}_r(e^{j\omega})^* \Phi_r(\omega) d\omega \right) + M_e$$

with $\bar{F}_r(z) = \frac{\Lambda_G(z, \theta_0)}{H_0}$ and M_e a matrix corresponding to the term u_e and y_e in the data. The matrix M_e can be evaluated via an experiment when $r = 0$ or neglected for experiment design since $M_e \geq 0$.

The modified feedback term (i.e. $y(t) - G_0(z)r(t)$) is a function of the unknown true system G_0 . Consequently, to realize the stealth excitation, we replace G_0 by an initial estimate $G_{init} = G(z, \theta_{init})$ in this modified feedback term. We follow in this way a similar approach as in Section 7.2 for the least costly experiment design problem. The stealth excitation procedure is illustrated in Figure 7.3. Note that ABB, our partner in the Autoprofit project, has submitted a patent to protect this idea (see B.01).

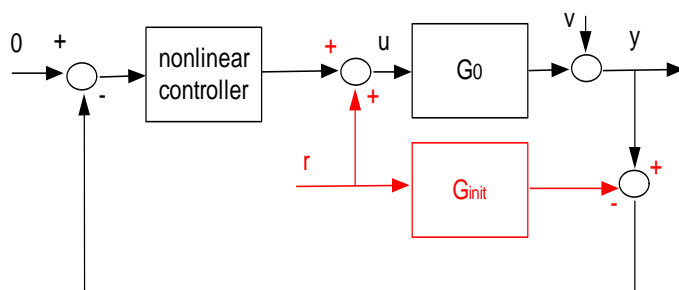


Figure 7.3: Stealth excitation r in the presence of a nonlinear controller C_{id}

Besides the stealth excitation, another solution specifically pertains to a controller C_{id} which is a MPC controller [34]. A MPC controller is nonlinear because it deals with input and output constraints. To obtain a tractable expression of P_θ^{-1} when C_{id} is a MPC controller, we propose another excitation setting. The classical setting (see Figure 6.1) consists of an excitation signal r added at the output of the controller C_{id} . In the new setting, it is the MPC controller C_{id} itself that produces both the control action and the excitation. For this purpose, we use the fact that a MPC controller is in essence an optimization algorithm subject to constraints. We indeed modify the MPC controller algorithm by adding the additional constraint that (7.7) has to be satisfied after the identification duration N . This approach remains a least costly approach since the modified MPC controller will still minimize a cost function aiming at reducing the variance of the input and the output of the system, and it will at the same time guarantee that the input-output data are sufficiently informative to obtain a model with sufficiently small uncertainty for control. From a technical point of view, integrating (7.7) as an extra constraint to the MPC algorithm is quite a challenge (e.g. the design variable is here the actual input sequence $u(t)$ and no longer a spectrum). Preliminary results are however presented in C.58.

Both stealth excitation and this modified MPC controller setting require further investigation. This will be one of the objectives of the PhD project of Max Potters (see Section 3.2).

7.5 Conclusions

With the optimal experiment design framework presented in this chapter, we are able to design cheap identification experiments for control. In theory, if the optimal identification experiment is performed, the identified model $G(z, \hat{\theta}_N)$ can be used to design the controller C and this controller is guaranteed to stabilize and to achieve sufficient performance with all systems in the uncertainty region \mathcal{D} identified along with the model. It is nevertheless always a good idea to perform on this controller the controller validation for stability and for performance presented in Chapter 6. We have indeed used some approximations in the optimal experiment design problem (e.g. the use of an initial estimate θ_{init} instead of θ_0 and $\hat{\theta}_N$).

The least costly identification experiment framework is currently tested in an industrial environment (i.e. at the sites of Boliden and Sasol) within the Autoprofit projet.

Chapter 8

Closed-loop performance diagnosis

8.1 Problem statement

In this chapter, we suppose that a model-based controller $C(\theta_{com})$ has been designed from an identified model $\{G(z, \theta_{com}), H(z, \theta_{com})\}$ of the true system $\{G_0 H_0\}$ (using e.g. the techniques of Chapters 6 and 7). In the sequel, we will call *commissioning* the period when the controller $C(\theta_{com})$ has been designed. We will assume that the objective of this controller is to reject the disturbance $v(t) = H_0(z)e(t)$ and that, at commissioning, the closed-loop performance was satisfactory (variances of the input and output signals were reasonably small in accordance with some pre-specified requirements).

This chapter considers the problem of the maintenance of the model-based control system over time. It is indeed important to maintain over time the satisfactory performance observed at commissioning. The performance of the closed-loop system can indeed be modified by changes in the true system $\{G_0 H_0\}$. Both the plant G_0 and the characteristics of the disturbance $v(t)$ can indeed change over time.

The performance of the closed-loop system can easily be monitored by estimating the present input/output variances and verifying whether the performance requirements are still satisfied (see [25] or D.01, D.02, D.03 for more details). If a performance drop is observed, a performance diagnosis step is necessary to determine whether the cause of this performance drop is¹ a change in disturbance characteristics (hypothesis \mathcal{H}_0) or a controller-relevant plant change (hypothesis \mathcal{H}_1). The closed-loop performance diagnosis problem can thus be considered as an hypothesis test [29]. As mentioned in Chapter 5, the distinction between \mathcal{H}_0 and \mathcal{H}_1 is necessary since these two causes will have different remedies. In the case of \mathcal{H}_0 , a controller retuning is often sufficient to restore the initial performance. In the case of \mathcal{H}_1 , a plant re-identification will have to be performed to be able to retune the controller and restore the initial perfor-

¹We assume that other causes such as sensor/actuator failures have been ruled out using available algorithms/methods.

mance. Since a plant re-identification is much more involved/expensive than a simple retuning, it is beneficial to decide such re-identification only when \mathcal{H}_1 is the most likely hypothesis.

The to-be-developed diagnosis step must be able to accurately distinguish between a (closed-loop) performance drop due to a plant change or due to a disturbance change. We will make no assumption on the possible plant or disturbance changes that may occur. In this respect, our work is different from the work presented e.g. in [37, 47]. Note finally that we are here not interested in detecting any plant change, but only those plant changes leading to a decrease of closed-loop performance. The diagnosis problem under consideration is thus different from the one considered e.g. in [4, 5, 3, 26, 28].

Our diagnosis procedure can nevertheless be related to the work in [19, 51]. Such as in these two papers, the diagnosis step we have developed is based on a cheap identification of the true system. By “cheap”, we mean an identification whose economical costs are much smaller than the full re-identification necessary for performance restoration. The advantage of using an identification approach as the basis for the diagnosis step is that the data collected for this diagnosis experiment can also be used for the (eventual) full re-identification step and therefore reduce the cost of this subsequent step. Besides the identification of a model, another similarity with [19, 51] is the introduction of a set $\mathcal{D}_{adm}(C(\theta_{com}))$ allowing to distinguish \mathcal{H}_0 and \mathcal{H}_1 . In our framework, the set $\mathcal{D}_{adm}(C(\theta_{com}))$ contains all plant transfer functions G resulting in a satisfactory closed-loop performance with the controller $C(\theta_{com})$ under the original disturbance level (or, more precisely, delivering satisfactory performance for the set of disturbance spectra considered as realistic at commissioning). Combining the identified model \hat{G}_N^{det} and the set $\mathcal{D}_{adm}(C(\theta_{com}))$, we introduced the following decision rule: if the identified model \hat{G}_N^{det} is outside of $\mathcal{D}_{adm}(C(\theta_{com}))$, we conclude that a plant change is the root cause of the performance drop and conversely we conclude that a change in the disturbance characteristics is the cause of the performance drop when $\hat{G}_N^{det} \in \mathcal{D}_{adm}(C(\theta_{com}))$.

Another important contribution of this chapter is to tackle the problem of optimal experiment design for the diagnosis problem at stake. This optimal design is done in the least-costly context i.e. the cost of the diagnosis experiment will be minimized while guaranteeing a certain pre-specified accuracy for the diagnosis. It is indeed important to ensure an optimal trade-off between the contradictory objectives of obtaining an accurate diagnosis, on the one hand, and of obtaining a cheap diagnosis experiment, on the other hand (especially with respect to the re-identification experiment). Moreover, due to the fact that diagnosis and re-identification experiment are quite closely intertwined, the proposed experiment design framework considers the design of both the diagnosis experiment and a possible re-identification experiment (when \mathcal{H}_1 is true).

Such as in the previous chapters, we will present the mathematical framework for a SISO true system (see (6.1)) and we will measure the performance according to the H_∞ framework. Note nevertheless that the proposed closed-

loop performance diagnosis method can be readily extended to MIMO systems and other performance measures as shown in D.04 (see Chapter 4).

8.2 Performance diagnosis

8.2.1 Hypothesis testing framework

The H_∞ control framework is adopted to quantify the ability of the controller $C(\theta_{com})$ in rejecting the disturbance $v(t) = H_0(z)e(t)$ that was present at commissioning. For this purpose, we can use the performance measure (6.12) with $T(G, C)$ defined as the matrix containing the weighted closed-loop transfer functions, (see (6.11)). The weights in (6.11) can be selected such that the performance measure is stated as a weighted function of $\frac{C}{1+GC}$ and $\frac{1}{1+GC}$. This enables relating the disturbance $v(t)$ to the inputs and outputs, respectively. More particularly, we will assume that these weights have been chosen in such a way that a loop $[C(\theta_{com}) G]$ that satisfies² $J(G, C(\theta_{com}), \omega) < 1 \forall \omega$ reject satisfactorily the disturbance $v(t)$ that was present **at commissioning**.

To shorten the notations, we define $J(G, C)$ as the H_∞ norm of $T(G, C)$:

$$J(G, C) = \sup_{\omega} J(G, C, \omega) \quad (8.1)$$

Consequently, we can say that a loop $[C(\theta_{com}) G]$ satisfying $J(G, C(\theta_{com})) < 1$ is a loop that is able to reject sufficiently the disturbances as they were at commissioning.

Next, the sets $\mathcal{D}_{adm}(C(\theta_{com}))$ and $\mathcal{V}_J(C(\theta_{com}))$ are defined in order to formulate the closed-loop performance diagnosis method.

Definition 1. $\mathcal{D}_{adm}(C(\theta_{com}))$ is defined as the set of all transfer functions G that are stabilized by $C(\theta_{com})$ and lead to the nominal performance level $J(G, C(\theta_{com})) < 1$.

Definition 2. The set $\mathcal{V}_J(C(\theta_{com}))$ contains the power spectra Φ_v of all disturbances $v(t)$ that are sufficiently rejected by all loops $[C(\theta_{com}) G]$ satisfying $J(G, C(\theta_{com})) < 1$. A disturbance $v(t)$ with spectrum Φ_v is considered to be sufficiently rejected by a loop $[C G]$ if the input and output signals have a reasonably small variance in accordance with some pre-specified requirements.

Definitions 1 and 2 suggest that the closed-loop performance of a loop $[C(\theta_{com}) G]$ is satisfactory only when $G \in \mathcal{D}_{adm}(C(\theta_{com}))$ and $\Phi_v \in \mathcal{V}_J(C(\theta_{com}))$. At commissioning, $G_0 \in \mathcal{D}_{adm}(C(\theta_{com}))$ and $\Phi_v \in \mathcal{V}_J(C(\theta_{com}))$ (the closed-loop performance is indeed assumed to be satisfactory at commissioning). However, the plant dynamics G_0 and/or the disturbance spectrum Φ_v may change over time, possibly leading to closed-loop performance deterioration. In the event of

²Here the performance threshold is chosen equal to one. It could also have been chosen equal to γ as in the previous chapters.

an observed performance drop (increased input/output variances), one of the following scenarios holds:

1. G_0 remains in $\mathcal{D}_{adm}(C(\theta_{com}))$, while the disturbance spectrum no longer lies in $\mathcal{V}_J(C(\theta_{com}))$. This implies that the performance drop is due to changes in disturbance characteristics.
2. G_0 has moved outside $\mathcal{D}_{adm}(C(\theta_{com}))$, suggesting that the performance drop is due to changes in plant dynamics.

Hence, using the set $\mathcal{D}_{adm}(C(\theta_{com}))$, the hypothesis test pertaining to the closed-loop performance diagnosis problem is formulated as:

$$\begin{aligned} \mathcal{H}_0 : G_0 &\in \mathcal{D}_{adm}(C(\theta_{com})) \\ \mathcal{H}_1 : G_0 &\notin \mathcal{D}_{adm}(C(\theta_{com})). \end{aligned} \tag{8.2}$$

Equation (8.2) pertains to the considered performance diagnosis test, as it indicates that the observed performance is due to a change in disturbance spectrum when hypothesis \mathcal{H}_0 is true and due to a control-relevant plant change when \mathcal{H}_1 is true.

Remark 1. When \mathcal{H}_0 is the correct hypothesis, G_0 may not be the same as the plant dynamics at commissioning. The hypothesis test (8.2) indicates that the changes in G_0 (if there are any) do not lead to a performance drop. When \mathcal{H}_1 is the correct hypothesis, the disturbance spectrum may have also moved outside $\mathcal{V}_J(C(\theta_{com}))$. In this case, another hypothesis test can be performed in a similar manner as above to distinguish between $\Phi_v \in \mathcal{V}_J(C(\theta_{com}))$ and $\Phi_v \notin \mathcal{V}_J(C(\theta_{com}))$.

Remark 2. As mentioned in the introduction, this closed-loop performance diagnosis method is inspired by [51, 19]. However, in [51], the objective is performance monitoring (detection of a performance drop) and not performance diagnosis (detection of the cause of the performance drop). The main differences with [19] is in the definition of the performance measure and in the disturbance description. In [19], the performance is indeed measured in terms of closed-loop stability margins, while we use here a more general closed-loop performance description using an H_∞ control setting³. In addition, our framework exploits a fully stochastic setting for disturbances, whereas deterministic disturbances are considered in [19].

8.2.2 Decision rule

To discriminate between the two hypotheses stated in (8.2), we will use a model of the unknown true plant G_0 identified in a full-order model structure. For this purpose, the closed-loop identification procedure of Section 6.1 can be followed and applied to the loop $[C(\theta_{com}) G_0]$. An excitation signal $r(t) = r_{det}(t)$

³Note also that our framework has also been extended to a large variety of other performance measures in D.04.

($t = 1 \dots N$) having a spectrum $\Phi_{r,det}$ is thus applied to this loop and data $\{u(t), y(t) | t = 1, \dots, N\}_{det}$ are collected. Let us denote by $\hat{\theta}_N^{det}$ the parameter vector identified with these data using the criterion (6.4), and by $P_{\hat{\theta}_N^{det}}$ its covariance matrix. Let us also introduce the notation $\mathcal{I}(\theta_0, \Phi_{r,det})$ to emphasize the dependence of $P_{\hat{\theta}_N^{det}}^{-1}$ on θ_0 and $\Phi_{r,det}$ (see (6.6)): $P_{\hat{\theta}_N^{det}}^{-1} \triangleq \mathcal{I}(\theta_0, \Phi_{r,det})$. Recall also that $\hat{\theta}_N^{det} \sim \mathcal{N}(\theta_0, P_{\hat{\theta}_N^{det}})$ asymptotically.

Once a model $\hat{G}_N^{det} = G(z, \hat{\theta}_N^{det})$ of the true plant is obtained, it can be utilized to choose between the hypotheses \mathcal{H}_0 and \mathcal{H}_1 (see (8.2)). The following decision rule is proposed to perform the hypothesis test

$$\begin{aligned} \hat{G}_N^{det} \in \mathcal{D}_{adm}(C(\theta_{com})) &\Rightarrow \text{choose } \mathcal{H}_0 \\ \hat{G}_N^{det} \notin \mathcal{D}_{adm}(C(\theta_{com})) &\Rightarrow \text{choose } \mathcal{H}_1. \end{aligned} \quad (8.3)$$

Note that verifying that $\hat{G}_N^{det} \in \mathcal{D}_{adm}(C(\theta_{com}))$ and $\hat{G}_N^{det} \notin \mathcal{D}_{adm}(C(\theta_{com}))$ can be straightforwardly done by evaluating if $J(\hat{G}_N^{det}, C(\theta_{com})) < 1$ and $J(\hat{G}_N^{det}, C(\theta_{com})) \geq 1$, respectively.

The decision rule (8.3) may lead to erroneous decisions since \hat{G}_N^{det} is an estimate of the true plant G_0 . The null hypothesis \mathcal{H}_0 may be chosen erroneously when $\hat{G}_N^{det} \in \mathcal{D}_{adm}(C(\theta_{com}))$ has been generated by $G_0 \notin \mathcal{D}_{adm}(C(\theta_{com}))$. This is in effect a wrong decision since the performance drop is not due to variations in disturbance characteristics, but due to changes in plant dynamics. Conversely, the choice of the alternative hypothesis \mathcal{H}_1 is erroneous when $G_0 \in \mathcal{D}_{adm}(C(\theta_{com}))$.

In hypothesis testing, the accuracy of the decision rule is determined by two probabilities: the probability $Pr_{\mathcal{H}_0}$ of deciding \mathcal{H}_0 when \mathcal{H}_0 is true and the probability $Pr_{\mathcal{H}_1}$ of deciding \mathcal{H}_1 when \mathcal{H}_1 is true

$$Pr_{\mathcal{H}_0} \triangleq Pr\{\hat{G}_N^{det} \in \mathcal{D}_{adm}(C(\theta_{com})) | G_0 \in \mathcal{D}_{adm}(C(\theta_{com}))\} \quad (8.4)$$

$$Pr_{\mathcal{H}_1} \triangleq Pr\{\hat{G}_N^{det} \notin \mathcal{D}_{adm}(C(\theta_{com})) | G_0 \notin \mathcal{D}_{adm}(C(\theta_{com}))\}. \quad (8.5)$$

The probability $Pr_{\mathcal{H}_1}$ is called *detection rate*, whereas the probability $1 - Pr_{\mathcal{H}_0}$ is called *false alarm rate* [29]. Clearly, both probabilities $Pr_{\mathcal{H}_0}$ and $Pr_{\mathcal{H}_1}$ should be high for the hypothesis test to be accurate. The probabilities depend not only on the (unknown) true plant dynamics G_0 when the diagnosis experiment is performed⁴, but also on the design of excitation signal used in the diagnosis experiment. Indeed, a diagnosis experiment leading to a model \hat{G}_N^{det} very close to G_0 will increase both probabilities. In Section 8.3, the diagnosis experiment will be designed optimally to guarantee pre-specified values for both probabilities $Pr_{\mathcal{H}_0}$ and $Pr_{\mathcal{H}_1}$. Next, the to-be-performed actions after closed-loop performance diagnosis are discussed.

⁴In other words, $Pr_{\mathcal{H}_0}$ and $Pr_{\mathcal{H}_1}$ will be different for different plant changes.

8.2.3 After performance diagnosis

When an observed performance drop is due to changes in disturbance characteristics (\mathcal{H}_0 is the correct hypothesis), it can be decided to let the controller intact (as disturbance changes are often temporary) or to restore the closed-loop performance by retuning the controller using the knowledge of the new disturbance characteristics $\hat{H}_N^{det} = H(z, \hat{\theta}_N^{det})$ identified along with \hat{G}_N^{det} . On the contrary when an observed performance drop is due to a control-relevant plant change (\mathcal{H}_1 is chosen in (8.3)), the controller should be redesigned based on a model of the new plant dynamics G_0 to restore the closed-loop performance to its nominal level. As the model $\{\hat{G}_N^{det}, \hat{H}_N^{det}\}$ may not be sufficiently accurate for redesigning the controller, the diagnosis step is typically proceeded with another identification step when \mathcal{H}_1 is the true hypothesis. In this case, a new excitation signal $r_{id}(t)$ is applied to the closed-loop system to collect the data set⁵ $\{u(t), y(t) | t = 1, \dots, N\}_{id}$.

Since the proposed performance diagnosis method relies on system identification, a link is established between the diagnosis step and the plant re-identification step. This is done by identifying the model $\{\hat{G}_N^{id}(z), \hat{H}_N^{id}(z)\}$ not only based on the data $\{u(t), y(t) | t = 1, \dots, N\}_{id}$, but also using the data $\{u(t), y(t) | t = 1, \dots, N\}_{det}$ obtained during diagnosis. This can be done by using $\hat{\theta}_N^{det}$ and its covariance $P_{\hat{\theta}_N^{det}}$ in a regularization term. Hence, the parameter vector of the re-identified plant model $\{\hat{G}_N^{id} = G(z, \hat{\theta}_N^{id}), \hat{H}_N^{id} = H(z, \hat{\theta}_N^{id})\}$ is determined by

$$\hat{\theta}_N^{id} = \arg \min_{\theta} \frac{1}{N} \left(\sum_{t=1}^N \epsilon^2(t, \theta) + \left\| \theta - \hat{\theta}_N^{det} \right\|_{P_{\hat{\theta}_N^{det}}^{-1}}^2 \right) \quad (8.6)$$

where $\epsilon(t, \theta)$ is computed using $\{u(t), y(t)\}_{id}$. The covariance matrix of $\hat{\theta}_N^{id}$ is given by

$$P_{\hat{\theta}_N^{id}} = \left(\mathcal{I}(\theta_0, \Phi_{r,id}) + \underbrace{\mathcal{I}(\theta_0, \Phi_{r,det})}_{P_{\hat{\theta}_N^{det}}^{-1}} \right)^{-1} \quad (8.7)$$

with $\mathcal{I}(\cdot, \cdot)$ as defined in Section 8.2.2. Using both data sets to identify $\hat{\theta}_N^{id}$ will enable us to increase the accuracy of $\hat{\theta}_N^{id}$ with respect to the situation where only $\{u(t), y(t) | t = 0, \dots, N-1\}_{id}$ would be used. Note that $P_{\hat{\theta}_N^{det}}^{-1}$ is an affine function of both $\Phi_{r,id}$ and $\Phi_{r,det}$ (the spectra of the excitation signals r_{id} and r_{det}).

Next, a unified experiment design framework is presented for designing diagnosis and re-identification experiments where requirements on the diagnosis accuracy are considered along with the requirement on accuracy of the to-be-re-identified model.

⁵For simplicity, it is assumed that the measurement sets $\{u(t), y(t)\}_{det}$ and $\{u(t), y(t)\}_{id}$ have the same length N .

8.3 Experiment Design Framework

The objective of experiment design is to design the spectra $\Phi_{r,det}$ and $\Phi_{r,id}$ ⁶ of the excitation signals $r_{det}(t)$ and $r_{id}(t)$ in such a way that the total economical cost of performance diagnosis and (possible) plant re-identification is minimized while guaranteeing the accuracy of performance diagnosis and, if \mathcal{H}_1 is true, the accuracy of the to-be-re-identified model $\hat{G}_N^{id}(z)$. We will use the same definition for the cost of an experiment as in the previous chapter (see (7.3)) and we will use the notation $\mathcal{J}_r(\Phi_r(\omega), \theta_0)$ for this cost to emphasize its dependence on $\Phi_r(\omega)$ and θ_0 .

The total economical cost of the performance diagnosis and plant re-identification procedure following an observed performance drop depends on the outcome of the hypothesis test (8.3). In the case where \mathcal{H}_0 is true, the cost will only be equal to the cost of the diagnosis experiment (i.e. $\mathcal{J}_r(\Phi_{r,det}, \theta_0)$). In the case where \mathcal{H}_1 is true, the cost will be equal to the sum of the costs of both diagnosis and re-identification experiments (i.e. $\mathcal{J}_r(\Phi_{r,det}, \theta_0) + \mathcal{J}_r(\Phi_{r,id}, \theta_0)$). However since the cause of an observed performance drop is not known a priori, the experiment design should be performed considering that both hypotheses can be true. In addition, the experiment cost in both cases of \mathcal{H}_0 and \mathcal{H}_1 depends on the unknown true plant parametrized by θ_0 . In S.02 and C.53, we have addressed this problem using a so-called two scenario approach. The two scenario approach will deliver an a-priori estimate $\theta_{0,\mathcal{H}_0}^{init}$ of θ_0 for the case where \mathcal{H}_0 is true and an a-priori estimate $\theta_{0,\mathcal{H}_1}^{init}$ of θ_0 for the case where \mathcal{H}_1 is true⁷. These two estimates can then be used to evaluate the costs of the experiments.

Another important consideration related to the existence of two hypotheses is to determine which cost should be minimized in the optimal experiment design. In this work, the cost $\mathcal{J}_r(\Phi_{r,det}, \theta_{0,\mathcal{H}_1}^{init}) + \mathcal{J}_r(\Phi_{r,id}, \theta_{0,\mathcal{H}_1}^{init})$ (corresponding to \mathcal{H}_1) is minimized, while constraining the cost $\mathcal{J}_r(\Phi_{r,det}, \theta_{0,\mathcal{H}_0}^{init})$ (corresponding to \mathcal{H}_0) to be smaller than a given threshold β , (i.e., $\mathcal{J}_r(\Phi_{r,det}, \theta_{0,\mathcal{H}_0}^{init}) < \beta$). The threshold β should be chosen such that it is (much) smaller than the cost of plant re-identification. Next, the quality objectives for the two to-be-designed experiments are described.

As mentioned in Section 8.2.2, one objective of the experiment design is to guarantee that the probabilities $Pr_{\mathcal{H}_0}$ and $Pr_{\mathcal{H}_1}$ are higher than user-specified values α_0 and α_1 :

$$Pr\{\hat{G}_N^{det} \in \mathcal{D}_{adm}(C(\theta_{com})) | G_0 \in \mathcal{D}_{adm}(C(\theta_{com}))\} \geq \alpha_0 \quad (8.8)$$

⁶The length of the experiments are supposed fixed a priori.

⁷The estimate $\theta_{0,\mathcal{H}_0}^{init}$ for \mathcal{H}_0 is obtained by assuming that $G_0 = G(\theta_{com})$ and by identifying a model of H_0 under this assumption. Conversely, the estimate $\theta_{0,\mathcal{H}_1}^{init}$ for \mathcal{H}_1 is obtained by assuming that $H_0 = H(\theta_{com})$ and by identifying a model of G_0 under this assumption. Due to the fact that a part of the model structure is fixed a-priori, such identification can be performed using routine closed-loop data. These data can e.g. be collected in the period between the detection of the performance drop and the decision to perform the diagnosis.

$$Pr\{\hat{G}_N^{det} \notin \mathcal{D}_{adm}(C(\theta_{com})) | G_0 \notin \mathcal{D}_{adm}(C(\theta_{com}))\} \geq \alpha_1. \quad (8.9)$$

Due to the dependence of the above constraints on the true plant, the a-priori estimates $\theta_{0,\mathcal{H}_0}^{init}$ and $\theta_{0,\mathcal{H}_1}^{init}$ (determined using the two scenario approach) can be used to rewrite (8.8)-(8.9) as follows:

$$Pr\{ J(G(z, \hat{\theta}_N^{det}), C(\theta_{com})) < 1 \mid \hat{\theta}_N^{det} \sim \mathcal{N}(\theta_0 \triangleq \theta_{0,\mathcal{H}_0}^{init}, P_{\hat{\theta}_N^{det}}) \} \geq \alpha_0 \quad (8.10)$$

$$Pr\{ J(G(z, \hat{\theta}_N^{det}), C(\theta_{com})) \geq 1 \mid \hat{\theta}_N^{det} \sim \mathcal{N}(\theta_0 \triangleq \theta_{0,\mathcal{H}_1}^{init}, P_{\hat{\theta}_N^{det}}) \} \geq \alpha_1 \quad (8.11)$$

Recall now that we are designing the diagnosis experiment. Consequently, $\hat{\theta}_N^{det}$ is an unknown random variable that is distributed as shown in (8.10)-(8.11). However, if we could build an uncertainty region \bar{U} that is guaranteed to contain $\hat{\theta}_N^{det}$ at a probability α_0 , the constraint (8.10) could be replaced by a more classical constraint: $J(G(z, \theta), C) < 1 \forall \theta \in \bar{U}$. Such uncertainty \bar{U} can be deduced using the distribution of $\hat{\theta}_N^{det}$:

$$\bar{U}(\theta_{0,\mathcal{H}_0}^{init}, P_{\hat{\theta}_N^{det}}^{-1}, \alpha_0) \triangleq \{ \theta \mid (\theta - \theta_{0,\mathcal{H}_0}^{init})^T P_{\hat{\theta}_N^{det}}^{-1} (\theta - \theta_{0,\mathcal{H}_0}^{init}) < \chi_{\alpha_0} \} \quad (8.12)$$

with $Pr(\chi^2(k) < \chi_{\alpha_0}) = \alpha_0$. Note the similarity/duality between this set \bar{U} and the set U (see (6.8)) that can be constructed after an identification experiment. The former is centered at the true parameter vector and contains the identified one at a certain probability, while the latter is centered at the identified parameter vector and contains the true parameter vector at a certain probability level. A similar approach can also be used to make (8.11) tractable. This leads to the following two constraints that are sufficient conditions for (8.10)-(8.11):

$$J(G(z, \theta), C(\theta_{com})) < 1 \quad \forall \theta \in \bar{U}(\theta_{0,\mathcal{H}_0}^{init}, \mathcal{I}_0, \alpha_0) \quad (8.13)$$

$$J(G(z, \theta), C(\theta_{com})) \geq 1 \quad \forall \theta \in \bar{U}(\theta_{0,\mathcal{H}_1}^{init}, \mathcal{I}_1, \alpha_1) \quad (8.14)$$

where $P_{\hat{\theta}_N^{det}}^{-1}$ is evaluated as $\mathcal{I}_0 = \mathcal{I}(\theta_{0,\mathcal{H}_0}^{init}, \Phi_{r,det})$ in (8.13) and as $\mathcal{I}_1 = \mathcal{I}(\theta_{0,\mathcal{H}_1}^{init}, \Phi_{r,det})$ in (8.14).

As mentioned in Section 8.1, in this experiment design framework, we do not want to restrict attention only to optimal diagnosis. Our objective is indeed to present an unified framework for diagnosis and re-identification. Consequently, in addition to the performance diagnosis constraints (8.13)-(8.14), an additional constraint is needed to guarantee that, if \mathcal{H}_1 happens to be true, the uncertainty of the to-be-re-identified model $G(z, \hat{\theta}_N^{id})$ will be sufficiently small for the design of a controller $C(\hat{\theta}_N^{id})$ that can replace the failing $C(\theta_{com})$ in the loop with the true system. Similarly as in Chapter 7, such a constraint can be expressed as follows⁸:

⁸Note that the performance weights in the definition (6.11) of T could be adapted based on $H(z, \hat{\theta}_N^{det})$.

$$J(G(z, \theta), C(\hat{\theta}_N^{id})) < 1 \quad \forall \theta \in U \triangleq \{\theta \mid (\theta - \hat{\theta}_N^{id})^T \mathcal{I}_{id} (\theta - \hat{\theta}_N^{id}) < \chi_{\alpha_{id}}\} \quad (8.15)$$

with $\mathcal{I}_{id} = \mathcal{I}(\theta_{0, \mathcal{H}_1}^{init}, \Phi_{r, det}) + \mathcal{I}(\theta_{0, \mathcal{H}_1}^{init}, \Phi_{r, id})$. Note that we here consider the ellipsoid U as defined in (6.8) and containing θ_0 with an user-chosen probability level α_{id} . Note that the unknown $\hat{\theta}_N^{id}$ must be replaced by an initial estimate of the parameter vector we would identify if \mathcal{H}_1 is true. A good candidate for this initial estimate is the parameter vector $\theta_{0, \mathcal{H}_1}^{init}$ estimated for the case \mathcal{H}_1 with the two-scenario approach.

We can now formulate our experiment design problem as an optimization problem:

$$\begin{aligned} \min_{\Phi_{r, det}, \Phi_{r, id}} \quad & \mathcal{J}_r(\Phi_{r, det}, \theta_{0, \mathcal{H}_1}^{init}) + \mathcal{J}_r(\Phi_{r, id}, \theta_{0, \mathcal{H}_1}^{init}) \\ \text{subject to} \quad & \mathcal{J}_r(\Phi_{r, det}, \theta_{0, \mathcal{H}_0}^{init}) < \beta \\ \text{and to} \quad & (8.13), (8.14) \text{ and } (8.15) \end{aligned} \quad (8.16)$$

The objective function and the first constraint of this optimization problem are linear in the decision variables $\Phi_{r, det}$ and $\Phi_{r, id}$ (see Chapter 7). The constraints (8.13) and (8.15) are equivalent from a technical point of view to the constraint (7.1) that we tackled in Chapter 7. The constraint (8.14) can be transformed (with some conservatism) as a constraint:

$$J(G(z, \theta), C(\theta_{com}), \omega^*) \geq 1 \quad \forall \theta \in U(\theta_{0, \mathcal{H}_1}^{init}, \mathcal{I}_1, \alpha_1) \quad (8.17)$$

for some well-chosen frequency⁹ ω^* and this constraint can also be transformed into an LMI in $\Phi_{r, det}$ using a similar procedure as the one presented in Section 6.3 for the constraint where J had to be smaller than one. Consequently, the optimization problem (8.16) can be reformulated as a convex optimization problem subject to LMI constraints.

8.4 Conclusions

In this chapter, we have presented an identification-based closed-loop performance diagnosis framework that can distinguish between a performance drop due to a change in disturbance characteristics (\mathcal{H}_0) and one due to a control-relevant plant change (\mathcal{H}_1). In addition, we have presented an optimization problem that allows to design cheap and accurate diagnosis experiments along with cheap and accurate re-identification experiments in the case where \mathcal{H}_1 happens to be true.

⁹To find the optimal frequency ω^* , the optimization problem (8.16) (with (8.17) instead of (8.14)) can be solved for different values of ω^* . The optimal frequency ω^* is the one resulting in the smallest objective function.

As concluding remarks, let us discuss how the results of the experiment design problem (8.16) can be implemented in practice. The outcomes of (8.16) are the optimal spectra $\Phi_{r,det}$ and $\Phi_{r,id}$. A signal r_{det} with spectrum $\Phi_{r,det}$ can thus be applied to the closed-loop system $[C(\theta_{com}) G_0]$ to perform the diagnosis experiment. Based on the collected data, a model \hat{G}_N^{det} of G_0 is identified and, subsequently, it is verified whether \hat{G}_N^{det} lies in $\mathcal{D}_{adm}(C(\theta_{com}))$ (see decision rule (8.3)).

If $\hat{G}_N^{det} \notin \mathcal{D}_{adm}(C(\theta_{com}))$, a plant re-identification should be performed. An excitation signal with spectrum $\Phi_{r,id}$ (determined together with $\Phi_{r,det}$) can be used for plant re-identification. Alternatively, the spectrum $\Phi_{r,id}$ can be re-designed using $\hat{\theta}_N^{det}$ as an estimate for the unknown $\hat{\theta}_N^{id}$ in (8.15). Clearly, the estimate $\hat{\theta}_N^{det}$ provides a more accurate description of the true system with respect to $\theta_{0,\mathcal{H}_1}^{init}$ which was used in (8.16) to approximate $\hat{\theta}_N^{id}$.

The model-based maintenance of control systems developed in this chapter is summarized in Figure 8.1.

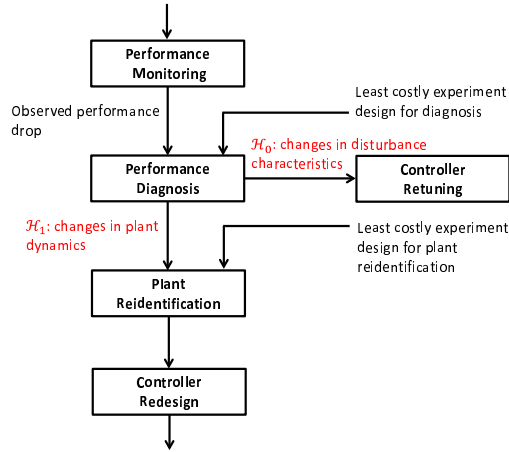


Figure 8.1: The proposed model-based maintenance of control systems

Chapter 9

Iterative model improvement for control

9.1 Problem statement

In this chapter, we consider the situation where we wish to improve the performance of a controller $C(M_1)$ designed with an initial model $M_1 = G(z, \hat{\theta}_1)$ of the true system. The least costly framework is an option to achieve this objective. As shown in Chapter 7, in this framework, a cheap identification experiment is performed on the system to obtain an identified model that is accurate enough for the design of a satisfactory controller i.e. a controller achieving a given closed-loop performance. Subsequently, a controller is designed with the identified model and applied to the true system.

When using this framework, even though the excitation signal is designed to be the least intrusive possible to guarantee the desired model accuracy, it could happen that even this smallest possible perturbation is too large to remain acceptable. One could in this case increase the duration N of the identification experiment (see Remark 1 in Section 7.2). However, the disadvantage would be then to keep the less performing controller $C(M_1)$ for a longer period. An elegant alternative to the least costly framework for these situations is to improve the model and also the controller throughout the lifetime of the closed loop via an excitation signal that may at all time be applied. The characteristics of this excitation signal are determined to maximize the overall control performance (see later) over the lifetime of the closed loop while guaranteeing at any time a minimal control performance. In this framework, there is thus no longer a clear separation between an identification phase and a control phase. Another characteristic of this new framework is that the desired performance has not to be specified a-priori by the user.

To achieve this objective, we will make the assumption that we a-priori know how long the closed loop will be operated at the current operating conditions. Given this assumption, we propose the following framework to improve the model and the controller throughout this period¹. We start by dividing this

¹Note that, instead of choosing this period as the entire lifetime of the closed loop, we can

period in n consecutive intervals. In each of these intervals, a specially tailored test signal can be applied (the characteristics of this signal can be different in each interval). After interval i , the informative data generated via r_i allows to reduce the uncertainty of the current model $M_i = G(z, \hat{\theta}_i)$. This yields a model $M_{i+1} = G(z, \hat{\theta}_{i+1})$ which is more accurate than M_i . The model M_{i+1} and its (reduced) uncertainty are then used to update the control action $C(M_{i+1})$ for the next learning interval $i + 1$. This procedure is illustrated in Figure 9.1.

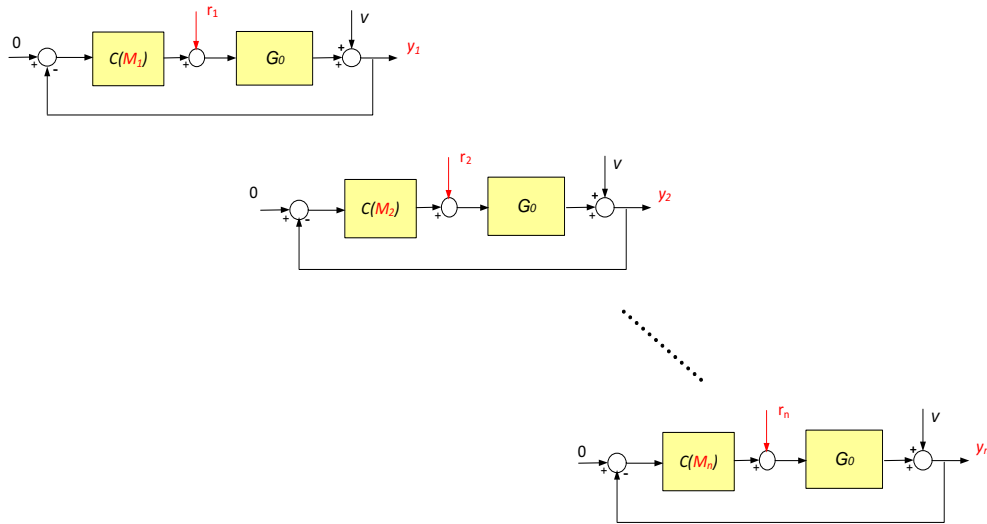


Figure 9.1: The n learning intervals with successive model updates and controller updates

It is important to stress the dual effect of the excitation signals r_i ($i = 1..n$). The application of r_i during interval i decreases the performance of this interval by inducing perturbations onto the normal operations. However, by decreasing the uncertainty of the model M_i , the application of r_i increases the performance of the next intervals.

To formalize our optimal experiment design problem, we characterize the closed-loop performance in each learning interval with a cost \mathcal{T}_i . The cost \mathcal{T}_i of the interval i is made up of two contributions. The first contribution is the *excitation cost* \mathcal{J}_{r_i} corresponding to the perturbations onto the normal operations caused by the excitation signal r_i . The second contribution is the *modeling error cost* \mathcal{V}_i corresponding to the performance loss caused by the uncertainty of the present model M_i from which the current controller $C(M_i)$ is designed.

As mentioned above, the power spectrum of the testing signals r_i ($i = 1..n$) have to be optimally designed in such a way that the overall performance over the n intervals is maximized while guaranteeing some minimal control quality in each learning interval. Maximizing the overall performance of the total period

also improve the model and the controller during a shorter period.

can be achieved by minimizing the sum $\sum_{i=1}^n \mathcal{T}_i$ of the costs of the n intervals. Moreover, enforcing a constraint on the minimal performance in each learning interval can also be easily realized by putting a threshold on the cost \mathcal{T}_i of each of these intervals. It is to be noted that the objective function $\sum_{i=1}^n \mathcal{T}_i$ somehow combines the objective function of the least costly framework via \mathcal{J}_{r_i} and, via \mathcal{V}_i , the one of the more classical optimal experiment design frameworks presented in e.g. [16]. Note also that the optimal design of the excitation signals r_i makes the proposed framework different from the iterative identification and control schemes developed in *identification for control* in the beginning of the nineties (see e.g. [44]). In those contributions, few attention was paid to the excitation signal.

Using the approach presented above, we will be able to determine the excitation signals r_i ($i = 1 \dots n$) for the n learning intervals before the start of the first learning interval. However, as also shown in Chapter 7, optimal identification experiment design requires information on the true system to design the optimal test signal(s). Consequently, the designed signals will be based on the information available at that moment (i.e. the model M_1) and could therefore be suboptimal. We consequently propose to only apply the test signal r_1 in the first interval and to redesign, before learning interval 2, the remaining test signals r_i ($i = 2 \dots n$) using a similar optimization problem, but now based on the more accurate information on the true system (i.e. model M_2). This redesign approach (which has a strong analogy with the *receding horizon mechanism* in model predictive control [34]) is repeated before each interval.

The possibility of applying this redesign mechanism is certainly one of the main advantages of the iterative procedure introduced in this chapter. Another advantage is of course the possibility to improve the performance as fast as possible even if this improvement is still limited after the first interval. Note that the choice of the duration of each learning interval is quite simple for plants which have to perform repetitive control actions (e.g. batch processes in the chemical industry and certain manipulators in robotics/mechatronics): the duration of one of these repeated actions is the duration of one interval. For other processes where this division is not so obvious, we have to make a trade-off between a too small number n (a situation where the plant will be operated for a long time with the controller $C(M_1)$ without any improvement) and a too large number n (a situation where the control law will have to be adapted too many times).

In this sense, our methodology is different from (active) adaptive control. Indeed, in our approach, the model of the plant and the control law are not updated at each time sample like in adaptive control. This different approach will allow us to solve the problem in a tractable way. In active adaptive control [50, 40], the considered problem is indeed very close to the problem considered in this chapter (the control input is optimized to be an optimal trade-off between control and identification objectives). However, the recursive setting leads to a stochastic dynamic programming problem that is never really tractable in practice [39]. As a consequence, the control input in adaptive control is generally only optimized for control objectives and thus not for identification objectives

[1, 7], often yielding identifiability problems and suboptimal performance.

The results of this chapter will be presented for a SISO true system (6.1) and for identification using a full-order model structure such as in the original papers C.57 and S.01.

9.2 Iterative identification and control design

Let us first present the procedure for the iterative identification of the true system (6.1). Suppose that the duration of each interval is equal to N and that we are at interval i . Consequently, the available model of the true system is $M_i = G(z, \hat{\theta}_i)$. Since it has been identified in a full-order model structure \mathcal{M} in the previous interval, the parameter vector $\hat{\theta}_i$ of this model is normally distributed around θ_0 with a covariance matrix $P_{\hat{\theta}_i}$ (see Section 6.1).

The excitation signal $r_i(t)$ ($t = 1 \dots N$) having a spectrum Φ_{r_i} is applied to the closed-loop system $[C(M_i) \ G_0]$ as shown in Figure 9.1 and the data $\{u(t), y(t) \mid t = 1, \dots, N\}_i$ are collected. These data will be used to reduce the uncertainty of the model M_i . For this purpose, like in Section 8.2.3, the parameter vector $\hat{\theta}_{i+1}$ will be determined with the following criterion:

$$\hat{\theta}_{i+1} = \arg \min_{\theta} \frac{1}{N} \left(\sum_{t=1}^N \epsilon^2(t, \theta) + \left\| \theta - \hat{\theta}_i \right\|_{P_{\hat{\theta}_i}^{-1}}^2 \right) \quad (9.1)$$

where $\epsilon(t, \theta)$ is computed using $\{u(t), y(t)\}_i$. The covariance matrix of $\hat{\theta}_{i+1}$ is given by

$$P_{\hat{\theta}_{i+1}} = \left(\mathcal{I}(\theta_0, \Phi_{r_i}) + P_{\hat{\theta}_i}^{-1} \right)^{-1} \quad (9.2)$$

with $\mathcal{I}(\cdot, \cdot)$ as defined in Section 8.2.2. We observe that the covariance matrix decreases from interval to interval. The same can be said about the size of the the uncertainty ellipsoid U_{i+1} that can be built using the distribution of $\hat{\theta}_{i+1}$ i.e. $\hat{\theta}_{i+1} \sim \mathcal{N}(\theta_0, P_{\hat{\theta}_{i+1}})$:

$$U_{i+1} = \{ \theta \mid (\theta - \hat{\theta}_{i+1})^T P_{\hat{\theta}_{i+1}}^{-1} (\theta - \hat{\theta}_{i+1}) < \chi_{\alpha} \} \quad (9.3)$$

This ellipsoid U_{i+1} contains the unknown true parameter vector θ_0 with probability α (with α such that $Pr(\chi^2(k) < \chi_{\alpha}) = \alpha$).

The new model $M_{i+1} = G(z, \hat{\theta}_{i+1})$ can be used to redesign the controller. We will suppose such as in the previous chapters that a control design method has been fixed a-priori and that the controller is thus a direct function $C(\cdot)$ of the model. The updated controller is thus $C(M_{i+1})$. Even though the uncertainty of the model has been reduced, it is always a good idea to validate the updated controller for stability and for performance over the plants in $\mathcal{D}_{i+1} = \{G(z, \theta) \mid \theta \in U_{i+1}\}$ (see Chapter 6) before applying it to the true system for the next interval.

Remark. The recursive equation (9.2) is initialized with $P_{\hat{\theta}_1}$ the covariance matrix of the initial model $M_1 = G(z, \hat{\theta}_1)$.

9.3 Cost \mathcal{T}_i of interval i

Even though other performance measures (such as the ones used in the previous chapters) are also possible, we will here define the performance in a relative way². The cost \mathcal{T}_i of the interval i is indeed defined by comparing the actual loop $[C(M_i) G_0]$ (i.e. the one in Figure 9.1) with the ideal loop $[C(G_0) G_0]$ (i.e. the loop that we would obtain if we would perfectly know the true system G_0). To make this comparison, it is important to have an expression for the output of these two loops. The output y_i of the actual loop is given by:

$$y_i(t) = \underbrace{\frac{H_0}{1 + C(M_i)G_0} e(t)}_{=y_{e,i}} + \underbrace{\frac{G_0}{1 + C(M_i)G_0} r_i}_{=y_{r,i}} \quad (9.4)$$

The output y_0 of the optimal loop is:

$$y_0(t) = \frac{H_0}{1 + C(G_0)G_0} e(t) \quad (9.5)$$

The main differences between (9.4) and (9.5) are the presence of r_i in (9.4) and the controllers present in the two loops. In the ideal loop, the controller is indeed the controller designed from the true system $G_0 = G(z, \theta_0)$.

The cost \mathcal{T}_i can now e.g. be defined as the power of the difference $y_i - y_0$ between these two outputs. Since r_i is independent of e , the total cost \mathcal{T}_i can be split up into the sum of a modelling error cost \mathcal{V}_i (i.e. the power of $y_{e,i} - y_0$) and an excitation cost \mathcal{J}_{r_i} (i.e. the power of $y_{r,i}$):

$$\mathcal{T}_i = \underbrace{\left\| \frac{H(\theta_0)}{1 + C(G(\theta_0))G(\theta_0)} - \frac{H(\theta_0)}{1 + C(M_i)G(\theta_0)} \right\|_2^2}_{=\mathcal{V}_i} \sigma_e^2 + \underbrace{\frac{1}{2\pi} \int_{-\pi}^{\pi} \left| \frac{G_0}{1 + C(M_i)G_0} \right|^2 \Phi_{r_i} d\omega}_{=\mathcal{J}_{r_i}} \quad (9.6)$$

Similarly as in (7.3) (with $\beta_u = 0$), the excitation cost \mathcal{J}_{r_i} is the power of the perturbation induced by r_i on the output of the system. This cost \mathcal{J}_{r_i} is linear in the to-be-designed spectrum Φ_{r_i} (such as also shown in Chapter 7). The modeling error cost \mathcal{V}_i is due to the uncertainty of the model $M_i = G(z, \hat{\theta}_i)$ which makes that $C(M_i) \neq C(G(\theta_0))$. This cost \mathcal{V}_i can be evaluated in the following way. Given a scalar γ_i , we know that $\mathcal{V}_i < \gamma_i$ (at a probability α) if

$$\underbrace{\left\| \frac{H(\theta)}{1 + C(G(\theta))G(\theta)} - \frac{H(\theta)}{1 + C(G(\hat{\theta}_i))G(\theta)} \right\|_2^2}_{=\mathcal{V}_i(\theta, \hat{\theta}_i)} \sigma_e^2 < \gamma_i \quad \forall \theta \in U_i \quad (9.7)$$

²such as has been done in C.57 and S.01.

with U_i defined similarly as U_{i+1} in (9.3).

Due to the relative definition of the performance, we can use the procedure in [22] to approximate³ $\mathcal{V}_i(\theta, \hat{\theta}_i)$ using a second-order Taylor expansion of this function around $\hat{\theta}_i$. More particularly, computing numerically the Hessian $\mathcal{H}(\hat{\theta}_i)$ of $\mathcal{V}(\theta, \hat{\theta}_i)$ at $\hat{\theta}_i$, (9.7) can be rewritten as:

$$(\theta - \hat{\theta}_i)^T \mathcal{H}(\hat{\theta}_i) (\theta - \hat{\theta}_i) < 2\gamma_i \quad \forall \theta \in U_i \quad (9.8)$$

The latter constraint is equivalent to the following LMI constraint linear in $P_{\hat{\theta}_i}^{-1}$:

$$P_{\hat{\theta}_i}^{-1} > \frac{\chi_\alpha}{2\gamma_i} \mathcal{H}(\hat{\theta}_i) \quad (9.9)$$

To sum up, we have that $\mathcal{V}_i < \gamma_i$ (at a probability α) if (9.9) holds. Minimizing $\sum_{i=1}^n \mathcal{V}_i$ can be thus formulated as minimizing $\sum_{i=1}^n \gamma_i$ under the constraint (9.9) at all i .

It is important to note that the smallest constant γ_i for which (9.9) holds decreases after each interval since $P_{\hat{\theta}_i}^{-1}$ increases after each interval. In other words, we see that, as expected, \mathcal{V}_i decreases after each interval in our framework.

Remark 1. Another possible definition for \mathcal{T}_i is the power of y_i . In this case, (9.7) would be replaced by:

$$\left\| \frac{H(\theta)}{1 + C(G(\hat{\theta}_i))G(\theta)} \right\|_2^2 \sigma_e^2 < \gamma_i \quad \forall \theta \in U_i \quad (9.10)$$

The results in J.13 could then be used to transform this constraint into a tractable one.

Remark 2. The excitation cost \mathcal{J}_{r_i} is also function of θ_0 . However, since this cost is not due to the model uncertainty, we will for simplicity not tackle \mathcal{J}_{r_i} using the uncertainty U_i . We will instead replace θ_0 in the expression of \mathcal{J}_{r_i} by an initial estimate as we have done in Chapter 7 (see also later). We can however also robustify the experimental design problem by using U_i for the dependence of \mathcal{J}_{r_i} on θ_0 (see S.01)

9.4 Optimal experiment design problem

Based on the result presented in the previous section, we can now formulate our experiment design problem leading to the spectra Φ_{r_i} ($i = 1 \dots n$) minimizing the overall cost $\sum_{i=1}^n \mathcal{T}_i$ over the n intervals as:

$$\arg \min_{\Phi_{r_i}, \gamma_i (i=1 \dots n)} \sum_{i=1}^n \gamma_i + \mathcal{J}_{r_i}$$

³This approximation is in fact not absolutely necessary, but is done for the simplicity of the presentation.

$$P_{\hat{\theta}_i}^{-1} > \frac{\chi_\alpha}{2\gamma_i} \mathcal{H}(\hat{\theta}_i) \quad i = 1 \dots n \quad (9.11)$$

$$\gamma_i + \mathcal{J}_{r_i} < \mathcal{T}_{max,i} \quad i = 1 \dots n$$

where $P_{\hat{\theta}_i}^{-1}$ is defined via the recursive equation (9.2) and $\mathcal{T}_{max,i}$ is an user-chosen threshold on the minimal control performance that is acceptable in each interval. The decision variable γ_i does not appear linearly in the first constraint of (9.11). However, the optimization problem (9.11) is equivalent to the following optimization problem with the slack variables t_i ($i = 1 \dots n$):

$$\begin{aligned} \arg \min_{\Phi_{r_i}, \gamma_i, t_i \ (i=1 \dots n)} \sum_{i=1}^n \gamma_i + \mathcal{J}_{r_i} \\ P_{\hat{\theta}_i}^{-1} > \frac{\chi_\alpha}{2} t_i \mathcal{H}(\hat{\theta}_i) \quad i = 1 \dots n \end{aligned} \quad (9.12)$$

$$\gamma_i + \mathcal{J}_{r_i} < \mathcal{T}_{max,i} \quad i = 1 \dots n$$

$$\begin{pmatrix} t_i & 1 \\ 1 & \gamma_i \end{pmatrix} > 0 \quad i = 1 \dots n$$

where the last constraint ensures that $t_i > \frac{1}{\gamma_i}$ at all i . The optimization problem (9.12) is now a convex optimization problem with LMI constraints. Indeed, $P_{\hat{\theta}_i}^{-1}$ and \mathcal{J}_{r_i} are both affine in the spectra Φ_{r_i} ($i = 1 \dots n$); see (9.2) and (9.6).

The chicken-and-egg problem is also present in (9.12). The optimization problem is indeed dependent on the unknown true parameter vector θ_0 (via \mathcal{J}_{r_i} and $P_{\hat{\theta}_i}$), but also on the to-be-identified parameter vectors $\hat{\theta}_i$ (via $\mathcal{H}(\hat{\theta}_i)$). All these unknowns can be replaced by the available estimate $\hat{\theta}_1$ defining M_1 . The receding horizon mechanism introduced in Section 9.1 can be used to refine the optimal spectra after each interval.

If there is no upper bound $\mathcal{T}_{max,i}$ on the cost of each interval (and in particular the first one), it can be proven that the solution of (9.12) puts all the excitation in the first interval i.e $\Phi_{r_i} = 0$ for $i \geq 2$. However, this excitation can be much too large in practice. Recall indeed that the cost \mathcal{J}_{r_1} is added to the cost \mathcal{V}_1 that is generally quite large since we want to improve $C(M_1)$. Consequently, these upper bounds are often necessary in practice. In the presence of these upper bounds $\mathcal{T}_{max,i}$, the numerical illustration of S.01 shows that our new iterative procedure achieves a significantly better overall performance $\sum_{i=1}^n \mathcal{T}_i$ than a procedure with a separate identification and control phase.

9.5 Conclusions

In this chapter, we have presented an alternative framework for *optimal identification experiment design for control*. This framework combines the objectives of the classical and of the least costly frameworks and is based on an iterative

scheme that updates the model and the controller during the lifetime of the control loop. Such a scheme allows one to maximize a measure of the overall performance while guaranteeing at all time a minimal level of performance.

In the paper C.54, a very similar iterative procedure has been applied in a simulation environment to improve the cooling profile (feedforward control) of a batch cooling crystallization process. For this purpose, the parameters of a nonlinear model of this process are re-identified after each batch⁴ and the cooling profile for the next batch is re-designed based on this improved model. In C.54, there is however no need for an optimal design of the excitation signal since the model improvement can be achieved in a satisfactory way using the internal excitation/perturbation of the system. Moreover, optimal experiment design for nonlinear systems is still an open research area.

In C.54, this identification-based technique is also compared to another model improvement technique i.e. Iterative Learning Control (see also C.48). It is to be noted that the iterative procedures presented in C.54 have been tested relatively successfully on a real-life crystallization process during a recent campaign at DSM.

⁴The batch plays here the role of the interval.

Chapter 10

Identification and feedforward control of inkjet printheads

10.1 Problem statement

In this chapter, we summarize the results we have obtained in collaboration with the printer manufacturer OCE within the Octopus projet (2008-2012). Our objective in this project have been to improve the print quality of a DoD (drop-on-demand) inkjet printhead using a system and control approach. An inkjet printhead is generally made up of a large amount of channels filled with ink (see Figure 10.1) and each of these channels can jet *a drop on demand* by applying, at the desired moment, an actuation pulse on the piezo-actuator at the top of the channel. In the sequel, the printhead under consideration is a printhead developed by *OCE Technologies* and consisting of two arrays of 128 channels each.

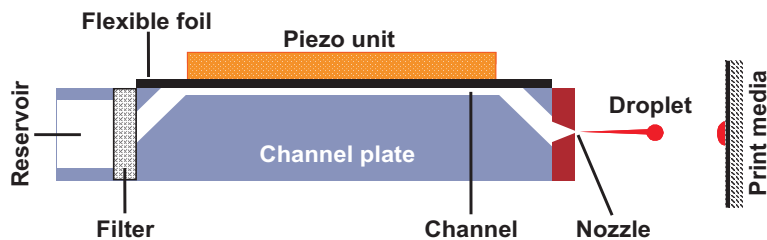


Figure 10.1: Cross-sectional representation of an ink channel

Inkjet technology is a relatively ancient technology when it comes to printing documents. However, this technology has recently emerged as a promising manufacturing tool. It has been successfully applied in various fields, namely, manufacturing of solar panels, PCBs and flat panel displays [36]. For these new applications, there are tighter requirements for the to-be-achieved “printing” performance and this performance should be achieved for jetting frequencies ranging from 20 to 70 *kHz*. By jetting frequency or *DoD frequency*, we mean the inverse of the time between two successive drops. An important performance requirement in this respect is that the jetted drops all have the same

speed irrespective of the DoD frequency. Unfortunately, the standard actuation pulse $u_{std}(t)$ [V] for the printhead under consideration (see Figure 10.2) is not able to achieve this objective.

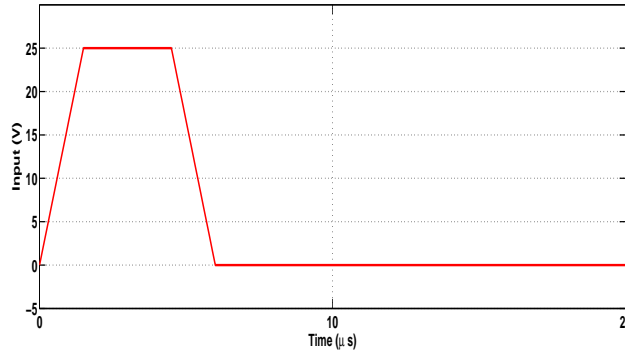


Figure 10.2: Standard actuation pulse $u_{st}(t)$ for the printhead under consideration

To illustrate this, let us use $u_{std}(t)$ to jet ten drops at a given DoD frequency and measure the speed of each of these ten drops. Subsequently, let us repeat this procedure at a certain number of other DoD frequencies. The speed of each of the ten drops can in this way be plotted as a function of the DoD frequency. This is done in Figure 10.3. Such figure is called the *DoD curve*. Since the speed of all the drops should be equal, the DoD curve should optimally be completely flat. We nevertheless observe in Figure 10.3 that this objective is far from met when the standard pulse is used as actuation pulse. The speed variation between the fastest and the slowest drop over the DoD range is equal to 12 m/s .

Let us investigate why the DoD curve is not flat. The standard pulse $u_{std}(t)$ has been designed to jet perfect drops when the system is at rest. For this purpose, this pulse creates, in the ink channel, a pressure wave represented in Figure 10.4. The signal represented in this figure is the so-called corrected PAINT signal, a sensor signal that is proportional to the derivative of the pressure in the ink channel (see J.19 for more details). It is important to note that the drop is jetted after $15\ \mu\text{s}$ or so. However, as we can see in Figure 10.4, the wave does not die out very fast after the drop has been jetted and remains significant for another $45\ \mu\text{s}$ or so.

These residual oscillations are the cause of the discrepancy between drop speeds that have been observed in Figure 10.3. Indeed, these oscillations perturb the jetting process if another drop is jetted before the ink channel is at rest. It is to be noted that undesired oscillations are also created in a given channel if the neighbouring channels are actuated. This phenomenon is called cross-talk and is due to the fact that the channels are all built on the same structure and influence therefore each other¹. The oscillations due to the cross-talk are less

¹Note that the cross-talk is not visible in Figure 10.3 since this figure results from an

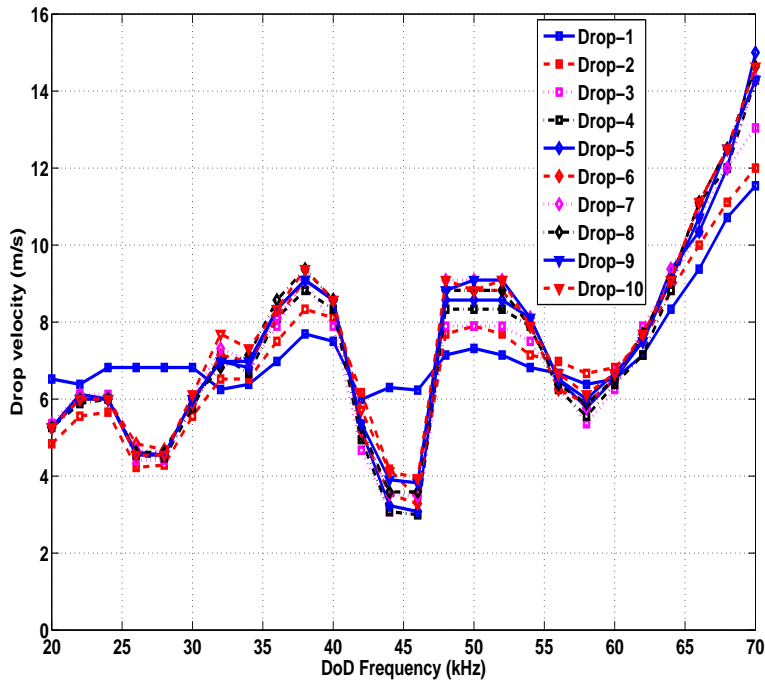


Figure 10.3: DoD curve corresponding to the standard pulse u_{st}

important than the residual oscillations, but they can generally not be neglected.

These two types of oscillations are the main factors that limit the performance of a printhead. In this chapter, we will show how we have redesigned the actuation pulse in order to compensate these oscillations and, in this way, improve the drop speed consistency. Our approach for this pulse redesign is a *model-based approach*. In our approach, an uncertain model is indeed deduced using system identification techniques and the pulse redesign methodology is inspired by the recent developments in robust feedforward control and robust filtering (see e.g. [42]). In this way, we provide a more systematic procedure than the experiment-based technique of [31, 30] and the learning-based technique of [52].

10.2 Modeling the inkjet printhead

Since, for this particular case, system identification has given the most complete results, we will here present the system identification procedure that we have used to deduce a model of the printhead. This model must relate the actuation pulse and an internal variable that can be measured and where the oscillations can be observed. This internal variable will be here the corrected PAINT signal

experiment where we have only actuated one channel.

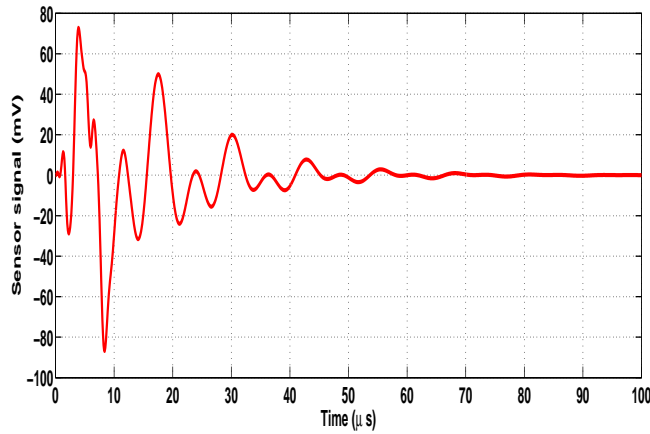


Figure 10.4: Measured PAINT signal when the standard actuation pulse $u_{st}(t)$ is applied

discussed in the previous section.

To simplify the modeling process, we will make the following assumptions based on the geometry of the printhead. The first assumption will be that the dynamics between the pulse u_n applied at channel n and the sensor signal y_n in this channel is identical for each channel n . We will also assume that the cross-talk is limited to the immediate neighbours and is identical on the left and right side. We can therefore write y_n as follows:

$$y_n(t) = G_{c,0} u_{n-1}(t) + G_{d,0} u_n(t) + G_{c,0} u_{n+1}(t) \quad (10.1)$$

where $G_{d,0}$ represents the direct dynamics and G_c the cross-talk dynamics. Note that the sensor signal will also be corrupted by additive noise, but we omit this noise in the previous equation to keep the notations simple. With these assumptions, we only need to identify a model for $G_{d,0}$ and a model for $G_{c,0}$ to entirely describe the printhead.

In order to identify these models, we apply an input signal u_n in open loop to channel n . This input signal is made up of a series of standard pulses² to be as close as possible to the operating conditions. We measure both the output y_n of channel n to identify the direct dynamics G_d and the output y_{n+1} of channel $n + 1$ to identify the cross-talk G_c . Using the prediction error criterion (6.4), a linear model G_d of $G_{d,0}$ and a linear model G_c of $G_{c,0}$, both having an order of six, are identified using the data sets $Z_d = \{u_n(t); y_n(t)\}$ and $Z_c = \{u_n(t); y_{n+1}(t)\}$, respectively. The Bode diagram of both models are represented in Figure 10.5. It is to be noted that the uncertainty \mathcal{D} of both models (see (6.9)) is negligible due to the small amount of noise in the data.

²The chosen input signal is a periodic signal (whose spectrum is a series of Dirac pulses at the harmonics of the DoD frequency) and can consequently be used in an identification procedure [33].

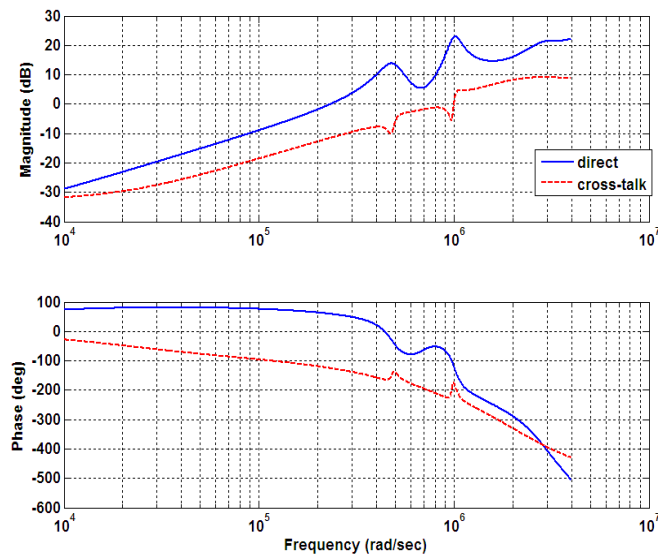


Figure 10.5: Bode diagram of G_d (blue solid) and G_c (red dashed)

A linear framework is nevertheless not entirely sufficient to accurately describe the relation between u_n and y_n . Indeed, if we apply the input signal (a series of standard pulses) at different DoD frequencies and we identify a linear model for each of these DoD frequencies, we obtain different dynamics as can be seen in Figure 10.6. This nonlinear phenomenon can be explained by the refill mechanism of the channel and is not observed for G_c (see J.19 and J.20 for more details).

Combining the set of models G_d identified at different DoD frequencies, we can build an uncertainty region \mathcal{D}_{DoD} that we will assume to contain all possible dynamics for G_d . This uncertainty region is built as a parametric uncertainty where the frequency and the damping factor of the first resonance peak of G_d is constrained to lie in a polytope (see J.19 for more details). We neglect the uncertainty of the second peak since this second peak is known to have much less influence on the performance. Note that this uncertainty \mathcal{D}_{DoD} is not due to the noise acting on the output of the system during the identification, but due to the nonlinear characteristics of the plant.

10.3 Model-based design of the actuation procedure

Using the model developed in the previous section, we will design an actuation procedure whose objective is to compensate the oscillations. When designing this actuation procedure, we must face a couple of limitations of the printhead hardware:

- The same pulse shape must be used for each channel. However, the pulses can be delayed in the even channels to deal with the cross talk

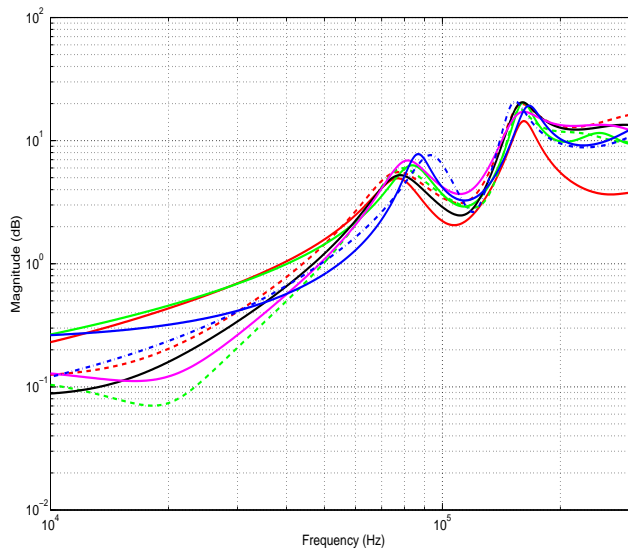


Figure 10.6: Models G_d identified with data generated at different DOD frequencies.

- The pulse shape is furthermore constrained to be trapezoidal (see Figure 10.7). We will therefore parametrize the actuation pulse with a parameter vector $\zeta = [t_{rR} \ t_{wR} \ t_{fR} \ V_R \ t_{dQ} \ t_{rQ} \ t_{wQ} \ t_{fQ} \ V_Q]^T$ corresponding to the characteristics of this trapezoidal pulse (see Figure 10.7)

Another limitation is that the pulse shape has to be unique, i.e. it cannot depend on the DoD frequency. Consequently, we will have to determine a pulse delivering good performance at all DoD frequencies, i.e. delivering good performance with all possible dynamics G_d in the uncertainty region \mathcal{D}_{DOD} .

Given the above limitations, our actuation design procedure reduces to determining in an optimal way the delay t_a between even and odd channels and the parameter vector ζ .

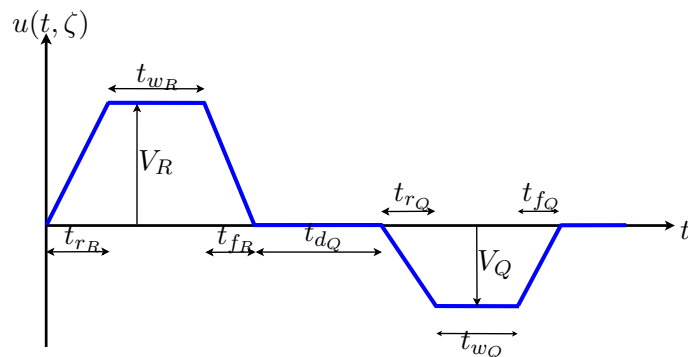


Figure 10.7: Parametrization of the pulse shape

An important ingredient for this purpose is to determine the optimal output we would like to achieve by tuning t_a and ζ . From the discussion in Section 10.1, an optimal output would be an output that has precisely the shape that allows to jet a drop with the desired velocity without any additional and undesired oscillation. To determine this desired output $y_{ref}(t)$, we recall that the standard pulse u_{std} is able to jet a perfect drop when the system is at rest. The output $y(t)$ corresponding to the standard pulse is given in red dashed in Figure 10.8 (see also Figure 10.4). Part A of the response $y(t)$ allows the drop to be jetted at the desired drop velocity. This happens at approximately $15 \mu\text{s}$. Consequently, $y_{ref}(t)$ should be the same as $y(t)$ in Part A. Part B of the response $y(t)$ represents the residual oscillations. Consequently, $y_{ref}(t)$ is brought to zero in this part.

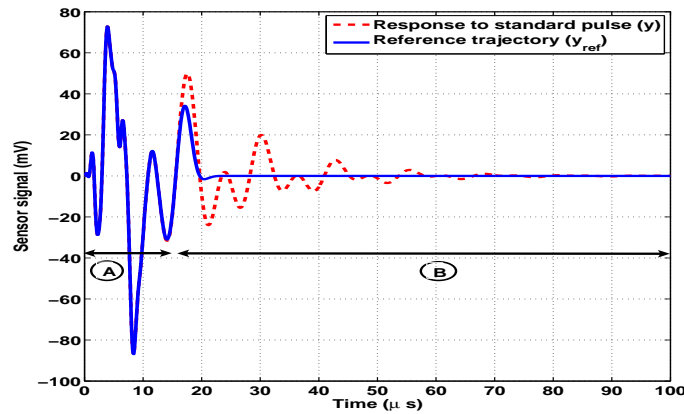


Figure 10.8: Sensor output y when the standard pulse is applied (red dashed) and desired output $y_{ref}(t)$ (blue solid)

Now that the desired output $y_{ref}(t)$ has been determined, we have to compare it with the actual output of a channel. This actual output depends on whether the two neighbouring channels are actuated or not. For example, suppose that n is odd and that channels n , $n - 1$ and $n + 1$ are actuated with the pulse $u(t, \zeta)$, the output y_n is then given by:

$$y_n(t) = G_d(z) u(t, \zeta) + 2 G_c(z) u(t - t_a, \zeta) \quad (10.2)$$

with G_d the model corresponding to the chosen DoD frequency. On the other hand, if the channels $n + 1$ and $n - 1$ are not actuated, the output y_n is given by:

$$y_n(t) = G_d(z) u(t, \zeta) \quad (10.3)$$

It is clear that y_n should be as close as possible to y_{ref} in all these situations³.

We can now propose the following optimization problem to determine optimal values for ζ and t_a :

$$\begin{aligned} & \arg \min_{\zeta, t_a} \max_{G_d \in \mathcal{D}_{DoD}} \mathcal{J}_{siso}(\zeta) + \lambda \mathcal{J}_{wc}(\zeta, t_a) \\ & \text{with } \mathcal{J}_{siso}(\zeta) = \sum_{t=1}^K (y_{ref}(t) - G_d(z)u(t, \zeta))^2 \\ & \mathcal{J}_{wc}(\zeta, t_a) = \sum_{t=1}^K (y_{ref}(t) - G_d(z)u(t, \zeta) - 2G_c(z)u(t - t_a, \theta))^2 \end{aligned} \quad (10.4)$$

where λ is an user-chosen weighting factor and K corresponds to 100 μs . The optimization problem (10.4) is a robust feedforward control problem. In comparison with robust feedback control problems, these problems are simpler and the robust control input can be directly determined by minimizing the worst case performance (i.e. $\mathcal{J}_{siso}(\zeta) + \lambda \mathcal{J}_{wc}(\zeta, t_a)$ in our case) over the plants in the uncertainty region \mathcal{D}_{DoD} (see e.g. [43]). However, due to the particular parametrization of the pulse, this optimization problem remains in our case a nonlinear optimization problem. Such nonlinear optimization problem can be solved offline using typical Matlab functions such as *fmincon*.

Remark 1. The uncertainty \mathcal{D}_{DoD} can be gridded to solve the optimization problem in an easy way. This is easily done since the uncertainty is a parametric uncertainty with only two uncertain parameters (see Section 10.2). As opposed to this simple approach, the papers C.42 and C.45 present methods to deal with the uncertainty as a compact set.

Remark 2. Since (10.2) and (10.3) pertain to odd channels, the optimization problem (10.4) focuses on these particular channels. In J.20, the optimization problem considers in fact both odd and even channels.

The solution of the optimization problem is $t_{a,opt} = 7.93 \mu s$ and the pulse shape $u(t, \zeta_{opt})$ given in Figure 10.9. In this figure, $u(t, \zeta_{opt})$ is compared with the standard pulse. The main difference between the optimal and the standard pulses is that the optimal pulse is made of two parts: one part to jet the drop and a second part (between 10 and 20 μs) to compensate/damp the oscillations.

10.4 Experimental results

Let us compare the performance of the optimal pulse $u(t, \zeta_{opt})$ with the one of the standard pulse using experiments on a real setup. A first evaluation can be

³Another situation is when channels n and $n + 1$ are actuated. However, the optimization problem presented in (10.4) delivers better results when only the extreme cases (10.2) and (10.3) are considered.

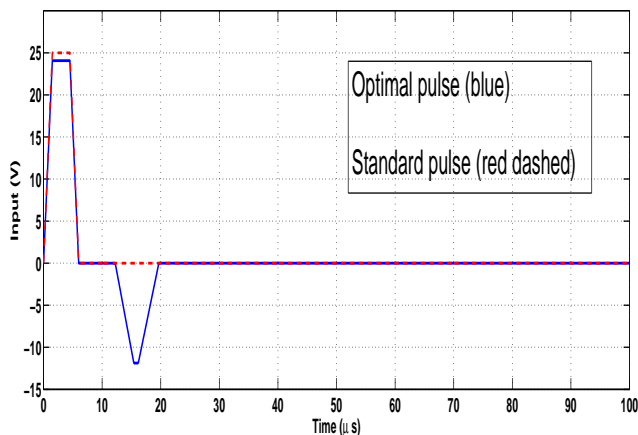


Figure 10.9: $u(t, \zeta_{opt})$ (blue solid) compared with $u_{st}(t)$ (red dashed)

obtained by comparing the DoD curve obtained with the two pulses. The DoD curve obtained with the standard pulse is given in Figure 10.3 while the DoD curve obtained with the optimal pulse $u(t, \zeta_{opt})$ is given in Figure 10.10. It is obvious the DoD curve is much flatter with the optimal pulse. The maximal speed difference is reduced from 12 m/s with the standard pulse to 2.5 m/s with the optimal pulse.

The DoD curve is obtained by actuating one single channel. In order to validate the complete actuation framework, we will print the bitmap represented in Figure 10.11. We see that this bitmap requires to actuate nine successive channels. The printed image when using $u(t, \zeta_{opt})$ and applying the optimal delay $t_{a,opt}$ between odd and even channels is given in Figure 10.12 and the printed image when using $u_{st}(t)$ and $t_a = 0$ is given in Figure 10.13. By comparing these two figures, it is evident that the proposed actuation procedure is very effective to improve the printing quality.

10.5 Conclusions

In this chapter, we have presented a model-based approach to improve the performance of a DoD inkjet printhead by damping undesired oscillations in the ink channel. The model of the printhead is developed using system identification techniques and assumptions based on the printhead geometry has allowed us to simplify the system identification procedure. We have observed that the direct ink channel behavior depends on the DoD frequency. Consequently, we consider a robust feedforward control problem to design an actuation framework damping the undesired oscillations. Experimental results have demonstrated that, with respect to the performance obtained with the standard pulse, a considerable improvement in the drop speed consistency is achieved with the proposed framework.

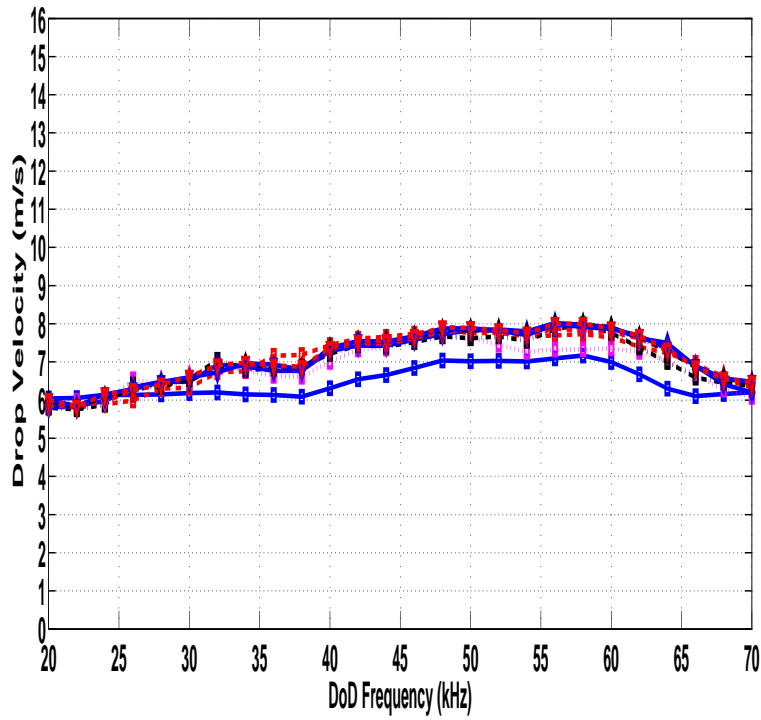


Figure 10.10: DoD curve corresponding to the optimal pulse $u(t, \zeta_{opt})$

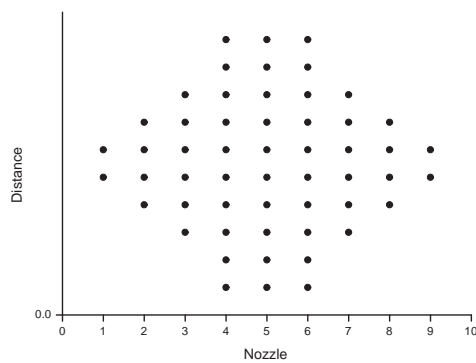


Figure 10.11: Bitmap to be printed



Figure 10.12: Printed image with $u(t, \zeta_{opt})$ and $t_{a,opt}$



Figure 10.13: Printed image with u_{st} and $t_a = 0$

Chapter 11

Informative data and network identification

11.1 Introduction

In this chapter, we present two series of results that both pertain to the fundamentals of system identification. The first series of results consider the question of the minimal characteristics an excitation signal should have to lead to a consistent estimate of the true system. The second series of results consider the identification of systems in a complex network.

11.2 How to get a sufficiently rich excitation signal?

Consider the identification framework presented in Section 6.1 which considers the identification (in a full-order model structure) of a true system (6.1) operated in closed loop with a controller C_{id} . The excitation signal applied at the output of the controller is denoted r . Even though this framework is a closed-loop identification framework, open-loop identification is equivalent to the case where $C_{id} = 0$ and where, thus, $r \equiv u$.

In Chapter 7, the excitation signal of the identification experiment is determined among other things to guarantee some constraint on the model accuracy. This model accuracy constraint is expressed as a function of the inverse P_θ^{-1} of the covariance matrix of the identified parameter vector $\hat{\theta}_N$. In this respect, a minimal constraint that must be satisfied by P_θ^{-1} is that it is strictly positive-definite: $P_\theta^{-1} > 0$. Consequently, since the excitation signal determines P_θ^{-1} (see e.g. (6.6)), the parametrization of the excitation signal¹ must be chosen in such a way that $P_\theta^{-1} > 0$. Different parametrizations can be used in practice (see Remark 2 in Section 7.2) and these parametrizations allow to generate the excitation signals that are generally used in system identification. For the most current parametrization where the excitation signal is a filtered version

¹As shown in Chapter 7, it is the spectrum $\Phi_r(\omega)$ of the excitation signal and not the excitation signal itself that is parametrized. However, this does not change the discussion in this chapter.

of a white noise, P_θ^{-1} is guaranteed to be strictly positive-definite [33]. However, when we choose the excitation signal as a multisine (i.e. the sum of a certain number of sinusoids at different frequencies), we must ensure that this number of sinusoids is sufficiently large to obtain a strictly positive-definite P_θ^{-1} .

The paper J.12 tackles this question by a careful analysis of the pseudoregression vector $\psi(t, \theta_0)$ defining the covariance matrix (see Section 6.1). This analysis is performed for both open-loop identification and closed-loop identification. The results for closed-loop identification case are particularly interesting. Indeed, as already mentioned in Remark 1 in Section 7.2, a strictly positive-definite P_θ^{-1} can be obtained with no excitation at all (i.e. $r = 0$) if the controller C_{id} is sufficiently complex. The particular conditions on the degree of the controller to enable such costless identification are presented in J.12. If the controller is not sufficiently complex, the closed-loop system will have to be excited by an external signal r to obtain $P_\theta^{-1} > 0$. If we choose a multisine as excitation signal, the minimal number of sinusoids to obtain $P_\theta^{-1} > 0$ is proportional to the difference between the degree that is required to enable costless identification and the actual degree of C_{id} .

An important question at this stage is to know whether the conditions obtained in J.12 also implies that the identified parameter vector $\hat{\theta}_N$ is a consistent estimate of the true parameter vector θ_0 . The consistency of $\hat{\theta}_N$ is indeed a very important requirement for a good identification. This consistency is obtained if the data set used for the identification is informative. An informative data set is a data set for which we have: $\epsilon(t, \theta) = e(t) \implies \theta = \theta_0$. In [15] (but also in J.07 for the particular case of costless identification), the conditions to obtain an informative data set are presented for both open-loop and closed-loop identification and it can be observed that these conditions are equivalent to the ones obtained in J.12.

The paper J.17 completes this work by establishing the precise relations existing between the notions of an informative data set, a strictly positive-definite P_θ^{-1} and the fact that θ_0 is the unique global minimum of the asymptotic identification criterion $\bar{V}(\theta) = \bar{E}\epsilon^2(t, \theta)$. We can in fact say that the papers J.12, J.17 and [15] extend the already existing theory on these issues (see e.g. [49, 33]). This is especially true for the closed-loop identification case.

Remark. These results have also been used to determine conditions on both the input signal and the scheduling variable for the identification of consistent estimates of LPV-ARX systems in open loop (see the paper C.46).

11.3 Identification of a particular system in a complex network

Until now, we have considered the case where the true system (6.1) is identified in an open-loop or a closed-loop setting. The open-loop and closed-loop settings are nevertheless only two of the possible ways in which a true system

can be operated. Indeed, an individual system (e.g. G_0^{21}) can also be operated in a setting such as the one in Figure 11.1 (called *network* in the sequel). The setting in this figure is obviously much more complex than the simple closed loop presented in Figure 6.1. Examples of such networks can be found in e.g. power grids and biological systems. Such network configurations will become more frequent in engineering systems that nowadays become increasingly complex and interconnected.

We will make some assumptions about the networks we will consider in this section. The first assumption is that we a-priori know the interconnection structure of the network. However, we do not assume to know the particular value of the transfer functions G_0^{ij} that are present in the network. In this situation, our particular objective is to obtain via system identification a consistent estimate of one of these transfer functions, say G_0^{21} in Figure 11.1. As such, our objective is different from the earlier works on network identification attempting at identifying both the structure and the entire dynamics of the network (see e.g. [35]).

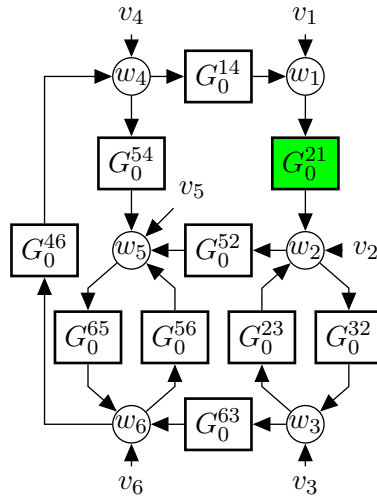


Figure 11.1: An example of a network

The input-output relation of the plant G_0^{21} in Figure 11.1 can be formulated as follows:

$$w_2(t) = G_0^{21}(z) w_1(t) + G_0^{23}(z) w_3(t) + v_2(t) \quad (11.1)$$

with v_2 defined similarly as $v(t)$ in (6.1) i.e. $v_2(t) = H_0^2(z)e_2(t)$. If w_2 , w_1 and w_3 can all be exactly measured, a consistent model for G_0^{21} (but also for $G_0^{23}(z)$ and $H_0^2(z)$) can be found using the prediction-error criterion (6.4) with the following prediction error:

$$\epsilon(t, \theta) = (H^{21}(z, \theta))^{-1} (w_2(t) - G^{21}(z, \theta) w_1(t) + G^{23}(z, \theta) w_3(t)) \quad (11.2)$$

The conditions for obtaining these consistent estimates are very similar to those for the case where (11.1) would be operated in a simple closed loop. The model

structure must indeed be full-order and the data set must be informative². The paper J.21 summarizes these conditions and, in addition to the classical direct identification technique (see above), this paper considers also other identification techniques such as the two-stage method.

The problem becomes even more interesting whenever some of the signals cannot be measured or are e.g. very expensive to measure. In this case, one could ask what are the signals that have absolutely to be measured in order to obtain a consistent estimate of $G_0^{21}(z)$. By signals, we here do not only mean the signals present in (11.1), but also the other signals w_4, w_5, w_6 of the networks. These other signals could indeed be easier to measure than the ones in (11.1). This question is addressed using insights of graph theory in the paper C.59.

²Such as for closed-loop identification, there is also an additional constraint on the presence of at least one pure delay in every loop that passes through w_2 .

Chapter 12

Other research projects

Hereunder follows a list of other research projects with a description.

- **Monitoring of industrial processes using large-scale first-principles models.** Since large-scale physical models of industrial plants are generally too complex to be used for the monitoring of industrial plants (state estimation), techniques have been developed to simplify those physical models while keeping the monitoring accuracy. The results of this project in collaboration with the research institute TNO-TPD are presented in the papers J.11, C.17, C.18 and C.23 as well as in the PhD thesis of Robert Bos (see Section 3.2) where the developed techniques have been applied to a large-scale physical model of the dryer section of a paper production machine.
- **Identification of irrigation channels.** In this project, we have used experimental data collected on an irrigation channel in Arizona to identify a dynamical model of this channel and in particular its resonating characteristics. This project is in collaboration with the Water Management Department of the TU Delft and the US Arid-Land Agricultural Research Center, Phoenix, Arizona. See the papers J.14 and C.52.
- **Optimal training sequences for telecommunication channels.** Training sequences are used to determine a model of a telecommunication channel that is required to reconstruct the emitted signal at the receiver end (deconvolution/equalization). These training sequences are here optimized to obtain the best reconstruction properties. This project is in collaboration with the Automatic Control and Telecommunication Departments of the KTH Stockholm. See the papers J.13 and J.22.
- **Automatic autorotation of a rotorcraft Unmanned Aerial Vehicle (UAV).** In this ongoing project in collaboration with the Dutch Aerospace Laboratory (NLR), our objective is to guarantee the safe landing of an UAV (drone) having lost its engine power. For this purpose, we have addressed the problem of optimal trajectory planning in the paper C.47 and we are for the moment using robust and LPV control techniques to follow these optimal trajectories. A first step towards this last objective

has been to devise methods to approximate complex nonlinear models (such as the UAV model) by simpler LPV models without losing too much accuracy: see C.60.

Chapter 13

Conclusions

In the previous chapters, I have presented in a concise manner my research activities in the last fifteen years. The main objective of this research has been to optimize the path starting at the collection of an informative data set on a real-life system and ending with a satisfactory control system. The followed approach has been to determine identification experiments that are specially optimized for the specific control objective and that are as cheap as possible. Within the Autoprofit project, this philosophy has been extended to comprise the whole maintenance of industrial control systems: performance monitoring, performance diagnosis and controller update via re-identification (see Figure 8.1). By doing this, our objective was to increase the autonomy of these industrial control systems. In the future, my main research objective will be to develop further this line of reasoning building on the experience of the Autoprofit project. The aim will therefore be to develop control systems that become increasingly autonomous.

Developing autonomous control systems is an important challenge for a large number of technological and industrial sectors. We indeed observe, on the one hand, an increasing demand for higher product quality, higher performance and higher efficiency. On the other hand, we also observe that control systems are becoming increasingly complex and interconnected. Due to this complexity and to these interconnections, control systems have to operate under circumstances that will more and more differ from the ones for which the control system has been designed at commissioning. A modern control system must therefore be able to monitor its performance, to detect the origin of any observed performance drop and to restore the desired level of performance in an autonomous way. All these actions must be performed using dedicated experiments that are optimized for their specific objectives.

Since optimal experiment design (for diagnosis or for re-identification) is central in our philosophy, the realization of this long-term objective will require that this paradigm becomes a fully mature theory. Several important challenges are indeed still ahead of us:

Optimal experiment design for network systems. A first challenge is to develop a comprehensive theory for designing optimal identification experi-

ments for systems embedded in a complex network. Indeed, as mentioned in the previous paragraph, control systems are becoming increasingly complex and interconnected. As we have seen in Chapter 11, we are just starting to understand how to identify models in a consistent way in such networks. An optimal experiment design framework for such networks is thus a complete new research area with interesting questions that are specific to this problem such as the optimal location in the network where the excitation has to be applied, the number of signals that have to be measured, etc.

Optimal experiment design for nonlinear systems. A second challenge is to make steps towards optimal experiment design for nonlinear systems, a topic which has remained almost unexplored despite its practical importance. The use of the nonlinear behaviour of engineering systems will indeed become increasingly important to fully optimize their performance. If identifying the linearized dynamics of a system already entails an important cost (especially in the process industry), the identification of the full nonlinear behaviour could be even more expensive. The design of cheap experiments for the identification of this nonlinear behaviour is therefore important. Different cases/situations can be considered.

- The first situation supposes that a nonlinear structure for the to-be-identified system is available and the objective of the identification is to determine the unknown (physical) parameters in this structure. Designing an optimal experiment in this case can be formulated as determining an excitation signal for the identification which perturbs as little as possible the system while guaranteeing a satisfactory accuracy for the estimated parameters (e.g. an accuracy allowing the design of a controller achieving satisfactory performance). Some preliminary work has been achieved towards this end in the PhD project of Marco Forgone (see Section 3.2).
- A second situation is when such a non linear structure is not available a-priori. In this case, a black-box nonlinear identification (such as LPV identification) has to be performed. Developing non-intrusive experiments for the identification of accurate LPV models is an important challenge. It involves the issues of obtaining informative data for such identification experiments, but also the issue of determining what is the optimal number of basis models that have to be considered in the LPV structure for an optimal trade-off between accuracy and excitation cost. Early results on these issues are available in C.37 and C.46.

Optimal experiment design with short data sets. Another challenge is to develop a comprehensive theory for the optimal design of short identification experiments. Indeed, cheap experiments are often short experiments while many optimal experiment design results are based on the assumption that the number of data is large; assumption which allows one to use asymptotic theory to evaluate the model uncertainty, but which could lead to errors when the number of data is small.

Optimal experiment design considering both variance and bias errors.

Almost all optimal experiment design results are based on the assumption that the identification is performed in a full-order model structure. Consequently, the model uncertainty is entirely determined by the variance error due to the stochastic noise corrupting the data. It would be very interesting to continue the work started in C.28 where an optimal experiment design framework is devised for the identification of a system in a reduced-order model structure. In this case, the optimal excitation must make a trade-off between the variance error and the bias error.

My ambition is thus to continue a strong fundamental line of research, but also to look for opportunities in the world of applications to valorize this fundamental research. Developing autonomous control systems is an important topic in a large variety of applications going from the process industry, the aerospace industry to manufacturers of mechatronic systems. I want therefore to further develop the collaboration with our industrial partners in the European Project (process industry) and with the NLR (aerospace) to finance this research. My ambition is also to pursue the collaboration on inkjet printers with OCE. OCE is indeed interested by our results on performance diagnosis via system identification (see Chapter 8).

Bibliography

- [1] K. Aström and B. Wittenmark. *Adaptive control*. Addison-Wesley Longman Publishing Co., Boston, MA, 1989.
- [2] M. Barenthin, H. Jansson, and H. Hjalmarsson. Applications of mixed H_2 and H_{∞} input design in identification. In *Proc. IFAC World Congress, Prague, 2005*.
- [3] M. Basseville. On-board component fault detection and isolation using the statistical local approach. *Automatica*, 34:1391–1415, 1998.
- [4] M. Basseville and A. Benveniste. Sequential segmentation of nonstationary digital signals using spectral analysis. *Information Sciences*, 29:57–73, 1983.
- [5] A. Benveniste, M. Basseville, and G. V. Moustakides. The asymptotic local approach to change detection and model validation. *IEEE Transactions on Automatic Control*, AC-32:583–592, 1987.
- [6] S. Boyd, L. El Ghaoui, E. Feron, and V. Balakrishnan. *Linear Matrix Inequalities in Systems and Control Theory*, volume 15 of *Studies in Appl. Math.* SIAM, Philadelphia, June 1994.
- [7] M. Campi and M. Prandini. Randomized algorithms for the synthesis of cautious adaptive controllers. *Systems and Control Letters*, 49:21–36, 2003.
- [8] B. Cooley and J. Lee. Control-relevant experiment design for multivariable systems described by expansions in orthonormal bases. *Automatica*, 37(2):273–281, February 2001.
- [9] P.M.J. Van den Hof. Closed-loop issues in system identification. *Annual Reviews in Control*, 22:173–186, 1998.
- [10] P.M.J. Van den Hof and R. Schrama. Identification and control - closed loop issues. *Automatica*, 31:1751–1770, 1995.
- [11] J.C. Doyle. Analysis of feedback systems with structured uncertainties. *IEE Proc.*, 129-D(6):242–250, November 1982.
- [12] U. Forssell and L. Ljung. Some results on optimal experiment design. *Automatica*, 36:749–756, 2000.
- [13] Lázló Gerencsér, Håkan Hjalmarsson, and Jonas Mårtensson. Identification of ARX systems with non-stationary inputs - asymptotic analysis with

- application to adaptive input design. *Automatica*, 45(3):623–633, March 2009.
- [14] M. Gevers. Towards a joint design of identification and control? In H.L. Trentelman and J.C. Willems, editors, *Essays on Control: Perspectives in the Theory and its Applications*, Birkhauser, New York, pages 111–151, New York, 1993. Birkhauser.
- [15] M. Gevers, A. S. Bazanella, and L. Miskovic. Informative data: how to get just sufficiently rich? In *Proc. 47th IEEE Conference on Decision and Control*, pages pp. 1962–1967, Cancun, Mexico, 2008.
- [16] M. Gevers and L. Ljung. Optimal experiment designs with respect to the intended model application. *Automatica*, 22:543–554, 1986.
- [17] K.C. Goh and M.G. Safonov. Robust analysis, sectors and quadratic functionals. In IEEE, editor, *Proc. IEEE Conf. on Decision and Control*, New Orleans, Louisiana, 1995.
- [18] G.C. Goodwin, M. Gevers, and B. Ninness. Quantifying the error in estimated transfer functions with application to model order selection. *IEEE Trans. Automatic Control*, 37:913–928, 1992.
- [19] F. Gustafsson and S. F. Graebe. Closed-loop performance monitoring in the presence of system changes and disturbances. *Automatica*, 34:1311–1326, 1998.
- [20] R.G. Hakvoort and P.M.J. Van den Hof. *IEEE Transactions on Automatic Control*, (11).
- [21] R. Hildebrand and M. Gevers. Identification for control: optimal input design with respect to a worst-case ν -gap cost function. *SIAM Journal on Control and Optimization*, 41(5):1586–1608, March 2003.
- [22] H. Hjalmarsson. System identification of complex and structured systems. *European Journal of Control*, 15(3-4):275–310, 2009.
- [23] H. Hjalmarsson, M. Gevers, and F. De Bruyne. For model-based control design, closed-loop identification gives better performance. *Automatica*, 32(12):1659–1673, 1996.
- [24] H. Hjalmarsson, M. Gevers, and F. De Bruyne. For model-based control design, closed-loop identification gives better performance. *Automatica*, 32:1659–1673, 1996.
- [25] B. Huang and S. Shah. *Performance Assessment of Control Loops. Theory and Applications*. Springer, 1999.
- [26] B. Huang and E. C. Tamayo. Model validation for industrial model predictive control systems. *Chemical Engineering Science*, 55:2315–2327, 2000.
- [27] H. Jansson and H. Hjalmarsson. Input design via LMIs admitting frequency-wise model specifications in confidence regions. *IEEE Transactions on Automatic Control*, 50(10):1534–1549, October 2005.

- [28] H. Jiang, B. Huang, and S. L. Shah. Closed-loop model validation based on the two-model divergence method. *Journal of Process Control*, 19:644–655, 2009.
- [29] S. M. Kay. *Fundamentals of Statistical Signal Processing: Detection Theory*. Prentice Hall, Piscataway, 1998.
- [30] K.S. Kwon. Waveform design methods for piezo inkjet dispensers based on measured meniscus motion. *Journal of Microelectromechanical Systems*, 18(5):1118–1125, 2009.
- [31] K.S. Kwon and W. Kim. A waveform design method for high-speed inkjet printing based on self-sensing measurement. *Sensors and Actuators A: Physical*, 140(1):75–83, 2007.
- [32] K. Lindqvist. *On experiment design in identification of smooth linear systems*. Licentiate Thesis, Royal Institute of Technology, Stockholm, Sweden, 2001.
- [33] L. Ljung. *System Identification: Theory for the User, 2nd Edition*. Prentice-Hall, Englewood Cliffs, NJ, 1999.
- [34] J.M. Maciejowsky. *Predictive control with constraints*. Pearson, Prentice Hall, 2002.
- [35] D. Materassi, M. Salapaka, and L. Giarre. Relations between structure and estimators in networks of dynamical systems. In *Proc. 50th IEEE Conference on Decision and Control*, Orlando, USA, 2011.
- [36] M.Singh, H.M. Haverinen, P. Dhagat, and G.E. Jabbour. Inkjet printing process and its applications. *Advanced Materials*, 22:673–685, 2010.
- [37] S. Olaru, J. A. De Doná, and M. M. Seron. Positive invariant sets for fault tolerant multisensor control schemes. In *Proceedings of the 17th IFAC World Congress*, pages 1224–1229, Seoul, 2008.
- [38] R. Pintelon and J. Schoukens. *System identification: a frequency domain approach*. Wiley - IEEE Press, 2004.
- [39] L. Pronzato. Optimal experimental design and some related control problems. *Automatica*, 44:303–325, 2008.
- [40] L. Pronzato, C. Kulcsar, and E. Walter. An actively adaptive control policy for linear models. *IEEE Transactions on Automatic Control*, 41:855–858, 1996.
- [41] Cristian R. Rojas, Juan C. Agüero, James S. Welsh, Graham C. Goodwin, and Arie Feuer. Robustness in experiment design. *IEEE Transactions on Automatic Control*, 57(4):860–874, 2012. QC 20120507.
- [42] C. Scherer and I.E. Kose. Robustness with dynamic IQCs: an exact state-space characterization of nominal stability with applications to robust estimation. *Automatica*, 44:1666–1675, 2008.

- [43] C. Scherer and S. Weiland. Linear matrix inequalities in control. Lectures notes, Dutch Institute for Systems and Control (DISC), available at <http://www.dsc.tudelft.nl/~cscherer/2416/lmi.pdf>, 1999.
- [44] R. Schrama. *Approximate Identification and Control Design*. PhD thesis, Delft University of Technology, 1992.
- [45] G. Scorletti. *Approche unifiée de l'analyse et de la commande des systèmes par formulation LMI*. PhD thesis, Université de Paris-Sud, U.F.R. scientifique d'Orsay, June 1997.
- [46] G. Scorletti. Robustness analysis with time delays. In *Proc. 36th IEEE Conference on Decision and Control*, San Diego, 1997.
- [47] M. M. Seron and J. A. De Doná. Actuator fault tolerant multi-controller scheme using set separation based diagnosis. *International Journal of Control*, 83:2328–2339, 2010.
- [48] Y.A.W. Shardt and B. Huang. Closed-loop identification with routine operating data: Effect of time delay and sampling time. *Journal of Process Control*, 21:997–1010, 2011.
- [49] T. Söderström and P. Stoica. *System Identification*. Prentice Hall International, Hemel Hempstead, Hertfordshire, UK, 1989.
- [50] E. Tse and Y. Bar-Shalom. An actively adaptive control for linear systems with random parameters via the dual control approach. *IEEE Transactions on Automatic Control*, 18:109–117, 1973.
- [51] M. Tyler and M. Morari. Performance monitoring of control systems using likelihood methods. *Automatica*, 32:1145–1162, 1996.
- [52] M.B.G. Wassink. *Inkjet printhead performance enhancement by feedforward input design based on two-port modeling*. PhD thesis, Delft University of Technology, 2007.
- [53] G. Zames. Feedback and optimal sensitivity: Model reference transformations, multiplicative seminorms, and approximate inverses. *IEEE Trans. Aut. Control*, AC-26(2):301–320, April 1981.
- [54] K. Zhou and J. Doyle. *Essentials of Robust Control*. Prentice Hall, Upper Saddle River, New Jersey, 1998.